Geometric Approach to the Feynman Integrals

Dissertation
zur
Erlangung des Doktorgrades (Dr. rer. nat.)
der
Mathematisch-Naturwissenschaftlichen Fakultät
der
Rheinischen Friedrich-Wilhelms-Universität Bonn

von
Reza Safari
aus
Ahvaz, Iran

Bonn, 17.09.2021

Angefertigt mit Genehmigung der Mathematisch-Naturwissenschaftlichen Fakultät der Rheinischen Friedrich-Wilhelms-Universität Bonn

1. Gutachter:	Prof. Dr. Albrecht Klemm
2. Gutachter:	PD Dr. Stefan Förste
Tag der Promotion:	23.12.2021
Erscheinungsjahr:	2022

Acknowledgment

I wish to thank everyone who helped me during my PhD and made these years one of the best period of my life.

First of all, I have to thank Prof. Albrecht Klemm, my supervisor, who patiently and kindly taught me many things and continuously supported me during my research. He proposed a very interesting and novel topic for my research that I am very passionate about it. I would like to thank PD. Dr. Stefan Förtse for accepting to be my second advisor and for many useful discussions we had. I am very thankful to Prof. Ursula Hamenstädt and Prof. Jochen Dingfelder for accepting to be my thesis referees. I appreciate all the crucial comments and kind supports by Prof. Hans Jockers. I express my warm gratitude to Prof. Victor Batyrev, Prof. Yang-Hui He and Prof. Claude Duhr for their useful comments during my research. I am also grateful to Dr. Babak Haghighat for being a great inspiration to me. Last but not least, we all have to thank Prof. Hans Peter Nilles for establishing a successful research institute, bctp.

I thank my colleagues Kilian Bönisch, Fabian Fischbach, Prof. Albrecht Klemm and Christoph Nega for our fruitful collaborations which resulted in two remarkable papers.

Special thanks goes to my fiance, Vahideh Eshaghian, for helping and supporting me in every step of my PhD, motivating me on this long way and for proofreading my thesis.

I am extremely thankful to the secretaries of the institute, Ms. Christa Börsch, Ms. Petra Weiss and Ms. Patricia Zündorf and also the scientific associate Dr. Andreas Wisskirchen for their countless helps during my PhD that made my life much easier in these years.

I am happy that I was a member of bctp with such a friendly and scientifically motivating atmosphere. I thank all the members and colleagues, specially, Bardia Najjari for playing Tar for me, Dr. Fazlollah Hajkarim for having tea together, Fabian Fischbach and Christoph Nega for many funny conversations, Alexandros Kanargias as the best office-mate and a great friend, Dr. Urmi Ninand, Joshua Kames-King, Dr. Christoph Liyanage, Dominik Köhler, Florian Domingo, Ruben Campos Delgado for the late chess games, Rahul Mehra, Thorsten Schimannek, Xin Wang, Andreas Gerhardus, Abhinav Joshi. I also thank my great friends like Dr. Makan Karegar, Dr. Ali Noori, Dr. Ameneh Sheikhan, Dr. Mojtaba Taslimi Tehrani, Dr. Haleh Ebadi and my close friend Mohsen Shamohammadi.

It is not possible to thank enough my parents and sisters, Nazanin and Niloofar, for their endless supports in every direction through my life and their special support and motivation during my PhD. I am also very thankful to my dear aunts Maryam, Hajar and Mahnaz and my dear uncle Ali for their kindness and supports.

Abtract

In this PhD thesis, the Feynman integrals are evaluated using an algebraic geometry approach known in string theory. The GKZ description of periods and certain classes of relative periods on Calabi-Yau $(l-1)$-folds has been used in order to solve the l-loop banana amplitudes with their general mass dependence.

There are different ways of computing Feynman integrals. These integrals satisfy a set of differential equations whose solutions give the answer of the integral. One of the approaches to derive a system of differential equations for Feynman integrals is the integration by part (IBP) identity. There is also an alternative approach to obtain these differential equations for a Feynman integral using the geometric interpretation of the Feynman integrals.

From the algebro-geometric point of view, Feynman integrals are the periods of the mixed Hodge structure on the relative cohomology groups. Varying physical parameters leads to a variation of the Hodge structure. The geometric interpretation comes from the polar locus of the integrand. The poles of the integrand define a Calabi-Yau manifold, which is often in a toric variety. These period integrals satisfy a system of linear homogeneous differential equations, so-called Picard-Fuchs differential ideal (PFDI). With toric geometry we can derive a finite set of differential operators, so-called GKZ hypergeometric system and extract PFDI. We obtain GKZ system from the variation of the Hodge structure and we benefit from the symmetries of the graphs more efficiently. GKZ systems are generalization of hypergeometric system and use the symmetries of the integrand, i.e. symmetries in its parameter space. As examples we compute the mass dependencies of the banana amplitudes up to the four-loop case.

For the two-loop banana Feynman integral, the so-called *sunset* diagram, the polar locus of the integrand is a special family of elliptic curves $\mathcal{E}$, i.e. a Calabi-Yau one-fold. The integral is related to the period integral of the local mirror M of the non-compact Calabi-Yau three-fold W, defined as the total space of the anti-canonical line bundle over the degree three del Pezzo surface S, which is $\mathbb{P}^2$ blown up in three generic points. For the three-loop case, the vanishing locus of denominator of the GKZ integral defines a $K3$ surface and obviously, it defines a Calabi-Yau $(l-1)$-fold for the l-loop case.

Later, we show that the coefficients of the linear combination of the solutions, which leads to the Banana Feynman integral, have geometrical interpretation and can be obtained by the so-called $\widehat{\Gamma}$-class evaluation in the ambient space of the mirror. We explain that in the equal mass case the relevant physical subslices in series of the Calabi-Yau manifolds are complete intersections of two constrains in $(\mathbb{P})^{l+1}$. We calculate the $\widehat{\Gamma}$-class for this case which happens to match perfectly with the coefficients that we obtain numerically.

Contents

Chapter 1

Introduction

In this PhD thesis, the Feynman integrals are evaluated using an algebro-geometric approach known in string theory. This work is mainly based on two papers [1, 2] as a joint work in collaboration with Kilian Bönisch, Fabian Fischbach, Albrecht Klemm and Christoph Nega.

Quantum field theoretic amplitudes are among the most fundamental quantities in physics that are crucial for understanding the fundamental interactions. To calculate these quantities, one needs to evaluate the Feynman integrals. Feynman integrals are multivalued functions of physical parameters that are defined by external momenta and internal masses. With higher energy colliders coming to the operation, for more accurate theoretical predictions of amplitudes, it needs to calculate higher loop orders in the perturbative expansions.

From theoretical point of view, there are different methods compute Feynman integrals. These integrals satisfy a set of differential equations whose solutions give the answer of the integral. There are different approaches to obtain these differential equations. One of them is by integration by part (IBP) identity. By defining a family of Feynman integral, one can find IBP identities between different members of this family. Members of a family of Feynman integral are different Feynman integrals with the same propagator structure but different integer exponents for each propagator. Having IBP identities in a family, one can obtain a basis, so-called *master integrals*, whose linear combinations result in the other members of the family. At the end, one can find a differential equation system which is satisfied by the master integrals and by solving those differential equations one can get the result of the master integrals [3–6]. There are different approaches of deriving a differential equation system for a Feynman integral using the geometric interpretation of them.

From the algebro-geometric point of view, Feynman integrals are the periods of the mixed Hodge structure on the relative cohomology groups. Varying physical parameters leads to a variation of the Hodge structure. The geometric interpretation comes from the polar locus of the integrand. The poles of the integrand define a Calabi-Yau manifold, which is often in a toric variety. These period integrals, which are over *closed cycles*, satisfy a system of linear homogeneous differential equations, so-called *Picard-Fuchs differential ideal* (PFDI). Then, by Griffiths-Dwork reduction method, PFDI can be derived from the cohomology of a smooth projective hyperspace [3, 7]. For the higher loop Feynman integrals, using the Griffiths-Dwork reduction method gets much more complicated. But, there is another approach which also benefits from the geometrical interpretation of Feynman integrals. With *toric geometry*, one

can derive a finite set of differential operators, so-called *GKZ hypergeometric system*.

It was observed already in [8] by Gelfand, Kapranov and Zelevinsky (GKZ) that *practically all integrals that arise in perturbative quantum field theory* have the form of residuum integrals of rational functions defined in a toric variety $\mathbb{P}_\Delta$. We will call these GKZ period integrals. In dimensional regularization, e.g. in $(4-2\epsilon)$ dimensions, the coefficients of the Laurent expansion of the Feynman integral in ϵ, are such period integrals [9]. In this approach, we derive a system of differential equations, GKZ system, from the variation of the Hodge structure and we benefit from the symmetries of the graphs more efficiently. GKZ systems are the generalization of hypergeometric systems that use the symmetries of the integrand, i.e. symmetries in its parameter space [10, 11]. GKZ period integrals with holomorphic forms integrated over closed cycles satisfy homogeneous systems of differential equations. But, there are GKZ integrals that are, unessentially holomorphic forms which are integrated over chains. It means the integration domain has non-trivial boundary and this yields inhomogeneities in the differential equation system. Such integrals are called *relative periods* [12]. In general, Feynman integrals have chains as their integration domains, in other words, the integration domains of the Feynman integrals have boundaries, therefore, they are related to relative periods. But, the *maximal cut* integrals of Feynman integrals are integrals with closed cycles as their integration domain and they satisfy homogeneous GKZ system.

We consider particular Feynman integrals that correspond to a class of l-loop Feynman diagrams in two space-time dimensions with two vertices of valence $l+1$, one invariant momentum K^2 and $l+1$ different masses M^i for each propagator, known as *Banana diagrams*. Banana Feynman integrals with different numbers of loops appear in various perturbation theory calculations. For instance, five-loop banana diagram in the Standard Model represents the spectral function for the process $q \to ql\nu_l gZH$, see Figure 1.0.1 [13]. They arise as master integrals in the two-loop electroweak computations or in the two-loop Higgs+jet production cross section [14, 15].

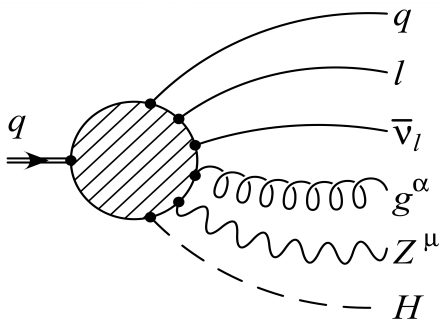

Figure 1.0.1: A half cut of five-loop banana diagram in the Standard Model representing the spectral function for the process $q \to ql\nu_l gZH$ [13].

After representing the banana Feynman integral by Feynman parametrization, in two space-time dimensions, the numerator of the integrand is trivial. The polar locus of the integrand in the l-loop banana Feynman integral defines a Calabi-Yau $(l-1)$-fold hypersurface.

The polynomial that defines the hypersurface corresponds to a Newton polytope, which is a reflexive integral polytope. After triangulating the corresponding Newton polytope, defining the ambient toric variety and obtaining the Mori cone generators, we derived the GKZ systems of differential equation for the banana Feynman integrals and solved them with the Frobenius method. Banana Feynman integrals, like most of the Feynman integrals, are relative periods, i.e. their integration domains have non-trivial boundaries. Therefore, together with solutions to the homogeneous equations, we need special solutions to the inhomogeneous equations.

In mirror symmetry a very important fact is that Calabi-Yau manifolds are expected to have at least one point of maximal unipotent monodromy in their moduli space. For Calabi-Yau hypersurfaces and complete intersections in toric ambient spaces, the location of these points can be calculated purely combinatorial from the triangulations of the toric polyhedron. At such a point the local exponents for the solutions of the Picard-Fuchs differential ideal are completely degenerate. This means that there exists a unique analytic solution, while all the other solutions are logarithmic at this point. There is also a unique solution with the highest power of logarithms which equals the dimension $l-1$. Moreover, the maximal cut integral corresponds to the unique holomorphic period and can be evaluated directly by a residuum integral over a l-dimensional torus in $\mathbb{P}_\Delta$. All logarithmic closed periods can be obtained by the Frobenius method. The solutions of the GKZ system are, however, redundant. It means it has more solutions than the Picard-Fuchs equations and not all of them are the answers of the Feynman integral. And also, we have to consider the inhomogeneous solution which cannot be obtained by the Frobenius method. By deriving the full differential ideal from the solutions, we reduce the number of logarithmic solutions and develop a method which yields to a smaller set of functions describing the l-loop banana Feynman integrals for generic internal masses. These functions are governed by a set of inhomogeneous differential equations. The inhomogeneity is determined at the point of maximal unipotent monodromy by integrating the banana Feynman integral directly after applying full differential ideal on its integrand.

For the two-loop banana Feynman integral, the so-called *sunset* diagram, the polar locus of the integrand is a special family of elliptic curves $\mathcal{E}$, i.e. a Calabi-Yau one-fold. The integral is related to the period integral of the local mirror M of the non-compact Calabi-Yau three-fold W defined as the total space of the anti-canonical line bundle over the degree three del Pezzo surface S, which is $\mathbb{P}^2$ blown up in three generic points. The masses are related in a simple way to the three new Kähler parameters in the blown up geometry. For the three-loop case, the vanishing locus of denominator of the GKZ integral defines a $K3$ surface and obviously, it defines a Calabi-Yau $(l-1)$-fold for the l-loop case.

Further, we showed that the coefficients of the linear combination of the solutions, which leads to the Banana Feynman integral, have geometrical interpretation and can be obtained by the so-called $\widehat{\Gamma}$-class evaluation in the ambient space of the mirror. We explain that in the equal mass case, the relevant physical subslices in series of the Calabi-Yau manifolds are complete intersections of two constraints in $(\mathbb{P})^{l+1}$. We calculate the $\widehat{\Gamma}$-class for this case which happens to match perfectly with the coefficients that we obtain numerically.

The full set of solutions to the Picard-Fuchs differential ideal and many aspects of their monodromies and analytic continuations have been intensively studied using the GKZ system in the context of mirror symmetry for period integrals of the holomorphic $(n,0)$-form for Calabi-Yau n-folds. For compact Calabi-Yau three-folds realized as hypersurfaces embedded

in toric ambient spaces, this was done in [16, 11, 10] for complete intersections embedded in such spaces in [17–19]. Higher dimensional Calabi-Yau spaces have been studied in [20–24]. A review of the subject can be found in [25].

To summarize, we clarify and extend the geometrical interpretation of the l-loop banana Feynman graphs. The new insights give important information about the analytic structure of the banana Feynman graphs.

Chapter 2

Algebraic geometry and toric geometry

2.1 Periods

Feynman integrals are interesting both for physicists and mathematicians. In this section, an overview on the concept of periods in mathematics is provided and then the approaches to obtain them are introduced.
As Zagier and Kontsevich explain in [26], first, we need to define algebraic numbers. ***Algebraic numbers*** are the set of all numbers $x \in \mathbb{C}$ that satisfy an algebraic equation with rational coefficients. $\sqrt{2}$ is the simplest irrational real algebraic number. All the numbers, that are not included in the algebraic numbers set, are ***transcendental***.
A complex number is called a ***period*** if its real and imaginary parts are values of absolutely convergent integrals of rational functions with rational coefficients . Periods are in general transcendental numbers. One of the most famous non-algebraic example of a period is π, with,

$$\pi = \iint_{x^2+y^2\leq 1} dx\ dy. \tag{2.1.1}$$

Logarithms of natural numbers, all values of Riemann zeta function and special values at algebraic arguments of *hypergeometric functions* are other examples of periods.

On the other hand, one can define periods as the values of integrals of algebraically defined differential forms over certain chains in algebraic varieties. In case these integrals depend on some parameters, i.e. the forms and the chains are functions of the parameters, one can expect the integrals satisfy linear differential equations with algebraic coefficients. Now that we are equipped with another approach to obtain periods, we have to find the linear differential equations which those integrals satisfy and solve them for the special values. These differential equations are called (generalized) *Picard-Fuchs differential equations* or *Gauss-Manin systems*. To obtain Picard-Fuchs equations, there are few approaches. GKZ and Griffiths-Dwork reduction are two of them. In this thesis, we have used mostly the GKZ method and provide three examples where we explain completely the GKZ method. Here, we only explain a bit the Griffiths-Dwork reduction method and postpone explaining the GKZ method to section 4.1.3.

2.2 Griffiths-Dwork reduction

As mentioned before Griffiths-Dwork reduction is an alternative method to derive a differential equation for a period in terms of its moduli. For a detailed explanation about Griffiths-Dwork reduction refer to [27].

First, let's define the mathematical concept of a period $\Pi_i(a)$,

$$\Pi_i(a) = \int_{\Gamma_i} \Omega(a), \tag{2.2.1}$$

where $\Gamma_i \in H_n(M)$ is a n-cycle and the nowhere vanishing $(n,0)$-form is given by,

$$\Omega(a) = \int_{\gamma} \frac{a_0 \mu}{P}, \tag{2.2.2}$$

here P is the Laurent polynomial, a_i is i-th monomial coefficient, a_0 the coefficient of monomial with degree 0 and μ is the top form. $P = 0$ is the hypersurface constraint with γ being the contour around it.

Let us consider the hypersurface case and define the graded ring by the Jacobian ideal $J = \{\partial_{x_i} P\}$ which is generated by partial derivatives of the weighted homogeneous polynomial $P(x)$ of degree $d = \sum_i w_i$. Now, we take derivatives of the period $\Pi(a)$ w.r.t. the complex structure moduli parameterized by the coefficients a's, until the numerator contains elements that are reducible w.r.t. to the ideal J. One has to first emerge expressions in the numerator using the Buchbinders algorithm for a Groeber basis, and then use integration by parts. This leads to the emerging expressions with lower powers of P in the denominator and lower homogeneous degree polynomials in x in the numerators. Finally, one can manipulate all the emergent terms into the form of moduli dependent rational functions times lower derivatives of $\Pi(z)$ w.r.t. to the moduli a. The relation derived in this way is one Picard-Fuchs operator. Let us clear this with an example.
Smooth quintic hypersurfaces in $\mathbb{P}$ are simple examples to show how Griffiths-Dwork reduction works. A quintic hypersurface in $\mathbb{P}$, which is a Calabi-Yau 3-fold, is define by the following polynomial constraint,

$$P = \sum_{i=1}^{5} \frac{1}{5} x_i^5 - a \prod_{i=1}^{5} x_i, \tag{2.2.3}$$

with x_i being homogeneous coordinates and a the moduli parameter. We take the derivative four times w.r.t. the moduli parameters from $\dfrac{\Pi(a)}{a} = \tilde{\Pi}(a) = \int_\gamma \dfrac{\mu}{P}$ and get:

$$\frac{\partial^4}{\partial a^4}\tilde{\Pi}(a) = \int_\gamma \frac{4! \prod_{i=1}^{5} x_i^4 \, \mu}{P^5} = \frac{4!(a^4 x_1^4 (x_2x_3x_4x_5)^3 \partial_{x_1} P + a^3 x_1^7 x_2^3 (x_3x_4x_5)^2 \partial_{x_2} P + a^2 (x_1x_2)^6 x_3^2 x_4 x_5 \partial_{x_3} P + a(x_1x_2x_3)^5 x_4 \partial_{x_4} P + (x_1x_2x_3x_4)^4 \partial_{x_5} P)}{(1-a^5)P^5}. \tag{2.2.4}$$

Now we have to obtain the third, second and first order derivative of the period in the ideal of $[\partial_{x_i} P]$. For this aim, repeatedly one needs to use the integration by part identities and represent the result by the derivatives of P w.r.t. a_i's. This leads to,

$$(a^5 - 1)\frac{\partial^4}{\partial a^4}\tilde{\Pi}(a) + 10a^4 \frac{\partial^3}{\partial a^3}\tilde{\Pi}(a) + 25a^3 \frac{\partial^2}{\partial a^2}\tilde{\Pi}(a) + 15a^2 \frac{\partial}{\partial a}\tilde{\Pi}(a) + a\tilde{\Pi}(a) = 0 \tag{2.2.5}$$

or by introducing the logarithmic derivative $a\partial_a = \theta$ it looks like,

$$[a^5\theta^4 - a\prod_{i=1}^{5}(\theta + \frac{i}{5})]\tilde{\Pi}(a) = 0. \tag{2.2.6}$$

The detailed derivation of the Picard-Fuchs equation for a quintic hypersurface is shown in the Appendix.

2.3 Toric geometry

In this section, we will provide a brief introduction to toric geometry and algebraic geometry. Later we will show how to define a polytope associated to a toric geometry. For more details about the toric geometry, we refer to *lectures on toric varieties* by David A. Cox.
To warming up, let us first introduce affine varieties. For given polynomials $f_1, \cdots, f_r \in \mathbb{C}[x_1, \cdots, x_n]$, ***affine varieties*** are defined as,

$$V(f_1, \cdots, f_r) = \{a \in \mathbb{C}^n | f_1(a) = \cdots = f_r(a) = 0\}. \tag{2.3.1}$$

We define projective varieties, but one needs to know what are projective spaces, first.
A n-dimensional ***projective space*** $\mathbb{P}$ is defined with the following relation,

$$\mathbb{P}^n = (\mathbb{C}^{n+1} \setminus \{0\})/\mathbb{C}^*, \tag{2.3.2}$$

where by applying the group $\mathbb{C}^*$, we create equivalence. It can be shown like following as well,

$$\mathbb{P}^n = (\mathbb{C}^{n+1} \setminus \{0\})/\sim, \tag{2.3.3}$$

where $\sim$ shows equivalence relation which means $(x_1, \cdots, x_{n+1}) \sim (y_1, \cdots, y_{n+1})$ iff there is a non-zero coefficient $\lambda \in \mathbb{C}^*$ which $(x_1, \cdots, x_{n+1}) = \lambda(y_1, \cdots, y_{n+1})$. This means that all points on a line through the origin in $\mathbb{C}^{n+1}$ are equivalent, or in the other word, $\mathbb{P}^{n+1}$ is the space of all lines which pass through the origin in $\mathbb{C}^{n+1}$. The coordinate of a point p in a projective space is given by *homogeneous coordinates*, $p = (x_1, \cdots, x_{n+1}) \equiv (x_1 : \cdots : x_{n+1})$.
Now we can define projective varieties. We know that if a polynomial $f \in \mathbb{C}[x_1, \cdots, x_{n+1}]$ is called *homogeneous of degree* d it means that all monomials this polynomial has total degree of d, or,

$$f(\lambda x_1, \cdots, \lambda x_{n+1}) = \lambda^d f(x_1, \cdots, x_{n+1}), \quad \lambda \in \mathbb{C}^*. \tag{2.3.4}$$

Then, given homogeneous polynomials $f_1, \cdots, f_r \in \mathbb{C}[x_1, \cdots, x^{n+1}]$, we can define the ***projective variety*** by,

$$V(f_1, \cdots, f_r) = \{a \in \mathbb{P}^n | f_1(a) = \cdots = f_r(a) = 0\} \subset \mathbb{P}^n. \tag{2.3.5}$$

It is also useful to introduce ***weighted projective space***. Given positive integers $d_1, \cdots, d_{n+1}$ which each two of them are relatively prime, $gcd(d_1, \cdots, d_{n+1}) = 1$, the weighted projective space is defined as,

$$\mathbb{P}(d_1, \cdots, d_{n+1}) = (\mathbb{C}^{n+1} \setminus \{0\})/\sim, \tag{2.3.6}$$

and $\sim$ means $(x_1, \cdots, x_{n+1}) \sim (y_1, \cdots, y_{n+1}) \Leftrightarrow \exists \lambda \in \mathbb{C}^*$ such that $(x_1, \cdots, x_{n+1}) = (\lambda^{d_1} y_1, \cdots, \lambda^{d_{n+1}} y_{n+1})$. This implies $\mathbb{P}(1, \cdots, 1) = \mathbb{P}^n$.
A ***toric variety*** $\mathbb{P}$, is a generalization of projective space. For an ambient space $\mathbb{C}^n$ we act an algebraic torus $(\mathbb{C}^*)^m$ for $m < n$ and instead of excluding the origin for defining projective space, we exclude a subset U which is fixed by a continuous subgroup of $(\mathbb{C}^*)^m$. It yields to,

$$\mathbb{P} = (\mathbb{C}^n \setminus U)/(\mathbb{C}^*)^n. \tag{2.3.7}$$

2.4 Mirror symmetry and Batyrev construction

Around mid-1980s a great discovery happened in the theoretical physics and algebraic geometry. It was triggered by an observation that string theory propagation on a target spaces of a circle of radius R and $1/R$ are equivalent [28, 29]. This is a modular group, the so-called T-duality. In the meanwhile, it has been also found out that Calabi-Yau manifolds are very appropriate candidates for expressing the geometry of string propagation [30]. Later Vafa, Lerche and Warner have been noticed that a topologically distinct pair of Calabi-Yau manifolds yield the same string propagation theory and they discovered the ***Mirror Symmetry*** between that two Calabi-Yau manifold [31]. *A mirror pair of Calabi-Yau manifold* have the following relation between their Hodge numbers,

$$h^{q,p}_{\mathscr{M}} = h^{d-p,q}_{\mathscr{W}}, \tag{2.4.1}$$

where d is the complex dimension of the Calabi-Yau manifolds $\mathscr{M}$ and $\mathscr{W}$. We gave a brief story of one of the most beautiful discoveries in the theoretical physics and mathematics, we refer the interested reader to [32, 33] for more details.
In 1993, Batyrev introduced an algebro-geometric approach to mirror symmetry [34]. He constructed mirror pair of hypersurfaces in toric ambient spaces by *reflexive polyhedra*. A year after, Batyrev and Borisov generalized it to complete intersections in Fano toric varieties by reflexive polyhedra with Neff partitions [35]. The main idea is that they found a correspondence between a toric variety and a polytope and relate the mirror pair of the toric Calabi-Yau manifold to the dual of that polytope.
For understanding the Batyrev construction of mirror symmetry we have to get familiar with few notions. First we start with the definition of a lattice polytope.
Consider $N \simeq \mathbb{Z}^n$ be a lattice whose dual is M, then a ***lattice polytope*** $\Delta \subset M_{\mathbb{R}} = M \otimes \mathbb{R}$ is the convex hull of a finite set of points in M. A *facet* of a polytope is codimension 1 face of a polytope and obviously the *vertices* of a polytope are dimension 0 faces. The ***dual polytope*** of a polytope is defined by,

$$\hat{\Delta} = \{v \in N_{\mathbb{R}} | \langle v, m\rangle \geq -1, \text{ for all } m \in \Delta\} \subset N_{\mathbb{R}}. \tag{2.4.2}$$

It follows $\hat{\hat{\Delta}} = \Delta$. A ***reflexive polytope*** Δ is a lattice polytope with origin in its interior and whose dual $\hat{\Delta}$ is also a lattice polytope. One can derive from Eq. (2.4.2) the relation between the faces of the dual pairs of polytope. Each n-dimensional face of polytope Δ corresponds to a $(d-n-1)$-dimensional face of $\hat{\Delta}$. Now let's get familiar with concept of cones and fans.
Consider $M \simeq \mathbb{Z}^n$ to be a free Abelian group of rank n and $N = Hom(M, \mathbb{Z})$ is its dual, i.e. $\langle m, v\rangle \in \mathbb{Z}$, for $m \in M$ and $v \in N$. Then, a ***rational polyhedral cone*** $\sigma \subset N_{\mathbb{R}}$ is a subset which defined by,

$$\sigma = \{\sum_{i=1}^{r} \lambda_i u_i \mid \lambda_i \geq 0\}, \tag{2.4.3}$$

for $u_1, \ldots, u_r \in N$. And the dual cone is given by,

$$\check{\sigma} = \{m \in M_{\mathbb{R}} \mid \langle m, v\rangle \geq 0, \ \forall v \in \sigma\}. \tag{2.4.4}$$

A cone is *strongly convex* if $\sigma \cap (-\sigma) = \{0\}$. A *face* of a cone σ is,

$$\tau = \{\ v \in \sigma |\ \langle m, v\rangle = 0\} \subset \sigma. \tag{2.4.5}$$

Obviously, every face of a cone σ is a rational polyhedral cone as well. The intersection of two faces of a cone is again a face of that cone. As in the case of polytopes, a *facet* of a convex polyhedral is a face of codimension 1. Faces of a cone range from $(\dim\sigma - 1)$-dimensional to 0-dimensional. This means a face of a face of a cone is again a face of that cone. Trivially, $\{0\}$ is a face of a cone. A *ray* is a 1-dimensional face of a cone.
We define a ***fan*** Σ as a finite collection of cones in $N_{\mathbb{R}}$ which has following properties:

- Each cone $\sigma \in \Sigma$ is a strongly convex polyhedral cone.
- If $\sigma \in \Sigma$ and τ is a face of the cone σ, then $\tau \in \Sigma$
- If $\sigma, \tau \in \Sigma$, then $\sigma \cap \tau$ is a face of each.

Consider a fan $\Sigma \in N_{\mathbb{R}}$, with $\Sigma(1)$ be the set of one-dimensional cones or rays of Σ. For each $\rho \in \Sigma(1)$ we denote $v_\rho \in N$ as the the unique *primitive generator* of $\rho \cap N$. we associate a coordinate x_ρ to each ray $\rho \in \Sigma(1)$. Now, if $\mathcal{S}$ be any subset of $\Sigma(1)$ which does **not** span a cone of Σ, then $V(\mathcal{S}) \subset \mathbb{C}^n$ is the linear subspace defined by setting $x^\rho = 0$ for all $\rho \in \mathcal{S}$. If $Z(\Sigma) \subset \mathbb{C}^n$ be the union of all $V(\mathcal{S})$, the toric variety is constructed as a quotient of $\mathbb{C}^n - Z(\Sigma)$ by a group G, which defined as follows [32].
Let's consider the map $\phi : \mathrm{Hom}(\Sigma(1), \mathbb{C}^*) \to \mathrm{Hom}(M, \mathbb{C}^*)$. Where $\mathrm{Hom}(\Sigma(1), \mathbb{C}^*)$ is a map of sets $f : \Sigma \to \mathbb{C}^*$ and $\mathrm{Hom}(M, \mathbb{C}^*)$ is a map of groups $m \mapsto \prod_{v\in\Sigma(1)} f(v)^{\langle m,v\rangle}$. We can represent this map ϕ as,

$$\phi : (\mathbb{C}^*)^n \to (\mathbb{C}^*)^r, \quad (t_1, \ldots, t_n) \mapsto (\prod_{j=1}^{n} t_j^{v_{j1}}, \ldots, \prod_{j=1}^{n} t_j^{v_{jr}}), \tag{2.4.6}$$

$(v_{j1}, \ldots, v_{jr})$ is coordinates of v_j and $n = |\Sigma(1)|$. Now we can define the group G as the kernel of ϕ:

$$G = \mathrm{Ker}(\mathrm{Hom}(\Sigma(1), \mathbb{C}^*) \xrightarrow{\phi} \mathrm{Hom}(M, \mathbb{C}^*)). \tag{2.4.7}$$

This means $G \subset \mathrm{Hom}(\Sigma(1), \mathbb{C}^*)$, therefore $g(v_\rho) \in \mathbb{C}^*$ for each $g \in G$ and $\rho \in \Sigma(1)$. An action of G on $\mathbb{C}^n$ looks like,

$$g \cdot (x_1, \ldots, x_n) = (g(v_1)x_1, \ldots, g(v_n)x_n). \tag{2.4.8}$$

Finally, a toric variety X_Σ is defined as,

$$X_\Sigma = (\mathbb{C}^n - Z(\Sigma))/G. \tag{2.4.9}$$

A toric variety X_Σ is compact if and only if the union of the cones $\sigma \in \Sigma$ is equal to all of $N_{\mathbb{R}}$ and an incomplete fan defines a non-compact toric variety.
Let us clear the steps of deriving a toric variety from a fan by an example. Consider the fan shown by Figure 2.4.1.
The three rays $\{(1, 0), (0, 1), (-1, -1)\}$ span this fan Σ. The cones of this fan are given by,

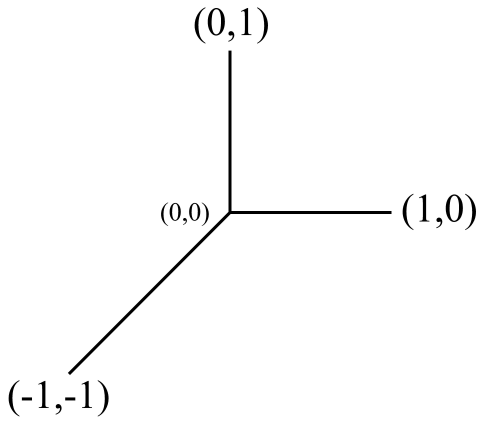

Figure 2.4.1: The corresponding fan of $\mathbb{P}^2$

- $\{0\}$ as the trivial 0-dimensional cone,
- the three 1-dimensional cones spanned by the vectors $\{(1,0)\}$, $\{(0,1)\}$ and $\{(-1,-1)\}$,
- the three 2-dimensional cones spanned by $\{(1,0),(0,1)\}$, $\{(1,0),(-1,-1)\}$ and $\{(0,1),(-1,-1)\}$.

For the next step, we need to find $Z(\mathcal{S})$. $\mathcal{S} = \{(1,0),(0,1),(-1,-1)\}$ is the only set of rays that does not span a cone in the fan Σ. This means we have $Z(\mathcal{S}) = \{(0,0,0)\} \subset \mathbb{C}^3$.
For the next step we need the kernel of the following map,

$$\phi : \quad (\mathbb{C}^*)^3 \to (\mathbb{C}^*)^2, \qquad (t_1,t_2,t_3) \mapsto (t_1^{-1}t_2, t_1^{-1}t_3). \tag{2.4.10}$$

The kernel of the this map is the diagonal group $G = \{(t,t,t)|t \in \mathbb{C}^*\} \simeq \mathbb{C}^*$. Now we can obtain the toric geometry by,

$$(\mathbb{C}^3 - \{(0,0,0)\})/\mathbb{C}^*, \tag{2.4.11}$$

which is the definition of $\mathbb{P}^2$.

Chapter 3

Different approaches to solve Feynman integrals

3.1 Introduction

To evaluate Feynman integrals, there are different approaches. It mostly depends on the type of considered integral. From the mathematical point of view, if we can find an algebro-geometric interpretation for the integrand, we can benefit from the methods explained in the previous chapter. There are some Feynman integrals, e.g. banana Feynman integrals, whose polar loci define hypersurfaces, hence using methods known in algebraic geometry one can obtain the corresponding periods. As mentioned before, these periods satisfy a system of differential equations and their solutions give the result of the integral. Griffiths-Dwork reduction is one the methods to derive the system of differential equations which was explained in the previous chapter with an example. GKZ is another method to get the system of differential equations and will be explained in the next chapter.

In this chapter, we focus on the other methods to obtain the result of the Feynman integrals. There are relations between the members of the so-called *Feynman integrals family*. By finding those relations, which are linear identities, one can derive basis integrals by which one can calculate the other integrals of the family. The basis are called *Master Integrals*. In the following sections we will explain what exactly are the relations between different integrals of a family and how to obtain them.

3.2 Integral families and basis

In 1981, Chetyrkin and Tkachov in [5] proposed a technique which could compute some of the Feynman integrals in a much easier way. By applying *integration by parts* (IBP) on a Feynman integral, they found an identity by which one can reduce the original integral to few simpler ones, the so-called ***Master Integrals*** (MIs). By evaluating MIs one can get the result of the original Feynman integrals. Nowadays, there are some computer programs which can calculate the IBP reductions and give the MIs, such as `FIRE`, `LiteRed`, `REDUZE`, `AIR`, `KIRA` [36–38].
In the following, we will show that MIs form a basis in the linear space of a ***family of Feynman integrals*** [39,40]. A family of Feynman integrals is the one where each Feynman integral has the same propagator structure, but each of them has propagators with arbitrary integer powers. Now, we will review the steps of obtaining the MIs with the one loop box Feynman integral as an example [40].

The one-loop box integral in D-dimension, depicted in Fig. 3.2.1, is given by,

$$I_{box} = \int \frac{d^D k}{i\pi^{D/2}} \frac{1}{k^2(k+p_1)^2(k+p_1+p_2)^2(k-p_4)^2}, \tag{3.2.1}$$

with k the loop momentum and p_i the external momentum that satisfy the momentum conservation $\sum_{i=1}^{4} p_i = 0$ and the on-shell conditions $p_i^2 = 0$. By applying a change of variables and using the so-called *dual coordinates*, which is often employed in planar integrals like box integral, the previous integral is transformed to,

$$I_{box} = \int \frac{d^D y}{i\pi^{D/2}} \frac{1}{(y-y_1)^2(y-y_2)^2(y-y_3)^2(y-y_4)^2}. \tag{3.2.2}$$

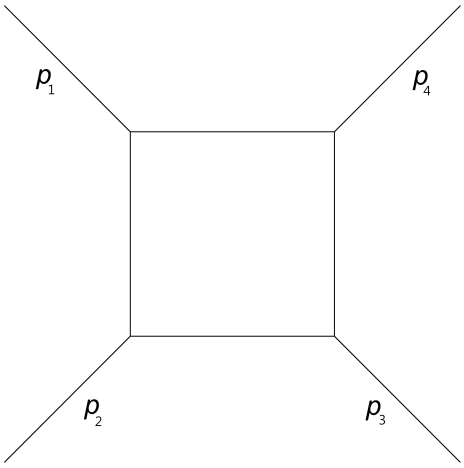

Figure 3.2.1: One-loop box integral

Now we want to derive the integral family of the one loop box integral. For this goal, we need to generalize this integral by assigning a general integer power to each propagator,

$$I_{a_1,a_2,a_3,a_4} = \int \frac{d^D y}{i\pi^{D/2}} \prod_{i=1}^{4} \frac{1}{[(y-y_i)^2]^{a_i}}. \tag{3.2.3}$$

The on-shell condition still holds, $(y_1-y_2)^2 = (y_2-y_3)^2 = (y_3-y_4)^2 = (y_4-y_1)^2 = 0$.
This integral is associated to the box Feynman graph with propagators up to a general powers if $a_i > 0$ for all i. By omitting one of the propagators, or in other words, annihilating one of the powers, i.e. $a_i = 0$ for the i^{th}-power, it yields a triangle integral and for $a_i < 0$ we have factors in the numerator. I_{a_1,a_2,a_3,a_4} with different integer value of a_i, as the arbitrary power of propagators, defines the integral family of the box diagram.
In principal, the integrals which are members of a family are not independent and one can find some relations between the members of this family. By *integration by part* (IBP) technique one can find linear relations which can relate different integrals of the family. In the following we will show how one can derive these relations.
One derives identities by knowing that total derivatives vanish in dimensional regularization, it means,

$$\int \frac{d^D y}{i\pi^{D/2}} \frac{\partial}{\partial y^\mu} \xi^\mu \prod_{i=1}^{4} \frac{1}{[(y-y_i)^2]^{a_i}} = 0, \tag{3.2.4}$$

where ξ can be $\xi = y - y_1$, as an example and it is a given vector. If we apply the differential operator on the rest of the integrand and expand the terms, we can obtain the linear relation between different integrals of the family, which have different powers $a_1, ..., a_4$. To show these relations in a more clear way, Henn in [40] introduced $Y_i^{\pm}$ operators as follows,

$$Y_1^{\pm} I_{a_1,a_2,a_3,a_4} = I_{a_1 \pm 1,a_2,a_3,a_4}, \tag{3.2.5}$$

and it operates in the same way for other integer values of $i \in \{1, \ldots, 4\}$ in Y_i. The operator $Y_i^{\pm}$ does not have a deep mathematical meaning, it has been introduced just to simplify showing the relations between different integrals with different powers. Then the IBP relations looks like,

$$[(D-2a_1-a_2-a_3-a_4)-(y_1-y_3)^2 a_3 Y_3^+ + (-a_2 Y_2^+ - a_3 Y_3^+ - a_4 Y_4^+) Y_1^-] I_{a_1,a_2,a_3,a_4} = 0. \quad (3.2.6)$$

For getting the basis, i.e. Master integrals, one has to continue applying this relation to reach integrals with minimum possible value of $a = \sum a_i$, where some of a_i's are possibly zero. For the box integral case there are three Master Integrals. They can be chosen to be the s- and t-channel[1] bubble integrals and the box integral itself, $I_{0,1,0,1}, I_{1,0,1,0}$ and $I_{1,1,1,1}$, respectively. As examples we have,

$$I_{2,1,1,1} = \frac{D-5}{s}\, I_{1,1,1,1} - \frac{4(D-5)(D-3)}{(D-6)st^2}\, I_{0,1,0,1} \quad (3.2.7)$$

$$I_{1,1,0,1} = \frac{2(D-3)}{(D-4)t}\, I_{0,1,0,1} \quad (3.2.8)$$

or schematically it can be shown like,

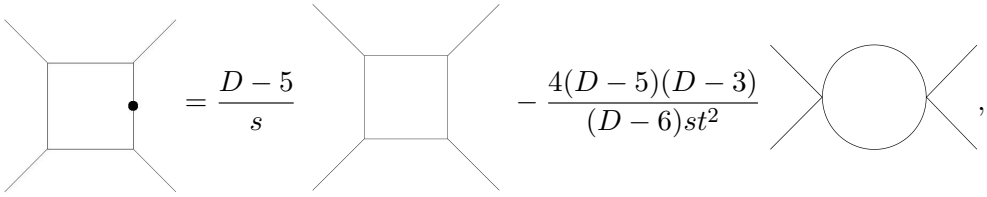

$$= \frac{D-5}{s} - \frac{4(D-5)(D-3)}{(D-6)st^2}, \quad (3.2.9)$$

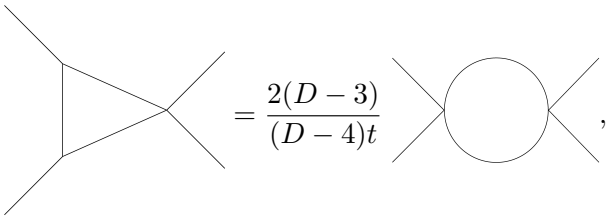

$$= \frac{2(D-3)}{(D-4)t}, \quad (3.2.10)$$

where dot shows a doubled propagator (a squared propagator).
Mainly if we can find IBP relations for a family integrals, it means that the master integrals are finite. Here, we showed a box integral as an example, but this approach for finding the basis of a family can be applied for other general cases, too.

3.2.1 Differential equations

So far we have shown that there is a finite-dimensional basis for a given family of Feynman integrals. By computing the basis, one can get the result of other members of the family by linear combinations of the basis. It means one just need to know the result of the Master Integrals. As it has been already outlined, one can calculate an integral by solving the differential

[1] In the dual coordinations it is $s = (y_1 - y_3)^2, t = (y_2 - y_4)^2$.

equations it satisfies. A family of Feynman integral is closed under the differentiating w.r.t the external momenta, therefore, one can represent the result of the differentiation by a linear combination of basis integrals.
In the case of family of one-loop box Feynman integrals, the kinematic variables are s and t and with the change of variables was done, they depend to vectors y_i only. We note that the differential operators, here ∂_s and ∂_t, have to commute with the on-shell and momentum conservation constraints. By applying some algebraic manipulations similar to the IBP process, one can see that the result of the differentiation on a member of the family have to be a linear combination of the basis $\vec{f}$, it means it looks like,

$$\partial_s \vec{f}(s,t;\epsilon) = A_s(s,t,\epsilon)\vec{f}(s,t;\epsilon) \tag{3.2.11}$$

$$\partial_t \vec{f}(s,t;\epsilon) = A_t(s,t,\epsilon)\vec{f}(s,t;\epsilon), \tag{3.2.12}$$

A_s and A_t are $N \times N$ rational function-valued matrices with N being the number of basis and $D = 4 - 2\epsilon$. For the one-loop box family integral, we have already mentioned the three basis integrals and we have,

$$A_s = \begin{pmatrix} 0 & 0 & 0 \\ 0 & -\epsilon/s & 0 \\ \frac{-2(1-2\epsilon)}{st(s+t)} & \frac{2(1-2\epsilon)}{s^2(s+t)} & \frac{-s+t+\epsilon t}{s(s+t)} \end{pmatrix}$$

$$A_t = \begin{pmatrix} -\epsilon/t & 0 & 0 \\ 0 & 0 & 0 \\ \frac{-2(1-2\epsilon)}{t^2(s+t)} & \frac{-2(1-2\epsilon)}{st(s+t)} & -\frac{s+t+\epsilon s}{t(s+t)} \end{pmatrix}.$$

3.2.2 Banana integrals as master integrals

Since this thesis is mostly about the banana Feynman integrals and how to evaluate them, in this subsection their importance as master integrals for other Feynman integrals is discussed.
One-loop case First we want to show the bubble integral which appears as inhomogeneous part of differential equation for the one-loop four-point function [41].
Fig.3.2.1 shows a one-loop four point function, the so-called box integral, with p_i as the external momenta. By taking logarithmic derivatives with respect to the external momenta we have,

$p_1^\mu \frac{\partial}{\partial_{p_1^\mu}}$ 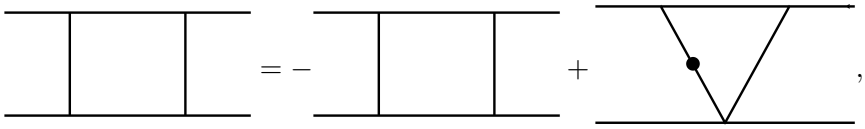 , (3.2.13)

where the right Feynman graph at the right hand side has a doubled propagator (a squared propagator) and a propagator has been canceled. Using IBP relations it yields,

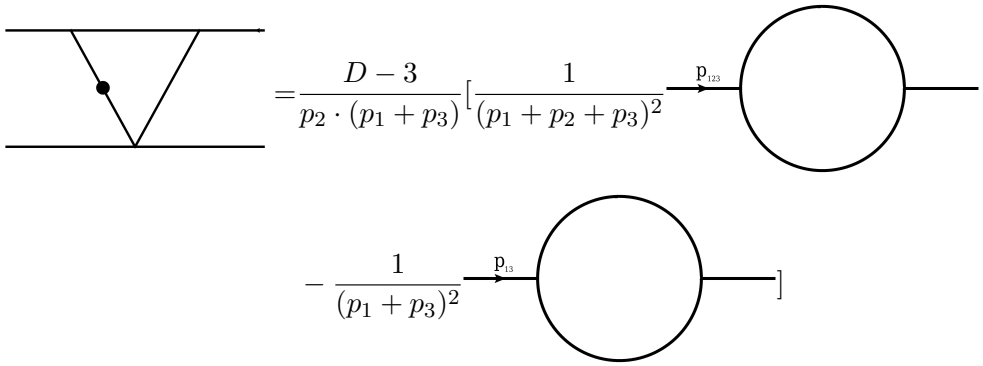

(3.2.14)

where $p_{ijk} \equiv p_1 + p_2 + p_3$. Upon inserting relation 3.2.14 in relation 3.2.13, one obtains an inhomogeneous first order differential equation. The bubble integral is not reducible to simpler subtopologies, therefore by knowing the result of bubble integral, it is possible to solve equation 3.2.13 and get the result of the one-loop box integral. In [41], one can find much more relations between the integrals of one-loop box Feynman integral.

Two-Loop case There are also interesting examples of sunset integral as master integrals for two-loop four-point functions in [41], like,

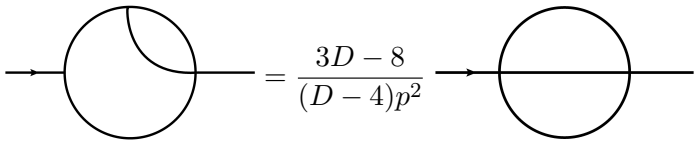

(3.2.15)

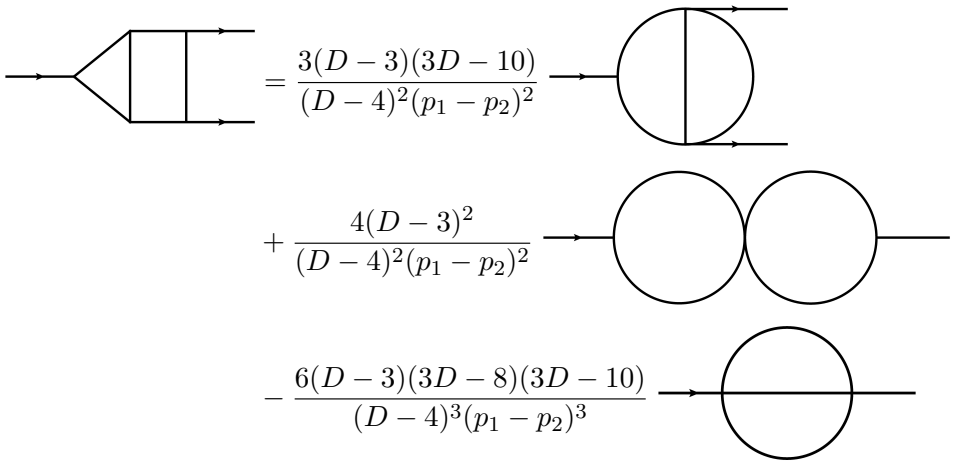

(3.2.16)

Three-Loop case Finally we want to show an example where three-loop banana integrals appears as the master integral for more complicated Feynman integrals. For this, we have to introduce the triangle with two massive loops shown in Fig. 3.2.2.

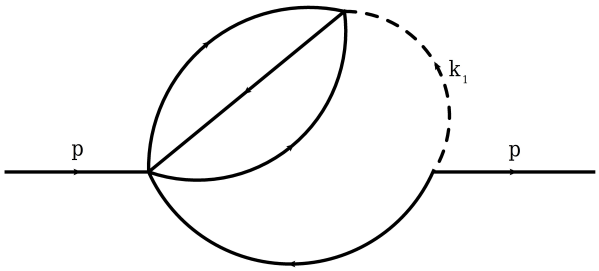

Figure 3.2.2: Triangle with two massive loops. Dashed lines present massless propagators.

The Family of this Feynman integral is given by [42]:

$$I(a_1,\ldots,a_5) = \frac{e^{3\epsilon\gamma}}{(i\pi^{D/2})^3}\int \frac{d^Dk^1 d^Dk^2 d^Dk^3}{(1-k_3^2)^{a_1}(1-(k_2+k_3)^2)^{a_2}(1-(k_1+k_2)^2)^{a_3}(1-(k_1+p)^2)^{a_4}(-k_1^2)^{a_5}} \tag{3.2.17}$$

and $D = 4-2\epsilon$. As mentioned before, by the help of IBP relations one can get seven master integrals for the family associated to the triangle with two massive loops,

$$\begin{aligned} &I(0,2,2,2,0),\ I(0,2,2,2,1),\ I(1,1,1,0,1),\ I(1,1,1,1),\\ &\qquad I(2,1,1,1),\ I(2,1,2,1),\ I(2,2,1,1,1). \end{aligned} \tag{3.2.18}$$

Here $I(1,1,1,1)$ is three-loop banana integral and $I(2,1,1,1)$ and $I(2,1,2,1)$ are three-loop banana integral with one and two squared propagators, respectively. Figure 3.2.3 shows these diagrams.

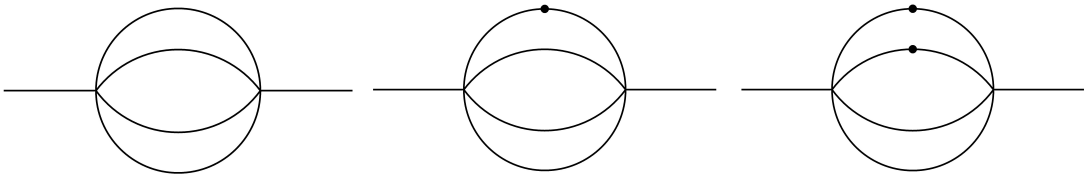

Figure 3.2.3: From left to right, $I(1,1,1,1)$, three-loop banana integral and $I(2,1,1,1)$ and $I(2,1,2,1)$ three-loop banana integral with one and two squared propagators, respectively.

Chapter 4

Banana Feynman integrals

4.1 l-loop banana diagram in the toric approach

The l-loop banana diagrams have a geometric interpretation that lets us to use toric geometry to evaluate them. This geometric interpretation originates from the graph polynomial representation of a Feynman diagram which is obtained after Feynman parametrization and evaluation of many Gaussian integrals[1]. First, we will show how to get to the Feynman parametrization. Later, we will show that for the banana type diagrams in two space-time dimensions, the exponent of the first *Symanzik polynomial* vanishes and the exponent of the *second Symanzik polynomial* is one. This simplifies the form of these integrals and offers an algebro-geometric approach, known in string theory, to evaluate them. The denominator of the integrand as a Newton polynomial defines a Calabi-Yau hypersurface. The corresponding banana diagram is viewed as a relative period of this Calabi-Yau hypersurface. Employing the GKZ system of differential equations, we can construct a basis of periods on the Calabi-Yau variety at the maximal unipotent monodromy point. Extending the GKZ system to inhomogeneous differential operators we can write down a complete set of functions parametrizing the full banana amplitude.

4.1.1 Feynman parametrization

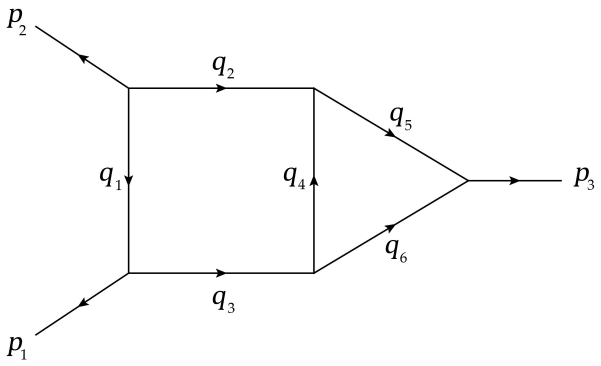

Figure 4.1.1: A two loop Feynman diagram

In this subsection we introduce Feynman parametrization which helps us to present Feynman integrals in a simpler form which is more suitable to extract the algebro-geometric interpretation.
Figure 4.1.1 shows a two loop graph with three external momenta and six internal momenta. All three external momenta are given to be outwards, therefore we have,

$$p_1 + p_2 + p_3 = 0. \tag{4.1.1}$$

In l-loop Feynman graphs, from n internal momenta only l number of them, the so-called loop momenta, are independent[2] and the other $(n-l)$ ones are fixed by the external and loop

[1] For a review of the graph theoretical representation of Feynman diagrams we refer to [4].
[2] l is the first Betti number of the graph, as well.

momenta. If k_i's are loop momenta, then the internal momenta q_i's, in our example, are given by,

$$q_1 = k_1, \qquad q_2 = p_2 + k_1, \qquad q_3 = p_1 - k_1 \tag{4.1.2}$$
$$q_5 = k_2, \qquad q_4 = p_1 + p_3 - k_1 - k_2, \qquad q_6 = p_3 - k_2. \tag{4.1.3}$$

Each internal momentum in general can be presented by a linear combination of the external momenta p_i's and the loop momenta k_i's [4],

$$q_i = \sum_{j=1}^{l} \alpha_{ij} k_j + \sum_{j=1}^{m} \beta_{ij} p_j, \qquad \alpha_{ij}, \beta_{ij} \in \{-1, 0, 1\}. \tag{4.1.4}$$

Now, let's start with the process of Feynman parametrization. We already know that a scalar Feynman l-loop integral in D dimensions with n propagators is given by [43, 44]:

$$I = (\mu^2)^{\nu - lD/2} \int \prod_{r=1}^{l} \frac{d^D k_r}{i\pi^{\frac{D}{2}}} \prod_{j=1}^{n} \frac{1}{(-q_j^2 + m_j^2)^{\nu_j}} \tag{4.1.5}$$

where μ is an arbitrary mass scale and q_j are linear combinations of the external and l loop momenta with an arbitrary power of ν_j. Also, k_r's are loop momenta. For applying the Feynman parametrization formula, we use an integral representation of the free scalar propagator as follows,

$$\frac{i}{q^2 - m^2} = \int_0^\infty d\alpha \; e^{i\alpha(q^2 - m^2)} \tag{4.1.6}$$

or for our case we have,

$$\prod_{j=1}^{n} \frac{1}{(-q_j^2 + m_j^2)^{\nu_j}} = \frac{\Gamma(\nu)}{\prod_{j=1}^{n} \Gamma(\nu_j)} \int_{x_j \geq 0} d^n x \delta(1 - \sum_{j=1}^{n} x_j) \frac{\prod_{j=1}^{n} x_j^{\nu_j - 1}}{(\sum_{j=1}^{n} x_j(-q_j^2 + m_j^2))^{\nu}} \tag{4.1.7}$$

for $\nu = \sum_{j=1}^{n} \nu_j$. Also there is the following identity,

$$\frac{1}{l_1 l_2} = \int_0^1 dx \; \frac{1}{(x l_1 + (1-x) l_2)^2}. \tag{4.1.8}$$

Then, we insert them into (4.1.5) and by the help of translational invariance of the loop integral, the Feynman integral looks like:

$$I = \frac{\Gamma(\nu - lD/2)}{\prod_{j=1}^{n} \Gamma(\nu_j)} \int_0^\infty \left(\prod_{j=1}^{n} dx_j x_j^{\nu_j - 1} \right) \delta(1 - \sum_{i=1}^{n} x_i) \frac{\mathcal{U}^{\nu - (l+1)D/2}}{\mathcal{F}^{\nu - lD/2}}, \tag{4.1.9}$$

x_i are Feynman parameters and obviously they are functions of loop momenta. $\mathcal{U}$ and $\mathcal{F}$, which are homogeneous functions of Feynman parameters, are called ***first and second Symanzik***

polynomials, respectively. And they are derived from the following steps. We can present the denominator of the integrand in (4.1.7) by,

$$\sum_{j=1}^{n} x_j(-q_j^2 + m_j^2) = -\sum_{r=1}^{l}\sum_{s=1}^{l} k_r M_{rs} k_s + \sum_{r=1}^{l} 2k_r \cdot Q_r + J, \tag{4.1.10}$$

with M, a $l \times l$ matrix with scalars as entries and Q as a l-dimensional vector with four-vector as entries. Then Symanzik polynomials are[3],

$$\mathcal{U} = \det(M), \qquad \mathcal{F} = \det(M)(J + QM^{-1}Q). \tag{4.1.11}$$

$\mathcal{U}$ is linear in each Feynman parameter and it is of degree l. But $\mathcal{F}$ is linear only for the massless case, i.e. when all internal masses are zero and it is of degree $l + 1$. For the shown example we have,

$$M = \begin{pmatrix} x_1 + x_2 + x_3 + x_4 & x_4 \\ x_4 & x_4 + x_5 + x_6 \end{pmatrix} \tag{4.1.12}$$

$$Q = \begin{pmatrix} (x_3 + x_4)p_1 - x_2 p_2 + x_4 p_3 \\ x_4 p_1 + (x_4 + x_6)p_3 \end{pmatrix} \tag{4.1.13}$$

$$J = -2x_4(p_1 \cdot p_3), \tag{4.1.14}$$

and we can derive easily $\mathcal{U}$ and $\mathcal{F}$ from them. But, there is a much easier way to get the Symanzik polynomials.

As it has been well explained in [4], one can obtain the Symanzik polynomials from the so-called ***spanning trees and spanning forests*** defined in the graph theory. For a given l-loop Feynman graph G a spanning tree T is a connected sub-graph that contains all vertices. We get a spanning tree by deleting l internal edges in a way that the graph remains connected and there would be no loop. Obviously, there could be more than one spanning tree for a graph. Figure 4.1.2 shows three examples of five possible spanning trees of the graph shown in Fig. 4.1.1. Those sub-graphs have been obtained by deleting two edges of the graph.

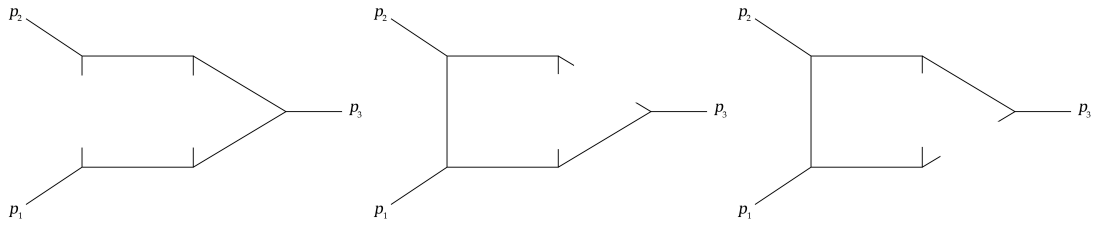

Figure 4.1.2: Three possible spanning trees of the graph shown in Fig. 4.1.1.

A spanning forest F of a given graph G is a generalization of spanning tree by omitting the

[3]For $\mu = 1$

requirement that the graph should be connected; but like spanning tree it has to contain all the vertices of G. A k-forest $\mathcal{T}_k$, has k connected trees T_i for $i = 1, \ldots, k$ and it is derived by deleting $l + k - 1$ edges. Figure 4.1.3 shows two examples of eleven possible 2-forests of the graph shown in Fig. 4.1.1.

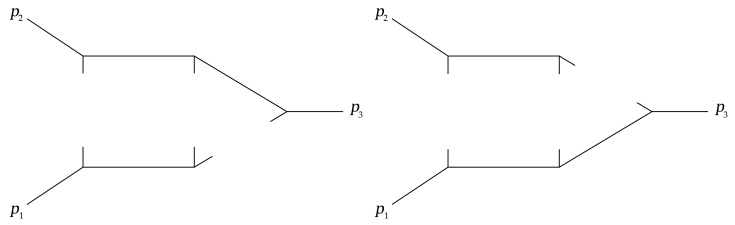

Figure 4.1.3: Two examples of eleven possible 2-forests of the graph shown in Fig. 4.1.1.

Now that we got familiar with the concept of spanning trees and spanning forests, we can show that the Symanzik polynomials can also be obtained by the following equations,

$$\mathcal{U} = \sum_{T \in \mathcal{T}_1} \prod_{q_i \notin T} x_i, \tag{4.1.15}$$

$$\mathcal{F} = \left(\sum_{(T_1,T_2) \in \mathcal{T}_2} \prod_{q_i \notin (T_1,T_2)} x_i \right) \left(\sum_{p_j \in P_{T_1}} \sum_{p_k \in P_{T_2}} p_j \cdot p_k \right) + \mathcal{U} \sum_{i=1}^{n} x_i m_i^2, \tag{4.1.16}$$

with $q_i \notin T$ it means the edge which has been cut to get the corresponding spanning tree T and P_{T_i} is the set of external momentum of T_i. For example, for the graph on the right in Figure 4.1.3 it is,

$$P_{T_1} = \{p_1\}, \qquad P_{T_2} = \{p_2, p_3\} \tag{4.1.17}$$

For the banana graph, obtaining the spanning trees and spanning forests is straightforward. As it can be seen in Figure 4.1.4, in the general case of banana Feynman graph, to get a spanning tree one has to remove all the internal edges but one and to obtain the only possible spanning forest, one has to cut all edges. Then for a l-loop banana diagram we have,

$$\mathcal{U} = \sum_{i}^{l+1} \prod_{j \neq i} x_j, \tag{4.1.18}$$

$$\mathcal{F} = x_1 x_2 \cdot x_{l+1} p^2 + \mathcal{U} \sum_{i=1}^{n} x_i m_i^2, \tag{4.1.19}$$

where p is the only external momentum.

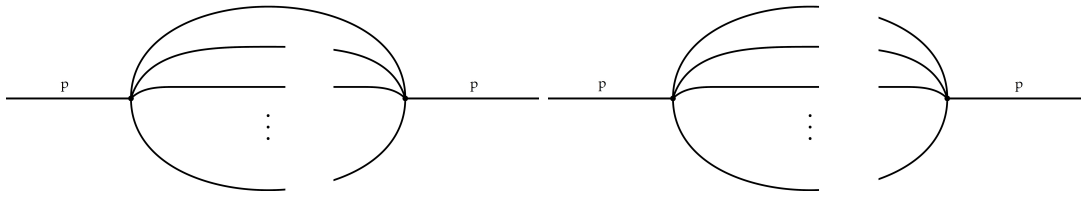

Figure 4.1.4: Respectively, the spanning tree and spanning forest of a general l-loop banana diagram

4.1.2 l-loop banana diagram

Now that we know how to do the Feynman parametrizations and to obtain the first and second Symanzik polynomials, we apply the same steps for the banana Feynman integrals to extract the geometric interpretation and benefit the method known in algebraic geometry to solve them.

The Feynman integral related to a *l-loop banana diagram* of a scalar field in 2d QFT with the corresponding interactions is shown in Figure 4.1.5. After a Feynman parametrization, it is given by:

$$\mathcal{F}_{\sigma_l}(t,\xi_i) = \int_{\sigma_l} \frac{\mu_l}{P_l(t,\xi_i;x)} = \int_{\sigma_l} \frac{\mu_l}{\left(t - \left(\sum_{i=1}^{l+1} \xi_i^2 x_i\right)\left(\sum_{i=1}^{l+1} x_i^{-1}\right)\right)\prod_{i=1}^{l+1} x_i} \ . \tag{4.1.20}$$

Here, x_i are the homogeneous coordinates of the projective space $\mathbb{P}^l$ and the l real dimensional integration domain σ_l is defined as

$$\sigma_l = \{(x_1 : \ldots : x_{l+1}) \in \mathbb{P}^l | x_i \in \mathbb{R} \text{ with } x_i \geq 0, \ \forall i\} \ . \tag{4.1.21}$$

With a holomorphic l measure μ_l,

$$\mu_l = \sum_{k=1}^{l+1} (-1)^{k+1} x_k \mathrm{d}x_1 \wedge \ldots \wedge \widehat{\mathrm{d}x_k} \wedge \ldots \wedge \mathrm{d}x_{l+1} \ . \tag{4.1.22}$$

The parameters or moduli in (4.1.20), t and ξ, are dimensionless parameters which are defined as $t = \frac{K^2}{\mu^2}$ and $\xi = \frac{M_i}{\mu}$ for $i = 1, \ldots l+1$, where K is the external momentum, M_i are the $l+1$ masses and μ is an infrared scale.

Later we will show that (4.1.20) is the GKZ period integral for a Calabi-Yau hypersurface in a toric ambient space.

4.1.3 Geometry associated to l-loop banana diagram

The zero locus of the denominator of the integral defines a singular family of $(l-1)$-fold Calabi-Yau hypersurfaces M_s as,

$$M_s = \left\{ P_l(t,\xi_i;x) = 0 | (x_1 : \ldots : x_{l+1}) \in \mathbb{P}^l \right\} \ . \tag{4.1.23}$$

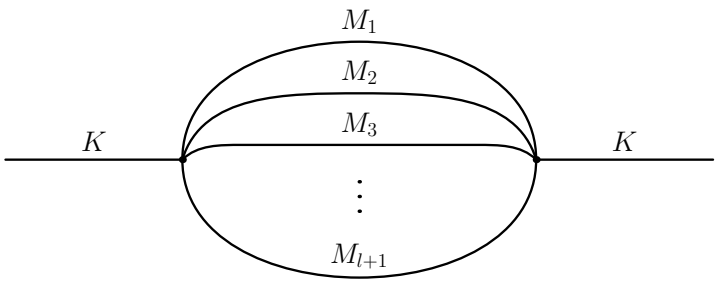

Figure 4.1.5: The l-loop banana diagram

Due to the standard arguments, see e.g. [45], M_s is a complex Kähler manifold with trivial canonical class $K = 0$, hence a Calabi-Yau space. The first fact follows by the definition of M_s as hypersurface in projective space $\mathbb{P}^l$ and the second as for a homogeneous polynomial P_l of degree $\deg(P)$ in $\mathbb{P}^l$ the canonical class is given in terms of the hyperplane class H of $\mathbb{P}^l$ as [45] $-K = c_1(TM_s) = [(l+1)-\deg(P)]H$ and $\deg(P) = (l+1)$. Note that given the scaling of (4.1.22) this degree makes the integrand of (4.1.20) well defined under the $\mathbb{C}^*$ scaling of the homogenous coordinates defining $\mathbb{P}^l$. Embedded in $\mathbb{P}^l$ the hypersurface is a singular Calabi-Yau space. Due to the Batyrev construction there is a canonical resolution of these singularities to define a smooth Calabi-Yau family, which we discuss next following [16, 11, 18, 25]. A Calabi-Yau manifold M of complex dimension $n = l - 1$ has two characteristic global differential forms. Since it is Kähler it has a Kähler $(1,1)$-form ω defining its Kähler– or symplectic structure deformations space. The triviality of the canonical class implies the existence of a nowhere vanishing unique holomorphic $(n,0)$-form that plays a crucial role in the description of the complex structure deformations space of M.

Calabi-Yau hypersurfaces in toric ambient spaces

The so-called ***Newton polynomial***, noted as P_{Δ_l}, is defined by,

$$P_l(t, \xi_i; x) =: P_{\Delta_l} \prod_i^{l+1} x_i \ . \tag{4.1.24}$$

The exponents of each monomial of P_{Δ_l}, w.r.t. the coordinates x_i, $i = 1, \ldots, l+1$, corresponds to a point in a lattice $\mathbb{Z}^{l+1}$. The convex hull of all these points in the natural embedding of $\mathbb{Z}^{l+1} \subset \mathbb{R}^{l+1}$ defines an l-dimensional lattice polyhedron. The dimension is reduced due to the homogeneity of P_{Δ_l} and we denote the polyhedron[4] that lies in the induced lattice $\mathbb{Z}^l \subset \mathbb{R}^l$ by Δ_l.

We considered a canonical basis e_i for $\Lambda = \mathbb{Z}^l \subset \mathbb{R}^l = \Lambda_{\mathbb{R}}$. The $l(l+1)$ vertices defined by (4.1.20) and (4.1.24) which span the polytope Δ_l [5], are,

$$\Delta_l = \mathrm{Conv}\left(\{\pm e_i\}_{i=1}^l \cup \{\pm(e_i - e_j)\}_{1 \le i < j \le l}\right). \tag{4.1.25}$$

[4] One calls P_{Δ_l} the Newton polynomial of Δ_l and Δ_l the Newton polyhedron of P_{Δ_l}.
[5] For $l = 1, 2, 3$ these polytopes are depicted in Figures 4.2.1, 4.2.2 and 4.2.3.

Note that Δ_l contains beside these vertices no further integral point other then the origen $\nu_0 = (0, \ldots, 0)$. These mean Δ_l is integral and reflexive, which implies that the dual polytope $\hat{\Delta}_l \subset \hat{\Lambda}_{\mathbb{R}}$,

$$\hat{\Delta}_l = \{y \in \hat{\Lambda}_{\mathbb{R}} | \langle y, x \rangle \geq -1, \forall\ x\ \ \in \Delta_l\}, \tag{4.1.26}$$

is also an integral and reflexive lattice polyhedron. Note that $\widehat{\hat{\Delta}_l} = \Delta_l$ and concretely $\hat{\Delta}_l$ is given by

$$\hat{\Delta}_l = \text{Conv}\left(\bigcup_{k=1}^{l} \bigcup_{r=1}^{\binom{l}{k}} \sum_{i=1}^{l} I_i^{(k),r} \hat{e}_i \cup \bigcup_{k=1}^{l} \bigcup_{r=1}^{\binom{l}{k}} \sum_{i=1}^{l} (-I_i^{(k),r} \hat{e}_i) \right) , \tag{4.1.27}$$

where $\hat{e}_i$ is a basis of the lattice $\hat{\Lambda}_{\mathbb{R}}$ and the $I^{(k),r}$ for $r = 1, \ldots, \binom{l}{k}$ are the sets of all distinct permutations of k-number of ones and $(l-k)$-number of zeros. Indeed the $2(2^l - 1)$ points listed in (4.1.27) are all integral points of $\hat{\Delta}_l$ beside the origin. For the polytope Δ_l itself it means that it has $2(2^l - 1)$ faces. From the structure of the vertices of Δ_l it can be proven that there is no integral point in the facets of the dual polytope. The combinatorics of all facets of $\hat{\Delta}$ are equal, in particular they all have 2^{l-1} vertices.

A central theorem in the toric mirror construction of Batyrev [16] says that a smooth resolution M of M_s with trivial canonical class is given by the constraint

$$P_{\Delta_l} = \frac{P_l(a; x)}{\prod_{i=0}^{p} x_i} = \sum_{\nu^{(i)} \in \Delta_l} a_i \prod_{\hat{\nu}^{(k)} \in \hat{\Delta}_l} x_k^{\langle \nu_i, \hat{\nu}_k \rangle} = 0 \tag{4.1.28}$$

in the coordinate ring x_i of $\mathbb{P}_{\hat{\Delta}_l}$, where ν_i, $i = 1, \ldots, p$ and $\hat{\nu}_k$, $i = 1, \ldots, \hat{p}$ run over all integer points in Δ_l and $\hat{\Delta}_l$ respectively[6]. Here $I(\Delta_l)$ is the number of lattice points in Δ_l and $p = I(\Delta_l) - 1$. Analogous definitions apply for $\hat{\Delta}_l$. Note that (4.1.28) defines an embedding of the physical parameters t and ξ_i, $i = 1, \ldots, l+1$ into convenient but redundant complex structure variables $a_i \in \mathbb{C}$, $i = 0, \ldots, l-1$. Both the physical as well as the a_i parameters are only defined up to scale. Note that we are a little cavaliar with the notations: The coordinate rings x_i, $i = 1, \ldots, l+1$ in the definition (4.1.20) and the one x_i, $i = 1, \ldots, \hat{p}$ in (4.1.28) are of course different. However, we can get the former by blowing down the latter. This is achieved by setting a suitable subset of $\hat{p} - (l+1)$ of the latter x_i variables to one. Likewise given P_{Δ_l} in x_i, $i = 1, \ldots, l+1$ as in (4.1.24) and all $\mathbb{C}^*$ action (4.1.30) we can uniquely extend it to $\hat{p}$ variables x_i by requiring that the extended polynomial (or strictly speaking the proper transform of (4.1.24)) is homogeneous, w.r.t. to all $\mathbb{C}^*$ rescalings in (4.1.30).

The space $\mathbb{P}_{\Delta_l}$ is a l-dimensional projective toric variety that can be associated to any reflexive lattice polyhedra Δ_l given a star triangulation [7] $\mathcal{T}$of Δ_l as

$$\mathbb{P}_{\Delta_l} = \frac{\mathbb{C}^p[x_1, \ldots, x_p] \setminus Z_{\mathcal{T}}}{(\mathbb{C}^*)^{p-l}} \ . \tag{4.1.29}$$

[6] P_{Δ_l} is a Laurent polynomial in which the minimal degree of the x_i is -1, while $P_l(a; x) = 0$ is a polynomial constraint, which also defines a smooth manifold in the coordinate ring .

[7] In a star triangulation all l-dimensional simplices of the triangulation covering the reflexive polyhedron share the inner point, as one of their vertices.

Here the $\mathbb{C}^*$ actions that are divided out are generated by

$$x_i \mapsto x_i(\mu^{(k)})^{l_i^{(k)}}, \quad \text{for } i = 1, \ldots, p \ , \tag{4.1.30}$$

where $\mu^{(k)} \in \mathbb{C}^*$ and the $l^{(k)}$ vectors span the $(p-l)$-dimensional space of all linear relations

$$L = \{(l_0^*, l_1^*, ..., l_p^*) \in \mathbb{Z}^{p+1} | l_0^* \bar{\nu}_0 + l_1^* \bar{\nu}_1 + ... + l_p^* \bar{\nu}_p = 0\} \tag{4.1.31}$$

among the points

$$\mathcal{A} = \{\bar{\nu}_0, \bar{\nu}_1, ..., \bar{\nu}_p | \bar{\nu}_i = (1, \nu_i), \nu_i \in \Delta_l \cap \mathbb{Z}^l\} \ . \tag{4.1.32}$$

The triangulation [8] $\mathcal{T}$ determine the set of generators $l^{(k)}$ of L and the Stanley-Reisner ideal $Z_{\mathcal{T}}$. The latter describes loci in $\mathbb{C}^p[x_1, \ldots, x_p]$, which have to be excluded so that the orbits of the $\mathbb{C}^*$ action (4.1.30) have a well defined dimension. Positive linear combinations of $l^{(k)}$, $k = 1, \ldots, n$ span the Mori cone, which is not necessary simplicial if $n > p - l$. It is dual to the Kähler cone of $\mathbb{P}_{\Delta_l}$ and all cones corresponding to all triangulations $\mathcal{T}$ of Σ_{Δ_l} form the secondary fan, see [46] for a review how to calculate the $l^{(k)}$ vectors and the Stanley-Reisner ideal combinatorial from a triangulation $\mathcal{T}$. This combinatorics is implemented in the computer package `SageMath` [47], which calculates the possible triangulations $\mathcal{T}$ and from them the generators $l^{(k)}$ and the Stanley Reisner ideal $Z_{\mathcal{T}}$.

The Calabi-Yau $(l-1)$-fold family defined as section of the canonical bundle $P_{\hat{\Delta}_l} = 0$ of $\mathbb{P}_{\Delta_l}$ is by Batryrev [16] conjectured to be the mirror manifold $W = X_{\hat{\Delta}_l}$ of the manifold M, i.e. (M, W) form a mirror pair with dual properties. A main implication of this proposal is that the complex structure deformation space of M denoted by $\mathcal{M}_{CS}(M)$ is identified with the complexified Kähler or stringy Kähler moduli space $\mathcal{M}_{KCS}(W)$

$$\mathcal{M}_{KCS}(W) = \mathcal{M}_{CS}(M) \tag{4.1.33}$$

and vice versa. Note that the real Kähler moduli space is parametrized by the Kähler parameters $t_k^{\mathbb{R}} = \int_{\mathcal{C}_k} \omega$, where $\omega \in H^{1,1}(M)$ and $\mathcal{C}_k$ span a basis of holomorphic curves in $H_{1,1}(M, \mathbb{Z})$. In string theory the complexification is due to the Neveu-Schwarz two-form field b also in $H^{1,1}(M)$. The complex variables $t_k = \int_{\mathcal{C}_k} \omega + ib$, $k = 1, \ldots, h_{1,1}(M)$ parametrize locally the complexified moduli space $\mathcal{M}_{KCS}(W)$ of W.

We will next discuss the space $\mathcal{M}_{cs}(M)$ of complex structure deformations of M. This space is redundantly parametrized by the complex coefficients a_i, $i = 0, \ldots, l(\Delta_l) - 1$ in (4.1.28). The a_i are identified by $l+1$ scaling relations on the coordinates of $\mathbb{P}_{\hat{\Delta}_l}$ and the automorphism of $\mathbb{P}_{\hat{\Delta}_l}$ that leaves M invariant but acts on the parametrizations of the polynomial constraint $P(a; x)$. The latter one parameter families of identifications of the deformation parameters are in an one-to-one correspondence to the points inside codimension one faces of Δ_l. Let us denote by Θ_k^j all faces of codimension k in Δ_l labeled by j. $I(\Theta_k^j)$ denotes the number of lattice points contained in Θ_k^j, while $I'(\Theta_k^j)$ denotes the number of lattice points that lie in the interior of $\Theta_k^{(j)}$. With this notation M has $I(\Delta_l) - (l+1) - \sum_j I'(\Theta_1^j)$ independent complex

[8] Δ_l defines canonically a fan Σ_{Δ_l} and the definition of a smooth $\mathbb{P}_{\Delta_l}$ may require to add integer points outside Δ_l and to triangulate the fan Σ_{Δ_l}. Such cases are discussed in [11, 10].

structure deformations. They correspond to elements in $H^1(M, TM)$ and are unobstructed on a Calabi-Yau manifold M. The cohomology group $H^1(M, TM)$ is related to the cohomology group $H^{l-2,1}(M)$ via the contraction with the unique holomorphic $(l-1,0)$-form.

Equation (4.1.33) implies that in particular the complex dimensions of these spaces have to match, i.e. $h_{1,1}(X_{\hat{\Delta}_l}) = h_{l-2,1}(X_{\Delta_l})$ and $h_{1,1}(X_{\Delta_l}) = h_{l-2,1}(X_{\hat{\Delta}_l})$. From theses facts it follows that the dimensions of these important cohomology groups are given by counting integral points in the polytops[9]

$$\begin{aligned} h_{1,1}(X_{\Delta_l}) &= I(\hat{\Delta}_l) - (l+1) - \sum_j I'(\hat{\Theta}_1^j) + \sum_j I'(\hat{\Theta}_2^i) I'(\Theta_{l-2}^i)) = 2^{l+1} - l - 2 \\ h_{l-2,1}(X_{\Delta_l}) &= I(\Delta_l) - (l+1) - \sum_i I'(\Theta_1^i) + \sum_i I'(\Theta_2^i) I'(\hat{\Theta}_{l-2}^i)) = l^2 \ . \end{aligned} \tag{4.1.34}$$

For $l = 3$ the Calabi-Yau manifold M will be a nine-parameter family of polarized $K3$ surfaces. In this case the transversal cycles in h_{11} are counted $h_{11}^T = I(\Delta_l) - (l+1) = 9$, i.e. in total one has eleven transcendental and eleven algebraic two-cycles, which are counted by $h_{11}^A = I(\hat{\Delta}_l) - (l+1) = 11$. For $l = 4$ the 16-parameter family of Calabi-Yau three-fold has $h_{11} = 26$ and $h_{21} = 16$ and hence Euler number $\chi = 20$. For $l = 5$ the Calabi-Yau four-fold has $h_{31} = 25$, $h_{11} = 57$, $h_{21} = 0$ and $\chi = 540$. Using an index theorem [22] one gets $h_{22} = 422$.

Since our polytope (4.1.25) has only $\sum_i I(\Theta_l^i) = l(l+1)$ corners and one inner points the manifold M has l^2 complex structure deformations, which have to be eventually mapped to our physical parameters t and ξ_i. Since the latter are equivalent up to scaling by μ we have $l+1$ independent physical parameters. Therefore, the map to the physical parameter space has a huge kernel for high l and special effort has to be made to specify the relevant physical subspace of $\mathcal{M}_{phys}(M) \subset \mathcal{M}_{cs}(M)$ as described concretely in the example sections 4.2.1, 4.2.2 and 4.2.3.

Actual properties of the smooth canonical resolution of M_s, in particular its Kähler cone, depend on the choice of the star triangulation $\hat{\mathcal{T}}$ of $\hat{\Delta}_l$. However, these detailed properties of the Kähler moduli space $\mathcal{M}_{KS}(M)$ of M do not affect the complex moduli space $\mathcal{M}_{CS}(M)$ and the integral (4.1.20) over closed cycles, like $\mathcal{F}_{T^l}$, the integral over the T^l torus. This maximal cut integral depends only on the complex structure parameters. The blow up coordinate ring allows however a useful description of the boundary contribution to $\mathcal{F}_{\sigma_l}$, see [48]. Moreover, the identification (4.1.33) turns out to be very useful to introduce suitable coordinates on $\mathcal{M}_{CS}(M)$ to obtain solutions for the integral (4.1.20). Different star triangulations $\mathcal{T}$ of the polyhedra Δ_l correspond to different Kähler cones of the ambient space $\mathbb{P}_{\Delta_l}$ of W and correspond eventually[10] to different Kähler cones of W. Each choice of the Kähler cone of W, defines by mirror symmetry and the identification (4.1.33) canonical so called Batyrev coordinates z_i, $i = 1, \ldots, h_{l-2,1}(M) = h_{1,1}(W)$ on $\mathcal{M}_{CS}(M)$, at whose origin $z_i = 0$ for all i

[9] The last terms after the first equal sign in the formulas in each line of (4.1.34) correspond to Kähler— or complex structure deformations, which are frozen by the toric realization of the manifolds, respectively. Likewise the third terms are absent in our case. The last equality holds only for the polyhedra given in (4.1.25) and (4.1.27).

[10] If all curves that bound the Kähler cone of $\mathbb{P}_{\Delta_l}$ descend to the hypersurface W.

there is a point of maximal unipotent monodromy in $\mathcal{M}_{CS}(M)$. The coordinates z_i are ratios of the coefficients a_i of P_{Δ_l} given for each triangulation by

$$z_k = (-a_0)^{l_0^{(k)}} \prod_i a_i^{l_i^{(k)}}, \quad k = 1, \ldots, p-l \ . \tag{4.1.35}$$

The definition of the z_k eliminates the scaling relation. Since in our case we have no codimension one points, i.e. no automorphism of $\mathbb{P}_{\hat{\Delta}}$ leaving the hypersurface invariant and further identifying the a_i deformations, the z_k are actual coordinates on $\mathcal{M}_{CS}(M)$. In other simple cases one can restrict in the definition of L (4.1.31) to linear relations of points, which are not in codimensions one, the general case is discussed in [11,10]. In the moduli space of $\mathcal{M}_{CS}(M)$ as parametrized by the independent a_i, the z_k are blow up coordinates resolving singular loci in discriminant components of the hypersurface $P_{\Delta_l} = 0$ in $\mathcal{M}_{CS}(M)$, so that these become in the resolved model of the complex moduli space $\widehat{\mathcal{M}_{CS}}(M)$ intersection points of normal crossing divisors $D_i = \{z_i = 0\}$, $i = 1, \ldots, h_{l-2,1}(M)$.

Of particular significance in the geometric toric construction of the differentials on M is the coefficient a_0 of the monomial $\prod_i^{l+1} x_i$ in $P(t, \xi; x)$ corresponding to the inner point in Δ_l, which is given in the physical parameters by

$$u \coloneqq a_0 = t - \sum_{i=1}^{l+1} \xi_i^2 \ . \tag{4.1.36}$$

The families that are just parametrized by u with the coefficients of all other points set to one, i.e. in particular $\xi^2 = 1$ for all $i = 1, \ldots, l+1$ is particularly symmetric. For $l = 4$, i.e. Calabi-Yau three-folds, the family is known as the Barth-Nieto quintic. The form of this family is conveniently given by a complete intersection in $\mathbb{P}^{l+1}$ that can be readily generalized to the ones

$$\sum_{i=1}^{l+2} x_i = 0 \quad \text{and} \quad \sum_{i=1}^{l+1} \frac{1}{x_i} + \frac{1}{u x_{l+2}} = 0 \ . \tag{4.1.37}$$

By solving for x_{l+2} and homogenizing one gets $P_{\Delta_l} = 0$ in the equal mass case parametrized by u and for equal masses $\xi_i^2 = 1$ for all $i = 1, \ldots, l+1$.

Period integrals on M and maximal cut amplitude

For the discussion of the period integrals, which are very close to the integral of interest (4.1.20), we start with a residue definition of the holomorphic $(n, 0)$-form Ω of the Calabi-Yau manifold M of complex dimension $n = l - 1$ defined as hypersurface in a toric ambient space

$$\Omega = \oint_\gamma \frac{a_0 \mu_l}{P_l(a; x)} \ , \tag{4.1.38}$$

where γ encircles the locus $P_l = 0$ in the toric ambient space and μ_l was defined in (4.1.22). Given a basis Γ_i of the cycles in the middle dimensional homology $H_n(M, \mathbb{Z})$ we can define closed string period integrals

$$\Pi(\Gamma) = \int_\Gamma \Omega \ . \tag{4.1.39}$$

The closed string periods are directly relevant as one of them describes the maximal cut integral. Moreover, by the local Torelli theorem $h^{n-1,1}$ of them can serve as projective coordinates of $\mathcal{M}_{CS}$ and by Griffiths transversality the periods fulfill differential relations for odd $n > 1$, algebraic relations for $n = 2$ and algebraic as well as differential relations for even $n > 2$.

At the point of maximal unipotent monodromy that is specified as the origin of the Batyrev coordinates z_i, $i = 1, \dots h$ from (4.1.35), which are simply defined by the Mori cone $l^{(k)}$ vectors of the mirror W, the Picard-Fuchs differential ideal is maximally degenerate. This point is a point of maximal unipotent monodromy or short MUM-point. As a consequence that near the MUM-point there is exactly one holomorphic period, and for $k = 1, \dots, n$ there are $h^{n-k,k}_{hor}$ periods whose leading multi-degree in $\log(z_i)$, $i = 1, \dots, h^{n-1,1}$ is of order k. For Calabi-Yau n-folds with $n > 2$ the full cohomology groups $H^{n,0}, H^{n-1,1}$ are horizontal. By complex conjugation this holds also for $H^{1,n-1}$ and $H^{0,n}$. In particular, for Calabi-Yau three-folds the whole middle cohomology is horizontal. Beside this general structure an additional bonus in the case of Calabi-Yau spaces given by hypersurfaces in toric ambient spaces is that there is a n-cycle with the topology of a n-torus $T^n \in H_n(M, \mathbb{Z})$ which yields that holomorphic period $\varpi \coloneqq \Pi(T^n)$ explicitly. With the definitions (4.1.38) and (4.1.39) this integral yields an $(n+1)$-times iterated residue integral over an T^{n+1} in the ambient space, that can be readily evaluated in terms of the $l^{(k)}$ vectors as

$$\varpi = \oint_{|x_1|=0} \frac{dx_1}{2\pi i} \dots \oint_{|x_{n+1}|=0} \frac{dx_{n+1}}{2\pi i} \frac{a_0}{P_l(a;x)} = \sum_{\{\underline{k}\}} \frac{\Gamma\left(-\sum_{\alpha=1}^h l_0^{(\alpha)} k_\alpha + 1\right)}{\prod_{l=1}^p \Gamma\left(\sum_{\alpha=1}^h l_l^{(\alpha)} k_\alpha + 1\right)} \prod_{\alpha=1}^h z_\alpha^{k_\alpha} \ . \tag{4.1.40}$$

Here we use the coordinate ring x as in (4.1.20) and set $x_{n+2} = 1$. In the tuple $\{\underline{k}\} = \{k_1, \dots, k_h\}$ each k_i runs over non negative integers $k_i \in \mathbb{N}_0$ and p is defined in (4.1.31). Note that by definition the sum of the integer entries in each $l^{(k)}$ is zero, therefore they have negative entries. For hypersurfaces and complete intersections the $l_0^{(k)}$ entry is non-positive $l_0^{(k)} \leq 0$ for all k. However, for $i > 0$ the $l_i^{(k)}$ can have either sign. Poles of the Γ-function at negative integers in the denominator make the summand vanishing. This effectively restricts the range of the $\{k_1, \dots, k_h\}$ to a positive cone

$$\sum_{\alpha=1}^h l_j^{(\alpha)} k_\alpha \geq 0 \ . \tag{4.1.41}$$

Restricting to the physical slice, i.e. to $\underline{z}(t, \xi_i)$ of the l-loop graph, means to parametrize the a_i, $i = 0, \dots, h = l^2$ by the physical variables t, ξ_i. Due to the definition of (4.1.35) one can find a splitting of the set of indices $\{\alpha_1, \dots, \alpha_h\}$ into $\{\alpha_1, \dots, \alpha_{l+1}\}$ and $\{\alpha_{l+2}, \dots, \alpha_h\}$ so that the variables $\{z_{\alpha_{l+2}}, \dots, z_{\alpha_h}\}$ are either set to constant values or identified with the variables $z_{\alpha_j}(t, \xi)$, $i = 1, \dots, l+1$. A key observation in the examples is that the range (4.1.41) is such that the contribution from the summation over the k_{α_j}, $j = l+2, \dots h$ to each monomial $\prod_{i=1}^{l+1} z_{\alpha_i}^{k_i}$ is finite. This implies in that (4.1.40) can also be given non-redundantly in $l+1$ physical parameters $z_{\alpha_j}(t, \xi)$, $i = 1, \dots, l+1$ exactly to arbitrary order. The range (4.1.41) and (4.1.40) can also be calculated directly as follows: Expanding in the integrand $a_0/P_l(x, a) = [1/\prod_i x_i]\,[1/(1 - 1/a_0(\dots))]$ the second factor as a geometric series and noticing

that only the constant terms of it contribute to the integral yields the result. Applying this to the P_l in (4.1.20) yields the all $(l = n + 1)$-loop maximal cut integrals

$$\mathcal{F}_{T^l}(t, \xi_i) = \frac{\varpi\left(\underline{z}(t, \xi_i)\right)}{t - \sum_{i=1}^{l+1} \xi_i^2} \tag{4.1.42}$$

as an exact series expansion with finite radius of convergence for regions in the physical parameters in which $z_k(t, \xi_i)$ are all small.

In principal, one can analytically continue this to all regions in the physical parameter space. This task can greatly aided if one knows the Picard differential ideal that annihilates ϖ and all other periods. The derivation of the latter will be discussed in the next section. It certainly helps if one knows all other periods near $z_k = 0$. Because of the structure of the logarithmic solutions at the MUM-point these can by easily given by the Frobenius method. This is done by introducing h auxiliary deformation parameters ρ_α in

$$\varpi(\underline{z}, \underline{\rho}) = \sum_{\{\underline{k}\}} c(\underline{k}, \underline{\rho}) \underline{z}^{\underline{k}+\underline{\rho}}, \tag{4.1.43}$$

where $\underline{z}^{\underline{k}+\underline{\rho}} := \prod_{\alpha=1}^{h} z_\alpha^{k_\alpha+\rho_\alpha}$ and

$$c(\underline{k}, \underline{\rho}) = \frac{\Gamma\left(-\sum_{\alpha=1}^{h} l_0^{(\alpha)}(k_\alpha + \rho_\alpha) + 1\right)}{\prod_{l=1}^{p} \Gamma\left(\sum_{\alpha=1}^{h} l_l^{(\alpha)}(k_\alpha + \rho_\alpha + 1\right)} \ . \tag{4.1.44}$$

With this definition $\varpi(\underline{z}) = \varpi(\underline{z}, \underline{\rho})|_{\underline{\rho}=0}$ the $h^{n-1,1}$ linear logarithmic solutions are given by

$$\Pi(\Gamma_\alpha) = [(1/(2\pi i)\partial_{\rho_\alpha} \varpi(\underline{z}, \underline{\rho})]|_{\underline{\rho}=0} = 1/(2\pi i)\Pi(T^n) \log(z_\alpha) + \mathcal{O}(z) \ . \tag{4.1.45}$$

It can be shown that $\Gamma_\alpha \in H_m(M, \mathbb{Z})$. All other solutions corresponding to the rest of the cycles $\Gamma_\beta \in H_n(M, \mathbb{Z})$ are of order $2 \leq k \leq n$ in the logarithms and of the form

$$\Pi(\Gamma_\beta) = [c_\beta^{\alpha_1 \dots \alpha_k} \partial_{\rho_{\alpha_1}} \dots \partial_{\rho_{\alpha_k}} \varpi(\underline{z}, \underline{\rho})]|_{\underline{\rho}=0} \ , \tag{4.1.46}$$

where the tensors $c_\beta^{\alpha_1 \dots \alpha_k}$ contain transcendental numbers fixed by the $\hat{\Gamma}$-class conjecture and classical intersection theory on W, see [25] for a review.

GKZ systems and Picard Fuchs differential ideal

Gel′fand, Kapranov and Zelevinskĭ [49] investigated integrals of the from

$$\mathcal{F}_\sigma^{GKZ} = \int_\sigma \prod_{i=1}^{r} P(x_1, \dots, x_k)^{\alpha_i} x_1^{\beta_1} \cdots x_k^{\beta_k} \mathrm{d}x_1 \cdots \mathrm{d}x_k \ , \tag{4.1.47}$$

which can be specialized to (4.1.20), which is in turn similiar to (4.1.40), even though in (4.1.40) we took the integration domain to be a closed cycle T^{n+1}, while [49] just speek of cycles σ.

In (4.1.20) σ is a closed cycle only for the maximal cut case which leads to (4.1.40), otherwise σ is a chain. In this case the corresponding differential ideal, which is fulfilled by the integral (4.1.47) is inhomogeneous. The GKZ integrals can be viewed as systematic multivariable generalization of the Euler integral ${}_2F_1(a,b,c;z) = \sum_{n=0}^{\infty} \frac{(a)_n (b)_n}{n!(c)_n} = \frac{\Gamma(c)}{\Gamma(b)\Gamma(b-c)} \int_0^1 t^{(b-1)}(1-t)^{(b-c-1)}(1-zt)^{-a}$, which solves Gauss hypergeometric systems and ϖ as a specially simple generalized multivariable hypergeometric series.

As mentioned at the end of the introduction to subsection (4.1.3) at least for integer exponents the requirement that these higher dimensional integrals are well defined under the scaling symmetries of the parameters, that appear in physical Feynman integrals, is equivalent to the vanishing of the first Chern class and hence these Feynman integrals with $r = 1$, $\alpha_1 = -1 = -n_1$ are closely related to period integrals over the holomorphic $(n,0)$-form in the cohomology group $H^{n,0}$ of the Calabi-Yau manifolds M defined as hypersurfaces in toric varieties [11, 50, 10]. The same argument relates integrals with $r > 1$ and $\alpha_i = -1 = -n_i$ to complete intersection Calabi-Yau spaces [17–19].

More general integrals are related to the former by taking derivatives w.r.t. to the independent complex moduli parameters say a. In particular, such derivatives change the Hodge type of the integrand as follows. Let $F^p(M) = \bigoplus_{l \geq p} H^{l,n-l}(M)$ a Hodge filtration $H^n = F^0 \supset F^1 \supset \ldots \supset (F^n = H^{n,0}) \supset F^{n+1} = 0$, then $H^{p,q}(M) = F^p(M) \cap \overline{F^q(M)}$, and the $F^p(M)$ can be extended to holomorphic bundles $\mathcal{F}^p(M)$ over the complex family M over $\mathcal{M}_{CS}(M)$, with

$$\partial_a^k \mathcal{F}^n(M) \in \mathcal{F}^{n-k}(M) \ . \tag{4.1.48}$$

Since the bundles $\mathcal{F}^p(M)$ are of finite rank, there will be differential relations among finite derivatives w.r.t. to the moduli, which implies that the period integrals over closed cycles are annihilated by finite order linear differential operators $\mathcal{D}_k$, where the derivations are w.r.t. the moduli and the coefficients are rational functions in the moduli. In particular, one can specify a differential ideal, called the Picard-Fuchs differential ideal, $\mathcal{D}_k$, $k = 1, \ldots, d$ that determines the periods as finite linear combination of its system of solutions.

One key tool to find the differential relations between these integrals is the Griffiths reduction method, which relies on the following partial integration formula, that is valid up to exact terms, i.e. holds under the integration over closed cycles [51]

$$\sum_{k \neq j} \frac{n_k}{n_j - 1} \frac{P_j}{P_k} \frac{Q \partial_{x_i} P_k}{\prod_{l=1}^r P_l^{n_l}} \mu \ = \frac{1}{n_j - 1} \frac{P_j \partial_{x_i} Q}{\prod_{l=1}^r P_l^{n_l}} \mu - \frac{Q \partial_{x_i} P_j}{\prod_{l=1}^r P_l^{n_l}} \mu \ , \tag{4.1.49}$$

where $Q(x)$ are polynomials of the appropriate degree to ensure the scale invariances and μ is straightforward generalization of the measure (4.1.22). Such $Q(x)$ arise automatically, when partial derivative w.r.t. the moduli are taken. Using these equations and Gröber basis calculus one can reduce higher derivatives w.r.t. to the moduli to lower ones and find eventually the complete differential ideal. These relations between rational functions are also used in the literature not only to compute differential equations for Feynman integrals but also for finding so called master integrals. If these master integrals are known with the partial integration relations (4.1.49) the whole Feynman integral is evaluated. For a review on master integrals in Feynman graph computation we refer to [52].

However, this method is computationally very expensive in multi moduli cases. Therefore, we employ as far as possible a different derivation of differential relations which follow from scaling symmetries that follow from the combinatorics of the Newton polytope, known as GKZ differential system. For this purpose we define

$$\hat{\Omega} = \oint_\gamma \frac{\mu_l}{P_l(a;x)} \quad \text{and} \quad \hat{\Pi}_\sigma = \int_\sigma \frac{\mu_l}{P_l(a;x)} \ . \tag{4.1.50}$$

Now each linear relation among the points in the Newton polytope as expressed by the $l^{(k)}$-vectors, $k = 1, \ldots, l^2$ yields a differential operator $\mathcal{D}_{l^{(k)}}$ in the redundant moduli a. Moreover, the infinitesimal invariance under the $(\mathbb{C}^*)^{n+2}$ scaling relations yields further differential operators $\mathcal{Z}_j$, $j = 1, \ldots, n+2$. Together they constitute an resonant GKZ system [8, 53]:

$$\hat{\mathcal{D}}_{l^{(k)}}\hat{\Pi}_\sigma = \left(\prod_{l_i^{(k)}>0} \left(\frac{\partial}{\partial a_i}\right)^{l_i^{(k)}} - \prod_{l_i^{(k)}<0} \left(\frac{\partial}{\partial a_i}\right)^{-l_i^{(k)}} \right) \hat{\Pi}_\sigma = 0 \quad \text{and} \tag{4.1.51}$$

$$\mathcal{Z}_j \hat{\Pi}_\sigma = \left(\sum_{i=0}^{p} \bar{\nu}_{i,j} \theta_{a_i} - \beta_j \right) \hat{\Pi}_\sigma = 0 \tag{4.1.52}$$

with $\beta = (-1, 0, ..., 0) \in \mathbb{R}^{n+2}$ for the hypersurface case and $\theta_a = a\partial_a$, in the form that applies to the integrals in Calabi-Yau hypersurfaces in toric varieties [16,11], for which the integration domain σ is also scale invariant. In this case we can use the relations $\mathcal{Z}_j\hat{\Pi}_\sigma = 0$ to eliminate the a_i in favour of the scale invariant z_i defined in (4.1.35) using $a_i\partial_{a_i} = \sum_{k=1}^{l^2} l_i^{(k)} z_k \partial_{z_k}$ and by the commutation relation $[\theta_a, a^r] = ra^r$ applied previously to a_0 we obtain operators $\mathcal{D}_{l^{(k)}}(z)$ that annihilate $\Pi(\Gamma)$. As it turns out these operators do not determine the $\Pi(\Gamma)$ as they admit further solutions [11]. To obtain the actual Picard-Fuchs differential ideal one can factorize the $\mathcal{D}_{l^{(k)}}(z)$ and disregard trivial factors that allow for additional solutions which have the wrong asymptotic to be periods [11, 17]. In practice the most efficient way to get the Picard-Fuchs differential ideal is often to make an ansatz for additional minimal order differential operators that annihilate (4.1.40) and check that the total system of differential operators allows no additional solutions then the ones specified in (4.1.45) and (4.1.46).

One of our main results is that we give the general strategy to derive the Picard-Fuchs differential ideal in the physical parameters $z_i(t, \xi)$, $i = 1, \ldots, l+1$ and give it explicitly for one, two and three loops in equations (4.2.5), (4.2.25) and in (A.1)-(A.4) for the three-loop banana graph. These operators determine the maximal cut integral everywhere in the parameter space. By applying these operators to the geometrical chain integral

$$\Pi_{\sigma_l} = \int_{\sigma_l} \frac{a_0 \mu_l}{P_l(a;x)} \tag{4.1.53}$$

and integrating explicitly over the boundary of the chain we can find the inhomogeneous differential equations and the corresponding special solutions describing the full l-loop banana graphs explicitly up to three loops.

Let us end this section with some remarks on additional structures for the periods of Calabi-Yau n-folds, which are relevant to understand the differential ideal that determines

the maximal cut integral better. For a given basis of transcendental n-cycles $\Gamma_i \in H_n(M, \mathbb{Z})$ one can find dual elements $\gamma_j \in H^n_{hor}(M, \mathbb{C})$ so that $\int_{\Gamma_i} \gamma^j = \delta^j_i$ and expand the holomorphic $(n,0)$-form $\Omega = \sum_i \Pi(\Gamma_i)\gamma^i$. Let us define for each set A of indices of order r the order r differential operator $\partial^r_A := \partial_{z_{a_1}} \dots \partial_{z_{a_r}}$. Then by (4.1.48) and consideration of type one gets the *transversality conditions* [54]

$$\int_M \Omega \wedge \partial^r_A \Omega \;=\; \Pi(\Gamma_i)\Sigma^{ij}\partial^r_A \Pi(\Gamma_j) \;=\; \begin{cases} 0 & \text{if } r < n \\ C_A(z) & \text{if } r \;=\; n \;, \end{cases} \tag{4.1.54}$$

where C_A are rational functions in the z_i, known as Yukawa couplings for $n = 3$. The form $\Sigma^{ij} = \int_M \gamma^i \wedge \gamma^j$ is integer and symmetric for n even and antisymmetric for n odd. In the latter case one can chose a symplectic basis for the γ^i. For the K3 or more generally $n \geq 2$ and n even it implies that the solutions to the Picard-Fuchs differential ideal fulfill nontrivial quadratic relations

$$\Pi(\Gamma_i)\Sigma^{ij}\Pi(\Gamma_j) = 0 \quad \text{and} \quad \Pi(\Gamma_i)\Sigma^{ij}\partial_{z_k}\Pi(\Gamma_j) = 0 \;, \quad \forall k \;. \tag{4.1.55}$$

We will discuss the consequences at the level of the differential operator more in section 4.2.3. For $n = 3$ it implies special geometry, see [25] for a review.

Geometrical and physical periods

The physical moduli space of the banana Feynman diagrams is parametrized by the $l + 2$ parameters $(t, \xi_1, \xi_2, \dots, \xi_{l+1})$, where additionally one of these can be scaled away. As mentioned, compared to the moduli space parametrized by all Batyrev coordinates z_i, the physical moduli space gets much smaller as l grows. In the following we explain how one can make a restriction onto the physical moduli space.

Besides this restriction there is another difficulty I have to mention. For the description of the large moduli space through the Batyrev coordinates z_i it is crucial to have a minimal number of Mori cone generators. They are determined from the triangulation $\mathcal{T}$ of the polytope[11] Δ_l. And from 4.1.34 we know that the minimum number of the Mori cone generators (l-vectors) is l^2. But there are few (and sometime no) fine and simplicial star-triangulations which yield l^2 Mori cone generators. Actually, for the sunset graph there is no triangulation which gives us 4 Mori cone generators. In such a situation one starts with a triangulation yielding a non-minimal number of Mori cone generators. We claim that one can still take out l^2 l-vectors describing the Feynman graph geometry appropriately. The choice of l^2 vectors is neither arbitrary nor unique but we can give some criteria[12] for choosing them correctly. Different proper selections of l-vectors should at the end yield the same results for the Feynman graph.

First of all the l^2 vectors should be all linear independent over the real numbers. Secondly, we want $l + 1$ l-vectors having a non-vanishing entry for the inner point which are important

[11] For $l = 3$ one can easily get all 2^6 star triangulations but for $l = 4$ there is an extremely large number of different star triangulations, which is 6^{20}. Listing all of them cannot be done by a desktop computer.

[12] We do not claim that these criteria are necessary or sufficient.

in the physical limit. Furthermore, we want that in the i-th components of all l-vectors there is at least a positive entry. This should be true for all components i without the one for the inner point. From the last condition we hope that it guarantees that the structure of solutions is as we explained in section 4.1.3. This one can check by analyzing that the GKZ operators defined in (4.1.52) do indeed annihilate the Frobenius solutions with positive powers (4.1.43).

We think that these conditions give a strategy to take out the required l^2 mori cone generators. For the sunset graph we have to follow this strategy and we give the results in section 4.2.2. Although there exist fine and star-triangulations with nine l-vectors for the three-loop banana diagram, we nevertheless applied our criteria on a non-simplicial cone. Also in the three-loop case the criteria select a proper set of nine l-vectors yielding the same results as presented in section 4.2.3 computed from a triangulation with minimal number of mori cone generators.

Now the restriction onto the physical moduli space starts with using the inequalities (4.1.41) such that the holomorphic solution (4.1.40) is evaluated exactly in the physical relevant Batyrev coordinates. Having found this period on the physical slice we search for operators annihilating it such that the set of common solutions to these operators form a basis of the periods on the physical slice. This finally yields a basis of periods on the physical moduli space. It is quite hard to give a universal description of these operators. In general they form a differential operator ideal of linear, homogeneous differential operators and their explicit form as for example their degree depend on the representation of the ideal. For our discussion we write down an ansatz for a differential operator in terms of logarithmic derivatives of the remaining Batyrev coordinates. Thereby, we start with second order operators with polynomial coefficients which we make of smallest degree as possible. Typically, this ansatz yields a large number of possible operators from which we have to take a generating set of the differential ideal. From cohomology arguments we expect as many single logarithmic solutions as the number of interesting physical parameters, which strongly depends on the concrete banana diagram. Therefore, we take as many operators until their number of logarithmic solutions fits to the cohomological prediction. If the resulting solutions do still not satisfy all expectations, e.g. the number of higher logarithmic solutions, one has to extend the set of operators with higher degree ones until all expected solutions are determined. In this way one finds a generating set of operators for the differential ideal describing the physical periods. This part of our method depends strongly on the given form of the physical holomorphic period which is why we refer to our examples. We only remark that later it is crucial that the operators and the physical solutions are expressed in the remaining physical Batyrev coordinates.

4.1.4 The complete banana diagram and inhomogeneous differential equations

So far, we have found a complete differential ideal with solutions spanning a basis of the physical periods. Or said differently, these functions after dividing by the inner point describe the maximal cut integral $\mathcal{F}_{T^l}$. Now we extend our method to find the missing functions which complete the function space for the full banana Feynman diagram $\mathcal{F}_{\sigma_l}$. By function space we mean a set of functions which suitably combined yield the complete banana Feynman integral (4.1.20). It turns out that for the banana graphs there is only a single additional function we

have to compute.

Basically, we extend the homogeneous differential ideal to a set of inhomogeneous differential operators such that its solutions describe the full Feynman graph. These inhomogeneities are found from the appropriate homogeneous operator by the following process: We let an operator directly act on the geometric differential, which is given as the integrand of (4.1.53), and perform then the integration over the domain σ_l. In this way we obtain for every homogeneous operator a corresponding inhomogeneous one.

For this task the original parametrization of the differential is changed to the Batyrev coordinates (4.1.35). This has a major advantage in the following. After applying the operators on the differential we can integrate over the simplex σ_l. In contrast to a period integral the integration range of the complete Feynman graph is not closed and such we get non zero after integration. Unfortunately, these integrals can not be carried out analytically with generic parameters. But they can be performed easily numerically. The advantage of including the inner point and using the Batyrev coordinates is now that the numerical results can simply be guessed. We claim that for the l-loop banana integrals they are only given as linear combinations of logarithms in the Batyrev coordinates. In our calculated examples given in section 4.2 we could always guess the inhomogeneities yielding a full set of inhomogeneous operators.

In the literature there are already some methods known for computing relative periods in a way that homogeneous differential equations describing usual periods are extended to inhomogeneous ones. For examples in [12] a method for general toric varieties is explained how to extend the GKZ method to relative periods. The key point for this method is the l-vector description of the variety and its relative cohomology. The l-loop banana diagrams are not entirely described through l-vectors and therefore this method can not be applied. Moreover, there is the Dwork-Griffith reduction to obtain the homogeneous differential equations which then can analogously be extended to inhomogeneous ones as in our method [3]. Although Dwork-Griffith reduction can in principle be applied in any situation as explained before, for computational reasons only the sunset graph can explicitly be done. Compared with known methods our strategy uses the structure of the l-loop banana diagrams more efficiently and produces results also for high loop orders.

Having found the inhomogeneous operators its solutions are given by the solutions of the homogeneous operators together with a single special solution of the inhomogeneous system. A special solution is found by an ansatz which has a similar logarithmic structure as the homogeneous solutions. Only the power of the highest appearing logarithm is increased by one compared to the other solutions. This closes the set of functions describing the l-loop banana Feynman graph.

Our method gives a relatively small set of functions necessary to compute the banana graphs. For example, with numerical computations the correct linear combination of these functions evaluating to the Feynman graph can be fixed. We exemplify this on the sunset graph in section 4.2.2. Moreover, a detailed analysis of the analytic structure of these functions based on the inhomogeneous differential equations can be elaborated and produce new insights of the Feynman graph, for instance branch cuts or singularities representing particle productions.

4.2 Examples

In this chapter we apply the GKZ method on three different examples, the one-, two- and three-loop banana diagram. This demonstrates how our general method is applied on explicit Feynman integrals and moreover shows the power of our method. For the reader the difficulty of our examples increases with the loop order and new appearing issues are highlighted and discussed case by case.

4.2.1 Example 1: The bubble graph

As the first example we discuss the one-loop banana diagram which is also called the bubble graph. This Feynman diagram can also be calculated directly with usual Feynman graph techniques [43]. Nevertheless, we will use this simple example to introduce our method.

In the Feynman parametrization the bubble integral is given by

$$\begin{aligned}\mathcal{F}_{\sigma_1}(t,\xi_1,\xi_2) &= \int_{x,y\geq 0} \frac{x\mathrm{d}y - y\mathrm{d}x}{xy\left(t-(\xi_1^2 x+\xi_2 y^2)(\frac{1}{x}+\frac{1}{y})\right)} \\ &= -\xi_1\xi_2 \int_{x,y\geq 0} \frac{x\mathrm{d}y - y\mathrm{d}x}{x^2+uxy+y^2}\ ,\end{aligned} \tag{4.2.1}$$

where in the second line the coordinates are rescaled and $u = \frac{\xi_1^2+\xi_2^2-t}{\xi_1\xi_2}$ is introduced.

Following our method we associate to the bubble graph (4.2.1) the polynomial constrain

$$P_1 = x^2 + uxy + y^2 \tag{4.2.2}$$

in projective space $\mathbb{P}$. For generic values of the parameter u this defines two different points in $\mathbb{P}$. It looks a bit artificial but we can give a toric description of this algebraic variety consisting of two points. We take the Newton polytope of (4.2.2) which is shown in Figure 4.2.1.

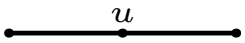

Figure 4.2.1: The toric diagram for the bubble graph

It has a single l-vector and Batyrev coordinate

$$l = (-2;1,1) \quad \text{and} \quad z = \frac{1}{u^2}\ . \tag{4.2.3}$$

As explained in section 4.1 we expect two functions spanning the function space of the bubble graph. One is coming from the maximal cut integral and the other one is a special solution of the inhomogeneous differential equation corresponding to the bubble graph. Furthermore,

there is only a single true parameter for which we take naturally the Batyrev coordinate z from (4.2.3).

The holomorphic period can be computed directly from the integral or from the l-vector (4.2.3)

$$\begin{aligned}\varpi &= \frac{1}{2\pi i}\int_{S^1}\frac{x\mathrm{d}y - y\mathrm{d}x}{\sqrt{z}(x^2+y^2)+xy} = -\frac{1}{2\pi i}\int_{S^1}\frac{1}{1+\sqrt{z}(v+\frac{1}{v})}\frac{\mathrm{d}v}{v} \\ &= -\frac{1}{2\pi i}\int_{S^1}\sum_{n=0}^{\infty}\sum_{m=0}^{n}(-1)^n\binom{n}{m}z^{n/2}v^{2m-n}\frac{\mathrm{d}v}{v} = -\sum_{n=0}^{\infty}\frac{(2n)!}{(n!)^2}z^n = -\frac{1}{\sqrt{1-4z}}\ ,\end{aligned} \tag{4.2.4}$$

where we have introduced the variable $v = \frac{x}{y}$. Moreover, ϖ satisfies the first order differential equation

$$\mathcal{D}\varpi = (1-4z)\theta\varpi - 2z\varpi = 0 \tag{4.2.5}$$

with the logarithmic derivative $\theta = z\partial_z$.

Now we apply the operator $\mathcal{D}$ from (4.2.5) on the integrand of the geometrical chain integral (4.1.53) containing the inner point of the polytope u expressed through the Batyrev coordinate z. At the end we relate this expression to the bubble graph simply by dividing through the inner point. Fortunately, the integral in the bubble case can be computed analytically

$$\mathcal{D}\Pi_{\sigma_1} = \mathcal{D}\int_{x,y\geq 0} u\frac{x\mathrm{d}y - y\mathrm{d}x}{x^2+uxy+y^2} = \int_{x,y\geq 0}\mathcal{D}\frac{x\mathrm{d}y - y\mathrm{d}x}{\sqrt{z}(x^2+y^2)+xy} = 1\ . \tag{4.2.6}$$

This extends the homogeneous differential equation (4.2.5) to an inhomogeneous one

$$(1-4z)\theta\ \Pi_{\sigma_1}(z) - 2z\ \Pi_{\sigma_1}(z) = 1\ . \tag{4.2.7}$$

A special solution to this inhomogeneous differential equation is given by

$$\varpi_S = \varpi\log(z) + 2z + 7z^2 + \tfrac{74}{3}z^3 + \tfrac{533}{3}z^4 + \cdots\ . \tag{4.2.8}$$

Then the general solution to the inhomogeneous differential equation (4.2.7) is given by $\Pi_{\sigma_1} = \varpi_S + \lambda\varpi$ with $\lambda \in \mathbb{C}$. We can relate this solution to the bubble graph by dividing with the inner point u and rescaling it by $-\xi_1\xi_2$. The parameter λ can be fixed by calculating the bubble graph (4.2.1) at a special point in moduli space, for example $u = 1$.

In the literature [55] the l-loop banana diagrams were analyzed in the equal mass case, i.e. $\xi_i = 1$ for $i = 1, \ldots l+1$. The one-loop bubble diagram satisfies the inhomogeneous first order equation

$$t(t-4)f_1'(t) + (t-2)f_1(t) = -2!\ . \tag{4.2.9}$$

After dividing Π_{σ_1} by the inner point this is exactly the differential equation it satisfies.

4.2.2 Example 2: The sunset graph

Our second example deals with the two-loop Banana diagram also known as the sunset graph. A different discussion of the sunset graph is given in [3] from which we adopt parts of our notation.

The sunset Feynman graph is defined by

$$\mathcal{F}_{\sigma_2}(t,\xi_1,\xi_2,\xi_3) = \int_{\sigma_2} \frac{\mu_2}{P_2(t,\xi_1,\xi_2,\xi_3;x)} = \int_{\sigma_2} \frac{x\mathrm{d}y\wedge\mathrm{d}z - y\mathrm{d}x\wedge\mathrm{d}z + z\mathrm{d}x\wedge\mathrm{d}y}{xyz\left(t-(\xi_1^2x+\xi_2^2y+\xi_3^2z)(\frac{1}{x}+\frac{1}{y}+\frac{1}{z})\right)} , \tag{4.2.10}$$

with the integration domain defined in (4.1.21). It can be interpreted as a relative period on an elliptic curve defined by the polynomial constraint

$$P_2 = txyz - \xi_1^2x^2y - \xi_1^2x^2z - \xi_1^2xyz - \xi_2^2xy^2 - \xi_2^2xyz - \xi_2^2y^2z - \xi_3^2xyz - \xi_3^2xz^2 - \xi_3^2yz^2 \tag{4.2.11}$$

in an ambient space given by two-dimensional projective space $\mathbb{P}^2$ as explained in section 4.1.3. Our approach is strongly based on this geometric interpretation. For convenience we rescale the coordinates and introduce a simpler parametrization of the elliptic curve. The polynomial is then given as

$$P_2 = xy^2 + yz^2 + x^2z + m_1xz^2 + m_2x^2y + m_3y^2z + uxyz \ . \tag{4.2.12}$$

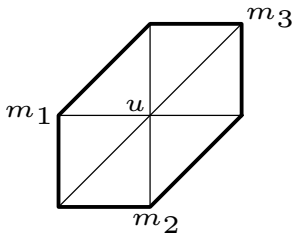

Figure 4.2.2: Toric diagram for the sunset graph

We notice that the polynomial (4.2.12) describes the blow up of $\mathbb{P}^2$ in three points which we call in the following $\mathcal{E}_{B3}$. In [56] a nice analysis of the different blow ups of $\mathbb{P}^2$ is carried out from which we can extract same information for the toric description. In Figure 4.2.2 the polyhedron corresponding to (4.2.12) is shown. The polyhedron's vertices are given by

$$\nu_2 = \{(0,-1),(1,0),(1,1),(0,1),(-1,0),(-1,-1),(0,0)\} \ . \tag{4.2.13}$$

The corresponding Mori cone generators are given by

$$\begin{aligned} \tilde{l}_1 &= (1,-1,1,0,0,0,-1)\ , & \tilde{l}_2 &= (0,1,-1,1,0,0,-1) \\ \tilde{l}_3 &= (0,0,1,-1,1,0,-1)\ , & \tilde{l}_4 &= (0,0,0,1,-1,1,-1) \\ \tilde{l}_5 &= (1,0,0,0,1,-1,-1)\ , & \tilde{l}_6 &= (-1,1,0,0,0,1,-1) \end{aligned} \tag{4.2.14}$$

generating a non-simplicial cone. From the general discussion in section 4.1.3 we only need four independent l-vectors and also that in all columns of (4.2.14) except the one corresponding to the inner point there is at least one positive entry. This does still not yield a distinct choice of four l-vectors but all of them can be used. We take for our collection of four l-vectors the ones which restrict to the Mori cone generators of the cubic in $\mathbb{P}^2$ and the other blow ups of $\mathbb{P}^2$ in one and two points. So we take in the following the four l-vectors

$$l_1 = \tilde{l}_1\ , \quad l_2 = \tilde{l}_2\ , \quad l_3 = \tilde{l}_3 \quad \text{and} \quad l_4 = \tilde{l}_4\ . \tag{4.2.15}$$

Toric geometry singles out a natural choice of parametrization of the algebraic variety given by the Batyrev coordinates (4.1.35). These parameters are related to the ones in (4.2.11) and (4.2.12) by

$$\begin{aligned} z_1 = -\tfrac{m_2 m_3}{u} &= -\tfrac{\xi_1^2}{\xi_1^2+\xi_2^2+\xi_3^2-t}\ , & z_2 = -\tfrac{1}{um_3} &= -\tfrac{\xi_3^2}{\xi_1^2+\xi_2^2+\xi_3^2-t} \\ z_3 = -\tfrac{m_1 m_3}{u} &= -\tfrac{\xi_2^2}{\xi_1^2+\xi_2^2+\xi_3^2-t}\ , & z_4 = -\tfrac{1}{um_1} &= -\tfrac{\xi_1^2}{\xi_1^2+\xi_2^2+\xi_3^2-t}\ . \end{aligned} \tag{4.2.16}$$

Upon collecting the main toric information of our problem we can start with our strategy. The first part of our strategy will be the computation of the periods corresponding to the maximal cut integral.

Let us note here in passing that in the elliptic curve case it is not necessary to solve any differential equation to obtain the period integrals and hence the mass dependence of the maximal cut integral. The periods are completely determined by modular functions as follows from [56]: We can bring the constraint $P_2 = 0$ (4.2.12) defining the elliptic curve into Weierstrass form $y^2 = 4x^3 - x g_2(u,\underline{m}) - g_3(u,\underline{m})$. This defines the modular parameter $\tau(u,\underline{m})$ from the definition of the Hauptmodul j of $\mathrm{PSL}(2,\mathbb{Z})$ as

$$\frac{1728 g_3^2(u,\underline{m})}{g_2^3(u,\underline{m}) - 27 g_3^2(u,\underline{m})} = j = \frac{1}{q} + 744 + 192688 q + 21493760 q^2 + \mathcal{O}(q^3)\ , \tag{4.2.17}$$

where $q = \exp(2\pi i \tau)$. Then the period $\int_a \Omega/u$ which yields the maximal cut integral is given in terms of the Eisenstein series as

$$\partial_u t(u) = \int_a \Omega = \sqrt{\frac{E_6(\tau(u,\underline{m})) g_2(u,\underline{m})}{E_4(\tau(u,\underline{m})) g_3(u,\underline{m})}}\ . \tag{4.2.18}$$

Moreover, the dual period $\int_b \Omega$ can be obtained by special geometry of non-compact three-folds as $\partial_t \int_b \Omega = -\frac{1}{2\pi i}\tau(u,\underline{m})) = \partial_t^2 F(t)$, where F is the prepotential that features in local mirror symmetry as generating function for the genus zero BPS invariants n_0^β, which is given by

$$F(Q) = -\frac{c^{ijk}}{3!}t_i t_j t_k + \frac{c^{ij}}{2}t_i t_j + c^i t_i + c \sum_{\beta \in H_2(W,\mathbb{Z})} n_0^\beta \mathrm{Li}_3(Q^\beta) \ . \tag{4.2.19}$$

Here t_i are the flat coordinates, $Q_i = \exp(t_i/2\pi i)$ and the c^* are classical intersection numbers on the mirror W. In [56] the Kähler classes t_i for $i = 1, \ldots, 4$ of the mirror have been identified. These are linearly related to the Batyrev coordinates (4.2.16). With $Q_i = \exp(t_i/2\pi i)$ they relate to the physical parameters as

$$Q = (Q_1 Q_2 Q_3 Q_4)^{\frac{1}{3}} \ , \quad m_1 = \frac{(Q_1 Q_3 Q_4)^{\frac{1}{3}}}{Q_2^{\frac{2}{3}}} \ , \quad m_2 = \frac{(Q_1 Q_2 Q_4)^{\frac{1}{3}}}{Q_3^{\frac{2}{3}}} \ , \quad m_3 = \frac{(Q_1 Q_2 Q_3)^{\frac{1}{3}}}{Q_4^{\frac{2}{3}}} \ . \tag{4.2.20}$$

This allows to relate the full integer genus zero BPS expansion n_0^β in the four Kähler parameters [56]

$$\begin{aligned} F \ = & \ cl. + L_{0,0,0,1} + L_{1,0,0,1} - 2L_{1,0,1,1} + 3L_{1,1,1,1} + 3L_{2,1,1,1} - 4L_{2,1,1,2} + 5L_{2,1,2,2} \\ & -6L_{2,2,2,2} + 5L_{3,1,2,2} - 6L_{3,1,2,3} + 7L_{3,1,3,3} - 36L_{3,2,2,2} + 35L_{3,2,2,3} - 32L_{3,2,3,3} \\ & +27L_{3,3,3,3} + 7L_{4,1,3,3} - 8L_{4,1,3,4} + 9L_{4,1,4,4} - 6L_{4,2,2,2} + 35L_{4,2,2,3} \\ & -32L_{4,2,2,4} - 160L_{4,2,3,3} + 135L_{4,2,3,4} - 110L_{4,2,4,4} + 531L_{4,3,3,3} \\ & -400L_{4,3,3,4} + 286L_{4,3,4,4} - 192L_{4,4,4,4} + \mathrm{Sym}_{ijk}(L_{a,i,j,k}) + \cdots \end{aligned} \tag{4.2.21}$$

to the full set of physical parameters. Here $L_\beta \coloneqq \mathrm{Li}_3(\prod_{i=1}^4 Q_i^{\beta_i})$. In [48] BPS invariants are given for the projective parametrization n_{ijk}. The relation to the geometrical BPS invariants is $\sum_a n_0^{aijk} = n_{ijk}$. It is clear from (4.2.20) and the symmetries of the polytop that the last formula is symmetric in the ijk indices. Moreover, the one parameter specialization also noted in [48] is given by $n_d = \sum_{a,i+j+k=d} n_0^{aijk}$. While we think that in the elliptic two-loop case this relation of the BPS expansion to the Feynman graph is remarkable but not very useful, it becomes more useful for the higher loop banana graphs as we explain in section 4.2.3.

The sunset maximal cut integral

The maximal cut integral of the sunset graph $\mathcal{F}_{T^2}(t, \xi_1, \xi_2, \xi_3)$ is defined by replacing the simplex σ_2 by a torus T^2. Instead of focusing on the maximal cut Feynman graph we rather deal with the related geometrical period which includes additionally the inner point u of the toric diagram. The expression

$$\Pi(T^2)(u, m_1, m_2, m_3) = \int_{T^2} u \frac{x\mathrm{d}y \wedge \mathrm{d}z - y\mathrm{d}x \wedge \mathrm{d}z + z\mathrm{d}x \wedge \mathrm{d}y}{xy^2 + yz^2 + x^2 z + m_1 xz^2 + m_2 x^2 y + m_3 y^2 z + uxyz} \tag{4.2.22}$$

describes a "usual" period on the elliptic curve $\mathcal{E}_{B3}$ and it is easily related to the maximal cut

integral $\mathcal{F}_{T^2}$ by dividing with u. At the point of maximal unipotent monodromy the geometrical period $\Pi(T^2) = \varpi$ is given by a single holomorphic power series (4.1.40). Evaluating the period (4.2.22) at a generic point in moduli space requires the knowledge of a period basis. Such a period basis can be found as follows: Homology theory of a generic elliptic curve tells us that there exists only a pair of one-cycles, i.e. $H_2(T^2) = \mathbb{Z}^2$. So if we take the $(1,0)$-form $\frac{a_0\mu_2}{P_2}$ with a_0 the inner point of the polytope and P_2 the hypersurface constraint defining the elliptic curve there are only two independent periods. Here it is important to remark that for elliptic curves this statement is independent of the parametrization, in particular, independent of the number of moduli. For the geometrical period $\Pi(T^2)$ and therefore also for the maximal cut integral $\mathcal{F}_{T^2}$ this means that there are two independent functions which linearly combined yield (4.2.22) at a generic point in moduli space.

In our toric analysis it is convenient to use the Batyrev parameters defined in (4.2.16). Later we will see that the usage of this particular choice of parametrization enables us to fully determine the sunset graph. Moreover, it simplifies many of the subsequent results.

From the Mori cone generators (4.2.15) one can directly write down the holomorphic period at the point of maximal unipotent monodromy given by

$$\begin{aligned}\varpi(\underline{z}) = \sum_{\underline{m}\geq 0} &\frac{\Gamma\left(1+m_1+m_2+m_3+m_4\right)}{\Gamma\left(1+m_1\right)\Gamma\left(1-m_1+m_2\right)\Gamma\left(1+m_1-m_2+m_3\right)\Gamma\left(1+m_3-m_4\right)} \\ &\cdot \frac{1}{\Gamma\left(1+m_4\right)\Gamma\left(1+m_2-m_3+m_4\right)} z_1^{m_1} z_2^{m_2} z_3^{m_3} z_4^{m_4}\end{aligned} \tag{4.2.23}$$

with the abbreviations $\underline{z} = (z_1, z_2, z_3, z_4)$ and $\underline{m} = (m_1, m_2, m_3, m_4)$. This is the most generic four-parameter holomorphic period of $\mathcal{E}_{B3}$. The geometrical period (4.2.22) has one less parameter since one-parameter can be scaled away. Therefore, we have to specialize the four-parameter solution (4.2.23) to a three-parameter one. We remark that from (4.2.16) the parameters z_1 and z_4 have the same value if expressed in the physical parameters. This means that the four-parameter solution (4.2.23) specialized on the subslice with $z_1 = z_4$ corresponds to the holomorphic solution of the geometrical period (4.2.22) at the maximal unipotent monodromy point.

This subslice is not as problematic as for the higher loop banana graphs because the sum over m_4 still contains a parameter, here z_1. But still we can use the Γ-functions in (4.2.23) to bound the summation over the index m_4 by $m_3 - m_4 \geq 0$. We obtain for the first few orders

$$\begin{aligned}\varpi(z_1, z_2, z_3) = 1 &+ 2z_1z_2 + 2z_1z_3 + 2z_2z_3 + 12z_1z_2z_3 \\ &+ 6z_1^2z_2^2 + 24z_1^2z_2z_3 + 24z_1z_2^2z_3 + 6z_1^2z_3^2 + 24z_1z_2z_3^2 + 6z_2^2z_3^2 + \cdots .\end{aligned} \tag{4.2.24}$$

Now our strategy is as follows: We compute the holomorphic solution to high order such that we can find a set of differential operators annihilating it. This set of differential operators has to be complete in a sense that its solutions form a basis of period integrals on the elliptic curve $\mathcal{E}_{B3}$. Therefore, a suitable ansatz for these operators is crucial. Again homology theory of the elliptic curve tells us what kind of solutions we expect and so the rare form of the operators. For $\mathcal{E}_{B3}$ only two solutions exist. At the point of maximal unipotent monodromy

the analytic structure of them is also known. One is a holomorphic function in the parameters and the other contains single logarithms of the parameters. For the differential operator ideal this implies that we are searching for first order operators in the parameters (z_1, z_2, z_3). Having found the first few operators one has to increase the number of operators until they are enough to fully determine the two different periods. As a possible generating set of the ideal we find

$$\begin{aligned}
\mathcal{D}_1 &= \theta_1 - \theta_2 + z_2\left(\theta_1 - \theta_2 + \theta_3 + 2z_3\left(\theta_1 + \theta_2 + \theta_3 + 1\right)\right) \\
&\quad - z_1\left(-\theta_1 + \theta_2 + \theta_3 + 2z_3\left(\theta_1 + \theta_2 + \theta_3 + 1\right)\right) \\
\mathcal{D}_2 &= \theta_2 - \theta_3 + z_3\left(\theta_1 + \theta_2 - \theta_3\right) - z_2\left(\theta_1 - \theta_2 + \theta_3\right) - 2z_1\left(z_2 - z_3\right)\left(\theta_1 + \theta_2 + \theta_3 + 1\right) \\
\mathcal{D}_3 &= \left(\theta_1 - \theta_2\right)\left(\theta_1 + \theta_2 - \theta_3\right) + z_1\left(\theta_1 - \theta_2 - \theta_3\right)\left(\theta_1 + \theta_2 + \theta_3 + 1\right) \\
&\quad + z_2\left(\theta_1 - \theta_2 + \theta_3\right)\left(\theta_1 + \theta_2 + \theta_3 + 1\right)
\end{aligned} \tag{4.2.25}$$

with $\theta_i = z_i\partial_{z_i}$ for $i = 1, 2, 3$. The missing period is then given by

$$\Pi(\Gamma_1)(z_1, z_2, z_3) = \varpi\left(\log(z_1) + \log(z_2) + \log(z_3)\right) + \Sigma_1 \tag{4.2.26}$$

with

$$\begin{aligned}
\Sigma_1 &= z_1 + z_2 + z_3 - \tfrac{z_1^2}{2} + 7z_1z_2 + 7z_1z_3 - \tfrac{z_2^2}{2} + 7z_2z_3 - \tfrac{z_3^2}{2} \\
&\quad + \tfrac{z_1^3}{3} + 3z_1^2z_2 + 3z_1^2z_3 + 3z_1z_2^2 + 3z_1z_3^2 + 48z_1z_2z_3 + \tfrac{z_2^3}{3} + \tfrac{z_3^3}{3} + 3z_2z_3^2 + 3z_2^2z_3 + \cdots .
\end{aligned} \tag{4.2.27}$$

These two solutions (4.2.24) and (4.2.26) form a basis of the periods for the elliptic curve $\mathcal{E}_{B3}$. Using the relations (4.2.16) we can divide by the inner point and transform this basis to the necessary point in moduli space such that they can be linearly combined to yield the maximal cut integral $\mathcal{F}_{T^2}$.

In the next section we extend the differential operator ideal (4.2.25) such that it governs all functions describing the full geometrical sunset Feynman graph Π_{σ_2}. By dividing with the inner point we can transfer these results to the actual Feynman integral (4.2.10).

Extension to inhomogeneous differential operators

As explained in section 4.1.4 we find as the first step the inhomogeneities of the operators (4.2.25). Again we use the Batyrev coordinates (z_1, z_2, z_3) which is crucial for the applicability of our method. We apply the operators (4.2.25) on the geometrical differential $\frac{u\mu_2}{P_2}$ and integrate afterwards over the two-dimensional simplex σ_2. These chain integrals can not in general be computed analytically with generic parameters but numerical evaluations of these integrals for fixed values of the parameters are possible. Now the advantage of the Batyrev coordinates is that we can guess the exact values of the numerical results. We claim that the differential operator ideal only produces simple logarithmic expressions in the Batyrev

coordinates (z_1, z_2, z_3). For (4.2.25) we find the following inhomogeneities[13]

$$\begin{aligned}\mathcal{D}_1\Pi_{\sigma_2} &= -\log(z_2) + \log(z_3)\\ \mathcal{D}_2\Pi_{\sigma_2} &= -\log(z_1) + \log(z_2)\\ \mathcal{D}_3\Pi_{\sigma_2} &= 0\ .\end{aligned} \tag{4.2.28}$$

We think that in another parametrization, for instance the physical parameters (t, ξ_1, ξ_2, ξ_3), and without the inner point these integrals can neither be computed analytically nor their numerical values can be guessed. Only the geometrical differential in the special parametrization with the Batyrev parameters guarantees the feasibility of our method.

Having found the complete set of inhomogeneous differential operators their solutions can be computed easily. One has to extend the solutions of the homogeneous system (4.2.25) by a special solution satisfying (4.2.28). As an ansatz for this solution we increase the power of logarithms in (z_1, z_2, z_3) up to two. Then we find as a possible choice of special solution

$$\begin{aligned}\varpi_S(z_1,z_2,z_3) = &\left(\log(z_1)\log(z_2) + \log(z_1)\log(z_3) + \log(z_2)\log(z_3)\right)\varpi_0\\ &+ 2\log(z_1) + 2\log(z_2) + 2\log(z_3) + 2z_1\log(z_1) + 2z_2\log(z_2) + 2z_3\log(z_3)\\ &- \tfrac{z_1^2}{2} + 10z_1z_2 - \tfrac{z_2^2}{2} + 10z_1z_3 - \tfrac{z_3^2}{2} - z_1^2\log(z_1) + 10z_1z_2\log(z_1)\\ &+ 10z_1z_3\log(z_1) + 6z_2z_3\log(z_1) + 10z_1z_2\log(z_2) - z_2^2\log(z_2) + 6z_1z_3\log(z_2)\\ &+ 10z_2z_3\log(z_2) + 6z_1z_3\log(z_3) + 10z_1z_3\log(z_3) + 10z_2z_3\log(z_3) - z_3^2\log(z_3) + \cdots\ .\end{aligned} \tag{4.2.29}$$

The general solution is then a linear combination of the form $\Pi_{\sigma_2} = \varpi_S + \lambda_0\varpi + \lambda_1\Pi(\Gamma_1)$ with $\lambda_0, \lambda_1 \in \mathbb{C}$. We can express Π_{σ_2} through the physical parameters (t, ξ_1, ξ_2, ξ_3) and divide it by the inner point to find the full sunset Feynman graph $\mathcal{F}_{\sigma_2}$ (4.2.10).

Comparison with the equal mass case and other known results

Many results about the sunset graph are already known in the literature [4, 57]. In particular, the equal mass case meaning $\xi_i = 1$ for $i = 1, 2, 3$ was analyzed many times. In this case, the maximal cut integral is up to a factor of $u = t - 3$ (4.1.36) the holomorphic period of the Barth-Nieto elliptic curve that can be represented as in (4.1.37). The equal mass sunset graph has to satisfy an inhomogeneous second order differential equation [55] in the momentum variable t

$$t(t-1)(t-9)f_2''(t) + (3t^2 - 20t + 9)f_2'(t) + (t-3)f_2(t) = -3!\ . \tag{4.2.30}$$

Our three-parameter solutions (4.2.24), (4.2.26) and (4.2.29) break down in the equal mass

[13] We checked this numerically up to more than 15 digits and for different values of the variables z_i for $i = 1, 2, 3$.

case[14] to the solutions of (4.2.30). This shows that they reproduces the well established equal mass results.

For the sunset graph a second test is possible since in [3] an inhomogeneous differential equation in all physical parameters is given which the sunset graph has to satisfy. Here we notice that our holomorphic and single logarithmic solutions expressed in the physical parameters fulfill this equation. The special solution (4.2.29) does not. A direct comparison between our special solution and the solutions to the inhomogeneous differential equation in [3] shows that the discrepancy between them is only in the terms having no logarithm in the variable $s = 1/t$. Such a small difference can be a result of a typo in the polynomials given in [3] but a general mistake in their derivation of the inhomogeneous differential equation can not be excluded.

$\Pi_{\sigma_2} = \lambda_S \varpi_S + \lambda_0 \varpi_0 + \lambda_1 \Pi(\Gamma_1)$	λ_S	λ_0	λ_1
order 5	0.9998	$-29.6275 + 42.7536i$	$-13.6122 - 18.8466i$
order 10	1.0000	$-29.6088 + 42.7407i$	$-13.6048 - 18.8496i$
order 5	$1.0004 + 0.0007i$	$70.0913 + 109.3340i$	$-34.7859 - 18.8389i$
order 10	$1.0004 + 0.0007i$	$70.0913 + 109.3340i$	$-34.7859 - 18.8389i$

Table 4.2.1: Linear combination of solutions for the sunset graph. In the first two rows are the values for our solutions whereas the last two give the ones for the solutions from [3].

To demonstrate the correctness of our solutions we made some numerical checks. We evaluated the sunset Feynman graph (4.2.10) at three different points[15] to fix the linear combination of our three solutions[16]. Having found the right combination of solutions given in Table 4.2.1 we checked for further values of the parameters and compare the precision for different expansion orders of $\varpi, \Pi(\Gamma_1)$ and ϖ_S. Our results are listed in Table 4.2.2. Notice, that it is important that the value of one ξ_i is fixed since there are only three physical degrees of freedom after rescaling. We choose ξ_3 to be fixed. With increasing expansion order our solutions fit better and better to the sunset graph which we could not observe for the solutions of [3]. Moreover, the factor λ_S of the special solution ϖ_S tends to the value one as expected.

[14] Notice that before one can apply the differential equation (4.2.30) on our solutions they have to be transformed at the same point in moduli space, which is here $t \mapsto \frac{1}{t}$.

[15] We took for the three points the values $(s, \xi_1, \xi_2, \xi_3) = (s_1 + i/10, 1/10, 1/20, 1/30)$, for $s_1 = 1/10,\ s_2 = 1/20$ and $s_3 = 1/30$.

[16] We fixed our basis of solutions such that the holomorphic solution starts with one and the constant piece in the single logarithmic solution is zero. Moreover, we fixed the special solution by requiring that the constant term and the constant term multiplied by $\log s$ is vanishing.

s, ξ_1, ξ_2, ξ_3	order 5	order 10	order 5	order 10
1/27 + i/20, 1/10, 1/20, 1/30	$9 \cdot 10^{-5}$	$5 \cdot 10^{-9}$	$2 \cdot 10^{-4}$	$2 \cdot 10^{-4}$
1/21+i/10, 1/10, 1/50, 1/30	$4 \cdot 10^{-4}$	$6 \cdot 10^{-9}$	30	30
1/24+i/10, 1/10+i/15,1/20,1/30	$6 \cdot 10^{-4}$	$5 \cdot 10^{-9}$	22	22

Table 4.2.2: The table shows how precise the relative periods combined as listed in Table 4.2.1 describe the Feynman graph. We show the absolute value of the difference between the numerical computation of the sunset graph and the evaluation of the linear combination of solutions. Increasing the expansion order increases the precision of our results given as the second and third column. The last columns give the results from [3] which do not increase their precision.

4.2.3 Example 3: The three-loop banana graph

As our last and most complicated example we demonstrate the applicability of our approach for the three-loop banana diagram

$$\mathcal{F}_{\sigma_3}(t, \xi_1, \xi_2, \xi_3, \xi_4) = \int_{\sigma_3} \frac{x\mathrm{d}y \wedge \mathrm{d}z \wedge \mathrm{d}w - y\mathrm{d}x \wedge \mathrm{d}z \wedge \mathrm{d}w + z\mathrm{d}x \wedge \mathrm{d}y \wedge \mathrm{d}w - w\mathrm{d}x \wedge \mathrm{d}y \wedge \mathrm{d}z}{xyzw \left(t - (\xi_1^2 x + \xi_2^2 y + \xi_3^2 z + \xi_4^2 w)(\frac{1}{x} + \frac{1}{y} + \frac{1}{z} + \frac{1}{w})\right)} \ . \tag{4.2.31}$$

The three-loop banana Feynman graph (4.2.31) can again be interpreted as a relative period now on a K3 surface. This K3 surface is defined by the constraint P_3 from the denominator in (4.2.31). After a rescaling of the coordinates we obtain

$$\begin{aligned} P_3 = {} & x^2yz + xyw^2 + xzw^2 + yzw^2 + m_1xy^2w + m_2x^2zw + m_3yz^2w + m_4x^2yw \\ & + m_5xz^2w + m_6y^2zw + m_7xy^2z + m_8xyz^2 + uxyzw \ . \end{aligned} \tag{4.2.32}$$

The polytope P_{Δ_3} corresponding to the banana graph together with a triangulation is shown in Figure 4.2.3. Its vertices are given by

$$\begin{aligned} \nu_3 = {} & \{(-1,1,0), (1,0,0), (0,-1,1), (0,0,1), (1,-1,0), (1,0,-1), (0,0,-1), (-1,0,1), \\ & (0,-1,0), (-1,0,0), (0,1,0), (0,1,-1), (0,0,0)\} \ . \end{aligned} \tag{4.2.33}$$

Furthermore, the Mori cone generators corresponding to the triangulation drawn in the polytope in Figure 4.2.3 are given by

$$\begin{aligned} l_1 &= (0,0,-1,0,1,0,0,1,0,0,0,0,-1) \ , & l_2 &= (0,-1,0,0,1,0,0,0,0,0,1,0,-1) \\ l_3 &= (0,-1,0,1,0,1,0,0,0,0,0,0,-1) \ , & l_4 &= (0,0,-1,1,0,0,0,0,1,0,0,0,-1) \\ l_5 &= (-1,0,0,-1,0,0,0,1,0,0,1,0,0) \ , & l_6 &= (0,0,0,0,-1,1,-1,0,1,0,0,0,0) \\ l_7 &= (0,0,1,0,0,0,0,-1,-1,1,0,0,0) \ , & l_8 &= (0,1,0,0,0,-1,0,0,0,0,-1,1,0) \\ l_9 &= (1,0,0,0,0,0,1,0,0,-1,0,-1,0) \ . \end{aligned} \tag{4.2.34}$$

They form a simplicial Mori cone generated by 3^2 vectors. For the subsequent discussion we

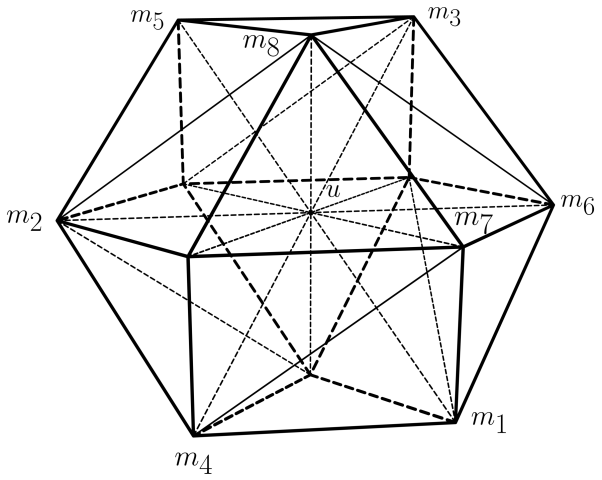

Figure 4.2.3: Toric diagram for the three-loop banana graph

need the Batyrev coordinates together with their relations to the physical paramters

$$\begin{aligned}
z_1 = -\tfrac{m_2 m_3}{m_5 u} &= -\tfrac{\xi_1^2}{\xi_1^2+\xi_2^2+\xi_3^2+\xi_4^2-t}\ , & z_5 = \tfrac{m_3 m_7}{m_6 m_8} &= 1 \\
z_2 = -\tfrac{m_2 m_7}{u} &= -\tfrac{\xi_2^2}{\xi_1^2+\xi_2^2+\xi_3^2+\xi_4^2-t}\ , & z_6 = \tfrac{m_4}{m_2} &= 1 \\
z_3 = -\tfrac{m_4 m_8}{u} &= -\tfrac{\xi_3^2}{\xi_1^2+\xi_2^2+\xi_3^2+\xi_4^2-t}\ , & z_7 = \tfrac{m_5}{m_3} &= 1 \\
z_4 = -\tfrac{m_8}{m_5 u} &= -\tfrac{\xi_4^2}{\xi_1^2+\xi_2^2+\xi_3^2+\xi_4^2-t}\ , & z_8 = \tfrac{m_1}{m_4 m_7} &= 1 \\
& & z_9 = \tfrac{m_6}{m_1} &= 1\ .
\end{aligned} \tag{4.2.35}$$

Having defined the most important information about the three-loop banana graph we want to find a set of functions describing it. We follow our general strategy but there are some subtleties which have not popped up for the sunset graph.

Maximal cut integral

As before, the maximal cut integral $\mathcal{F}_{T^3}(t,\xi_1,\xi_2,\xi_3,\xi_4)$ is related through the inner point to the K3 period integral

$$\Pi(T^3)(u,m_1,m_2,m_3,m_4) = \int_{T^3} \frac{u\mu_3}{P_3}\ . \tag{4.2.36}$$

We want to compute a basis for the periods on the K3 surface. Cohomology theory of the K3 surface can tell us again how many independent periods we expect. Differently as for elliptic curves the number of independent two-cycles depends on the number of moduli. For a r parameter model we expect $r+2$ independent two-cycles and similarly $r+2$ independent periods. Moreover, the analytic structure of these periods can be specified further. There

is exactly one holomorphic and one double logarithmic period on the K3. The remaining r periods are single logarithmic ones.

The starting point of our method is the holomorphic period expressed through the Batyrev parameters which are much more as the physical parameters. From (4.2.35) five Batyrev parameters are set to one after identification with the physical parameters. The remaining four coordinates (z_1, z_2, z_3, z_4) are related to the physical parameters and are such the only ones important in the following. From the Mori cone generators it is always possible to write down the general form of the holomorphic period but in all nine Batyrev parameters. We can expand this holomorphic solution in the "unphysical" parameters $(z_5, z_6, z_7, z_8, z_9)$ exactly and set them afterwards to one. This yields the holomorphic solution in the physically relevant four parameters. To insure that our expansion is exact in the unphysical parameters we use the particular form of the holomorphic periods in terms of Γ-functions. Since the numerator does never diverge for positive values of the index parameters $m_i,\ i = 1, \dots 9$ the Γ-functions in the denominator give bounds on the index parameters m_i. Concretely we obtain

$$\begin{aligned}\varpi(z_1, z_2, z_3, z_4) = \sum_{\mathcal{M}} & \frac{\Gamma(1+m_1+m_2+m_3+m_4)}{\Gamma(1+m_3+m_4-m_5)\Gamma(1+m_1+m_2-m_6)\Gamma(1+m_1+m_5-m_7)\Gamma(1+m_4+m_6-m_7)} \\ & \cdot \frac{z_2^{m_2} z_3^{m_3} z_4^{m_4} z_5^{m_5}}{\Gamma(1-m_1-m_4+m_7)\Gamma(1+m_2+m_5-m_8)\Gamma(1+m_3+m_6-m_8)\Gamma(1-m_2-m_3+m_8)} \\ & \cdot \frac{1}{\Gamma(1+m_7-m_9)\Gamma(1+m_8-m_9)\Gamma(1-m_5+m_9)\Gamma(1-m_6+m_9)}\end{aligned} \tag{4.2.37}$$

with the summation range given by

$$\begin{aligned}\mathcal{M} = \{ & 0 \le m_1 \le \infty,\ 0 \le m_2 \le \infty,\ 0 \le m_3 \le \infty,\ 0 \le m_4 \le \infty,\ 0 \le m_5 \le m_3 + m_4, \\ & m_2 + m_3 \le m_8 \le m_2 + m_5,\ 0 \le m_6 \le m_1 + m_2,\ m_1 + m_4 \le m_7 \le m_1 + m_5, \\ & m_6 \le m_9 \le m_7\} \ .\end{aligned} \tag{4.2.38}$$

We find

$$\begin{aligned}\varpi(z_1, z_2, z_3, z_4) = 1 & + 2\,(z_1z_2 + z_1z_3 + z_1z_4 + z_2z_3 + z_2z_4 + z_3z_4) \\ & + 12\,(z_1z_2z_3 + z_1z_2z_4 + z_1z_3z_4 + z_2z_3z_4) + \cdots \ .\end{aligned} \tag{4.2.39}$$

Then our strategy is the same as before. We expand the holomorphic solution (4.2.39) high enough that we can find a set of operators annihilating it. This time we are looking for second order operators in such a way that their solutions are given by a single holomorphic and a single double logarithmic solution and further four single logarithmic solutions. As a choice we take the operators $\mathcal{D}_1, \dots, \mathcal{D}_4$ as generators for the differential operator ideal. They are listed in appendix C. Then a period basis is given by four single logarithmic solutions

$$\begin{aligned}\Pi(\Gamma_1^1) &= \varpi \log(z_1) + \Sigma_1^1 \\ \Pi(\Gamma_1^2) &= \varpi \log(z_2) + \Sigma_1^2 \\ \Pi(\Gamma_1^3) &= \varpi \log(z_3) + \Sigma_1^3 \\ \Pi(\Gamma_1^4) &= \varpi \log(z_4) + \Sigma_1^4 \ ,\end{aligned} \tag{4.2.40}$$

with

$$\begin{aligned}\Sigma_1^1 = &-z_1 + z_2 + z_3 + z_4 + \tfrac{z_1^2}{2} + z_1z_2 + z_1z_3 + z_1z_4 - \tfrac{z_2^2}{2} + z_2z_3 + 5z_2z_4 - \tfrac{z_3^2}{2} + 5z_3z_4 - \tfrac{z_4^2}{2} \\ &- \tfrac{z_1^3}{3} - 3z_1^2z_2 - 3z_1^2z_3 - 3z_1^2z_4 + 3z_1z_2^2 + 3z_1z_3^2 + 3z_1z_4^2 + 16z_1z_2z_3 + 16z_1z_2z_4 \\ &+ 16z_1z_3z_4 + \tfrac{z_2^3}{3} + 3z_2^2z_3 + 3z_2^2z_4 + 3z_2z_3^2 + 3z_2z_4^2 + 52z_2z_3z_4 + \tfrac{z_3^3}{3} + 3z_3^2z_4 \\ &+ 3z_3z_4^2 + \tfrac{z_4^3}{3} + \cdots \ .\end{aligned} \tag{4.2.41}$$

The other Σ_1^i for $i = 2, 3, 4$ are given as permutations, namely $\Sigma_1^2 = \Sigma_1^1(z_1 \leftrightarrow z_2)$, $\Sigma_1^3 = \Sigma_1^1(z_1 \leftrightarrow z_3)$ and $\Sigma_1^4 = \Sigma_1^1(z_1 \leftrightarrow z_4)$. Additionally, there is a double logarithmic solution

$$\begin{aligned}\Pi(\Gamma_2) = \varpi\,&[\log(z_1)\log(z_2) + \log(z_1)\log(z_3) + \log(z_1)\log(z_4) + \log(z_2)\log(z_3) \\ &+ \log(z_2)\log(z_4) + \log(z_3)\log(z_4)] + \left(\Sigma_1^2 + \Sigma_1^3 + \Sigma_1^4\right)\log(z_1) \\ &+ \left(\Sigma_1^1 + \Sigma_1^3 + \Sigma_1^4\right)\log(z_2) + \left(\Sigma_1^1 + \Sigma_1^2 + \Sigma_1^4\right)\log(z_3) \\ &+ \left(\Sigma_1^1 + \Sigma_1^2 + \Sigma_1^3\right)\log(z_4) + \Sigma_2\end{aligned} \tag{4.2.42}$$

with

$$\begin{aligned}\Sigma_2 = &\,4\left(z_1z_2 + z_3z_2 + z_4z_2 + z_1z_3 + z_1z_4 + z_3z_4\right) + 6\left(2z_1^2z_2 + 2z_1^2z_3 + 2z_1^2z_4 + 2z_1z_2^2\right. \\ &+2z_1z_3^2 + 2z_1z_4^2 + 11z_2z_3z_1 + 11z_1z_2z_4 + 11z_1z_3z_4 + 2z_2z_3^2 \\ &\left.+2z_2z_4^2 + 2z_3z_4^2 + 2z_2^2z_3 + 2z_2^2z_4 + 2z_3^2z_4 + 11z_2z_3z_4\right) + \cdots \ .\end{aligned} \tag{4.2.43}$$

Together with the holomorphic period (4.2.39) this completes the period basis.

There is another very compact way of expressing the double logarithmic solution. We define the so called mirror maps

$$t_i = \tfrac{\Pi(\Gamma_1^i)}{2\pi i\varpi} \quad \text{for } i = 1, \ldots, 4 \ . \tag{4.2.44}$$

Now we can express the double logarithmic solution $\Pi(\Gamma_2)$ in terms of the mirror maps t_i for $i = 1, \ldots, 4$. For this one has to solve equation (4.2.44) for the variables z_i and plug it into $\Pi(\Gamma_2)$. One obtains

$$\Pi(\Gamma_2) = \varpi(t_1t_2 + t_1t_3 + t_1t_4 + t_2t_3 + t_2t_4 + t_3t_4) \ , \tag{4.2.45}$$

which is so simple since on a K3 surface there are no instanton corrections, see also the discussion in section 4.2.3.

Again after dividing by the inner point and a transformation into the physical parameters (4.2.35) these six basis solutions can be linearly combined to give the maximal cut integral $\mathcal{F}_{T^3}$ at all points in moduli space.

Extension to inhomogeneous differential operators

For the full three-loop banana graph we have to extend the differential operator ideal to an inhomogeneous set of operators. We find these inhomogeneities again when we apply the homogeneous system $\mathcal{D}_1, \ldots, \mathcal{D}_4$ on the geometrical differential $\frac{u\mu_3}{P_3}$ and perform afterwards an integration over the simplex σ_3. These integrals can only be performed numerically in all four Batyrev coordinates, but fortunately we can guess their exact values. They are[17]

$$\begin{aligned}
\mathcal{D}_1\Pi_{\sigma_3} &= 0 \\
\mathcal{D}_2\Pi_{\sigma_3} &= 5\log(z_1) - 5\log(z_2) \\
\mathcal{D}_3\Pi_{\sigma_3} &= \log(z_1) + \log(z_2) + \log(z_3) - 3\log(z_4) \\
\mathcal{D}_4\Pi_{\sigma_3} &= -5\log(z_3) + 5\log(z_4)\ .
\end{aligned} \tag{4.2.46}$$

These inhomogeneous differential equations describe all the functions appearing in the Feynman graph (4.2.31). The missing special solution can be computed with a triple logarithmic ansatz. For example we can take the following function

$$\begin{aligned}
\varpi_S = &- \varpi\left[\log(z_1)\log(z_2)\log(z_3) + \log(z_1)\log(z_3)\log(z_4) + \log(z_1)\log(z_3)\log(z_4)\right. \\
&\left. + \log(z_2)\log(z_3)\log(z_4)\right] - 2\left[(z_1+z_2)\left(\log(z_1)+\log(z_2)\right) + (z_1+z_3)\left(\log(z_1)+\log(z_3)\right)\right. \\
&+ (z_1+z_4)\left(\log(z_1)+\log(z_4)\right) + (z_2+z_3)\left(\log(z_2)+\log(z_3)\right) \\
&\left.+(z_2+z_4)\left(\log(z_2)+\log(z_4)\right) + (z_3+z_4)\left(\log(z_2)+\log(z_4)\right)\right] \\
&+ 2\left[(-3z_1+z_2+z_3+z_4)\log(z_1) + (z_1-3z_2+z_3+z_4)\log(z_2)\right. \\
&\left.+(z_1+z_2-3z_3+z_4)\log(z_3) + (z_1+z_2+z_3-3z_4)\log(z_4)\right] \\
&+ 12(z_1+z_2+z_3+z_4) + \cdots\ .
\end{aligned} \tag{4.2.47}$$

Again, the general solution is then a linear combination of the form $\Pi_{\sigma_3} = \varpi_S + \lambda_0\varpi + \sum_{i=1}^{4}\lambda_1^i\Pi(\Gamma_1^i) + \lambda_2\Pi(\Gamma_2)$ with $\lambda_0, \lambda_1^i, \lambda_2 \in \mathbb{C}$ for $i = 1,2,3,4$. We can express Π_{σ_3} through the physical parameters $(t, \xi_1, \xi_2, \xi_3, \xi_4)$ and divide it by the inner point to yield the full three-loop banana Feynman graph (4.2.31).

The equal mass case and general properties of the ideal of differential operators

For the three-loop banana graph not too many results are known in the literature[18]. In the equal mass case there is an inhomogeneous differential equation

$$t^2(t-4)(t-16)f_3'''(t) + (6t^3 - 90t^2 + 192t)f_3''(t) + (7t^2 - 68t + 64)f_3'(t) + (t-4)f_3(t) = -4! \tag{4.2.48}$$

[17] Also here we checked this numerically up to more than 15 digits and for different values of the variables z_i for $i = 1,2,3$.

[18] For a discussion on the maximal cut integral in the equal mass case we refere to [58].

computed in [55]. Restricting our solutions (4.2.39), (4.2.40), (4.2.42) and (4.2.47) to the equal mass case, dividing by the inner point and transform them to the point at infinity in moduli space they satisfy equation (4.2.48) showing consistency in this limit.

Let us make some general remarks on the properties of the homogeneous part of the differential operators for periods on K3. We first highlight the structure, which is related to the vanishing string world sheet instantons or unreduced Gromov-Witten invariants on K3 manifolds [59, 60], which is expected to hold more generally for hyperkähler manifolds. This together with (4.1.54) for $n = 2$ and $r = 0, 1$ implies a structure for the solutions which is reflected also in the classical W invariants of the homogeneous operator $\mathcal{D}_{K3}$ in $\mathcal{D}_{K3}f(t) = -4!$ of (4.2.48) that determines the Feynman graph. To explore the consequences of the vanishing instantons we have to transform the operator for the periods $\int_\Gamma \Omega$ with Ω as in (4.1.38) to the point of maximal unipotent monodromy, where the instantons are calculated by mirror symmetry in the B-model. That amounts to change the variable from t to $z = -1/u$ by (4.1.36) and change the dependent function to $f(z) = f_3(z)/z$ which yields the operator

$$[\theta^3+2z\theta(1+3\theta+2\theta^2)-16z^2(6+\theta(16+15\theta+5\theta^2)+96z^3(6+\theta(13+9\theta+2\theta^2))]f(z) = 0\ . \quad (4.2.49)$$

At $z = 0$ the unique holomorphic solution is $\varpi = \Pi(T^2) = 1 + 12z^2 - 48z^3 + \mathcal{O}(z^3)$, while the single logarithmic solution starts with $\Pi(\Gamma_1) = \frac{1}{2\pi i}[\varpi \log(z) - 2z + 17z^2 + \mathcal{O}(z^3)]$. The mirror map is defined as $\tau(z) = \Pi(\Gamma_1)/\Pi(T^2)$ and with $q = \exp(2\pi i\tau)$ one realises that its inverse is

$$\frac{1}{z(q)} = \frac{1}{q} - 2 + 15q - 32q^2 + 87q^3 - 192q^4 + 343q^5 - 672q^6 + 1290q^7 + \mathcal{O}(q^8)\ . \quad (4.2.50)$$

This was identified[19] as $1/z(q) = \left(\frac{\eta(\tau)\eta(3\tau)}{\eta(2\tau)\eta(6\tau)}\right)^6 + 4$ the total modular invariant or Hauptmodul of the group $\Gamma_0(6)^+3$ [61]. Such identifications have been made for many one-parameter K3 families [62] based on tables for invariants of Hauptmodules for modular groups that features in the monstrous moonshine conjecture [63].

Let $\Pi(\Gamma_2)$ be the double logarithmic solution. Because mirror symmetry maps the period vector $\Pi^T = (\Pi(T^2), \Pi(\Gamma_1), \Pi(\Gamma_2))$ to the central charges of branes in integer vertical classes $(H_{00}, H_{11}^{vert}, H_{22})$ of the mirror K3, we can calculate Σ^{ij} on the mirror and infer that the $n = 2$ and $r = 0$ relation in (4.1.54) reads $2\Pi(T^2)\Pi(\Gamma_2) + m\Pi(\Gamma_1)^2 = 0$, where m is the self intersection of the primitive holomorphic curve spanning $H_{11}^{vert}(M, \mathbb{Z})$. One finds that the period vector can be written as $\Pi^T = \Pi(T^2)(1, \tau, -\frac{m}{2}\tau^2)$. There is also a modular parametrization of $\Pi(T^2)$ namely $z\Pi(T^2) = \frac{(\eta(2\tau)\eta(6\tau))^4}{(\eta(\tau)\eta(3\tau))^2}$ is the square of periods of a family of elliptic curves associated to $\Gamma_1(6)$. The term $\frac{m}{2}$ encodes the classical intersection of the mirror K3 and the absence of q^n terms indicates the vanishing of all instanton corrections.

The classical theory see e.g. [64] that goes back to Hermann Schwarz, that was applied already to the one-parameter K3 in [65], relates the latter fact to the vanishing of the W_3 invariant of the K3 operator written generically as

$$Df = f''' + 3p(v)f'' + 3q(v)f' + r(v)f = 0\ . \quad (4.2.51)$$

[19] Today such identifications of the group and the η quotient for a wide class of groups are given by the Webpage of the "On-line Encylopedia of Integer Sequences" at **w**ww//oeis.org given enough coefficients of series as in (4.2.50).

By a change of the dependent function $g(v) = f(v)\exp(\int p dv)$ one eliminates the second derivative

$$g''' + 3Q(v)g' + R(v)g = 0 \tag{4.2.52}$$

with $R = r - 3pq + 2p^3 - p''$ and $Q = q - p^2 - p'$. Here Q is an invariant of the differential equation, which can be used to introduce a new variable τ, determined as a solution of the Schwarzian equation

$$\{\tau, v\} = \frac{3}{2}Q \ . \tag{4.2.53}$$

If the second invariant $W_3 = R - \frac{3}{2}Q' = 0$ vanishes, the function $h = \frac{d\tau}{dv}g$ satisfies the differential equation [20]

$$\frac{d^3}{d^3\tau}h(\tau) = 0 \tag{4.2.54}$$

with the solution space $\mathbb{C} \oplus \tau\mathbb{C} \oplus \tau^2\mathbb{C}$. Schwarz theory determines also the second order linear differential equation

$$\mathfrak{D}\mathfrak{f} = \mathfrak{f}'' + 2\mathfrak{q}(v)\mathfrak{f}' + \mathfrak{q}\mathfrak{f}(v) = 0 \ , \tag{4.2.55}$$

whose ratio of solutions $\tau = \mathfrak{f}_1/\mathfrak{f}_2$ fulfills (4.2.53) and which has the property $D = \mathrm{Sym}_2(\mathfrak{D})$, which means that the solutions to $Df = 0$ are $\mathfrak{f}_1^2, \mathfrak{f}_1\mathfrak{f}_2, \mathfrak{f}_2^2$. It can be found by inverting the following steps: After the trivial observation that $\mathfrak{g} = \mathfrak{f}e^{\int \mathfrak{p}dv}$ fulfills $\mathfrak{g}'' + \mathfrak{Q}\mathfrak{g} = 0$, where $\mathfrak{Q} = \mathfrak{q} - \mathfrak{p}^2 - \mathfrak{p}'$, Schwarz noted that with $\{\tau, v\} = 2\mathfrak{Q}$ defining $\mathfrak{h} = \sqrt{\frac{d\tau}{dv}}\mathfrak{g}$ the function $\mathfrak{h}$ fulfills $\frac{d^2}{d\tau^2}\mathfrak{h}(\tau) = 0$ and hence has solution space $\mathbb{C} \oplus \tau\mathbb{C}$.

If $\mathfrak{Q} = \frac{3}{4}Q$ then the two $\tau(v)$ above are identified. Obviously, the solutions h and g are a symmetric square of the solutions $\mathfrak{h}$ and $\mathfrak{g}$ respectively and one can arrange $\mathfrak{p}$ so that also the solutions f are a symmetric square of the ones of $\mathfrak{f}$. Verrill [61] gives this second order equation for (4.2.48)[21] and [57] relates this by changes of the dependent and the independent variable to the differential equation for the equal mass sunset graph (4.2.30).

Four our solutions of the three-loop banana graph with general masses the analogous structures are the equations (4.1.55). The first equation together with the vanishing of the genus one worldsheet instantons on K3 [59, 60], implies the simple form in (4.2.45). The coefficients of the double logarithmic terms are fixed by the intersection theory of the dual curve classes on the mirror K3. The second equation (4.1.55) becomes more powerful in the multi moduli case and restricts the structure of the solutions as well as the differential ideal in (C.0.1) – (C.0.4). One of the strongest hints that automorphic forms also gover the maximal cut graph as solution to (C.0.1) – (C.0.4) is the mirror map. The analog of (4.2.50) given as the multi parameter inversion of (4.2.40) leads to $1/z_i(q_1, \ldots, q_4)$ for $i = 1, \ldots, 4$, which have also integer expansions in the $q_i = \exp(2\pi i t_i)$, where $t_i = \Pi(\Gamma_1^i)/(2\pi i\varpi)$ are the Kähler parameters of the mirror K3. The natural candidate for these automorphic forms are Borcherds lifts of the type discussed in [66] and applied to lattice polarized K3 as in [67, 68]. As can be seen from the last two papers the automorphic forms are written naturally in terms of the Kähler parameters t_i of the mirror. The relations to the physical parameters are given by the mirror map defined by (4.2.40) and by (4.2.35).

[20] To prove this one uses the property $\{x, y\} = -\left(\frac{dx}{dy}\right)^2\{y, x\}$.

[21] Here λ is related to t in (4.2.48) by $\lambda = t - 4$.

Finally, let us comment on the higher loop Banana graphs. For example the analog of the differential operator (4.2.49) at suitable large volume coordinates derives analogously from the $n = 5$ entry of Table 1 in [55] as (4.2.49) from (4.2.48). It also appears in the Web database explained in [69, 70] as AESZ34 and is given by

$$\begin{aligned}\mathcal{D} = \theta^4 - z(35\theta^4 + 70\theta^3 + 63\theta^2 + 28\theta + 5) + z^2(\theta+1)^2(259\theta^2 + 518\theta + 285) \\ - 225z^3(\theta+1)^2(\theta+2)^2 \ .\end{aligned} \tag{4.2.56}$$

One advantage of the solutions at the MUM point is that because of the log structure, in case a factorization of the solutions exist, the analytic solution ϖ must be a pure power of solutions of the lower system [22]. If one tries to factorize in this way it will not work. The reason can be again understood from (4.1.54), see [25] for a review. Special geometry implies that the solutions will be $\Pi^T = \Pi(T^3)(1, \tau, \frac{10}{2}\tau^2 + \mathcal{O}(q), -\frac{10}{6}\tau^3 + \mathcal{O}(q))$ and that $\Pi_3 = -\partial_t\Pi_4$. The reason that this cannot be a symmetric cube are the genus zero world sheet instantons encoded in the higher series in q. For this geometry of the one-parameter family of Barth-Nieto quintics they are not vanishing to all degrees. Subtracting the multi-covering contributions the first $n_d^{(0)} \in \mathbb{Z}$ are given for degree $d = 1, \ldots, 7$ by $24, 48, 224, 1248, 8400, 62816, 516336$. Despite the integer structures in the $n_d^{(0)}$ and the mirror map $1/z = 1/q + 8 + 28q + 104q^2 + 654q^3 + \mathcal{O}(q^4)$ it will be much more complicated to give closed automorphic expressions for the equal mass four-loop graph then for the general mass three-loop graph.

There are however interesting relations of the periods to modular forms of $\Gamma_0(N)$ and algebraic extensions at the rank two attractor points that (4.2.56) as studied in [71]. At these points the numerator of the Hasse Weil factorises and the exact values of maximal cut integral are given by L-function values of holomorphic Hecke Eigenforms forms of weight two and four of $\Gamma_0(N)$ [71] or extensions and the quasi-periods of the corresponding meromorphic forms [72].

[22] The easiest way to find the operator (4.2.55) on a computer might be indeed to take the square root of the unique holomorphic solution ϖ and search for a second order operator that annihilates it.

Chapter 5

Different approaches to solve general banana Feynman integrals

In this chapter, we use a different approach to solve general banana Feynman integrals. We give a representation of the Feynman integral in terms of Bessel functions valid for small momenta and solve them in the large momenta regime where we calculate the maximal cut integral.

5.1 The l-loop banana amplitude and its geometrical realization

A key observation is that (4.1.20) can be understood as a (relative-) period integral for a smooth family of Calabi-Yau hypersurfaces $M_{l-1}^{l^2}$ with generically $\dim H^1(M_{l-1}^{l^2}, TM_{l-1}) = h^{l-2,1} = l^2$ complex structure deformations[1]

$$M_{l-1}^{l^2} = \{P_{\Delta_l}(\underline{y}) = 0 \,|\, \underline{y} \in \mathbb{P}_{\hat{\Delta}_l}\} \,, \tag{5.1.1}$$

defined as vanishing locus of the Laurent polynomial $P_{\Delta_l} = P_l(t, \xi_i; x)/\prod_{i=1}^{l+1} x_i$ in the coordinate ring of the toric ambient space $\mathbb{P}_{\hat{\Delta}_l}$, where Δ_l is the l-dimensional reflexive Newton polytope of the polynomial P_{Δ_l} and $\hat{\Delta}_l$ is its dual. By Batyrev's mirror construction [16] the mirror W_{l-1} is given as in (5.1.1) but with the rôle of Δ_l and $\hat{\Delta}_l$ exchanged.

We note that a single residuum integral $\Omega_{l-1} = \mathrm{Res}_{P_l(t,\xi_i;x)=0}\,(\mu_l/P_l(t, \xi_i; x))$ yields an expression for the holomorphic $(l-1, 0)$-form on the Calabi-Yau manifolds $M_{l-1}^{l^2}$. This was used in [1] to derive from the Gelfand-Kapranov-Zelevinskĭ (GKZ) differential system up to three loops the differential D-module describing those geometrical integrals over Ω_{l-1} that yield the physical Feynman amplitude (4.1.20) in all regions of their physical parameter space in t and ξ_i for $i = 1, \ldots, l+1$.

We extend this program [1] to banana Feynman diagrams of all loop orders l. As in [1] a key technical step is to reduce the solutions of the l^2 parameter GKZ system to the subset of solutions that describe the physical periods in the $l+1$ physical parameters, which we achieved starting from the GKZ system of $M_{l-1}^{l^2}$. Even though the full differential D-module $\mathcal{D}^l$ is lengthy to write down and will be made explicit only up to $l = 4$, we can provide a complete analytic description for the amplitude for the l-loop banana graph $\mathcal{F}_{\sigma_l}(t, \xi_i)$ in all regions of the moduli space. The latter is based on the identification of certain universal operators in $\mathcal{D}^l$ and systematic analytic continuation formulas valid for all l, which involves a systematic occurrence of products of zeta values with highest transcendentality l. It is natural to expect that the latter are related to the $\widehat{\Gamma}$-class of the mirror Fano threefold $\mathbb{P}_{\hat{\Delta}_l}$. Due to the very high co-dimension of the Kähler subslice dual to the $(l+1)$-dimensional physical slice of parameters of $M_{l-1}^{l^2}$ this is an increasingly complicated task. However, Matt Kerr pointed out to us that for the Fano variety that is associated to the equal mass three-loop banana diagram there is a realization of its Hodge structure that is an alternative to the redundantly parametrized one of $\mathbb{P}_{\hat{\Delta}_l}$ and is simply a degree $(1, 1, 1, 1)$ hypersurface in $(\mathbb{P}^1)^4$. This key observation was made by identifying the holomorphic solution associated to the differential

[1] See [1] for a more detailed description of the reflexive pair of lattice polyhedra $(\Delta_l, \hat{\Delta}_l)$ and the associated almost Fano– $(\mathbb{P}_{\Delta_l}, \mathbb{P}_{\hat{\Delta}_l})$ and Calabi-Yau (mirror) geometries $(M_{l-1}, \widehat{M_{l-1}})$.

system of this amplitude with the one that appears in an example[2] in the list [73] and has the same description. This suggests that the relevant physical subslices in the series of the Calabi-Yau manifolds $M_{l-1}^{l^2}$ (5.1.1) are complete intersections of two degree $(1,\dots,1)$ constraints in $(\mathbb{P}^1)^{l+1}$. The GKZ systems of complete intersections have been studied in [17] under the aspect of mirror symmetry. So a good model for the Calabi-Yau $(l-1)$-fold W_{l-1} is the complete intersection of two degree $(1,\dots,1)$ constraints in $(\mathbb{P}^1)^{l+1}$ that reads in the notation of [17]

$$W_{l-1}^{l} = \left(\begin{array}{c|c|c} \mathbb{P}^1_1 & 1 & 1 \\ \vdots & \vdots & \vdots \\ \mathbb{P}^1_{l+1} & 1 & 1 \end{array} \right) \begin{array}{c} \\ \\ \\ \end{array} \begin{array}{c} \Big\} \\ \Big\} \\ \Big\} \end{array} \begin{array}{c} \\ \\ l+1 \end{array} \Bigg) \subset \left(\begin{array}{c|c} \mathbb{P}^1_1 & 1 \\ \vdots & \vdots \\ \mathbb{P}^1_{l+1} & 1 \end{array} \right) \begin{array}{c} \\ \\ \\ \end{array} \begin{array}{c} \Big\} \\ \Big\} \\ \Big\} \end{array} \begin{array}{c} \\ \\ l+1 \end{array} \Bigg) = F_l \ , \tag{5.1.2}$$

which is here suitably embedded[3] in the Fano l-fold F_l. According to [17] the mirror manifold M_{l-1}^{l+1} is given by a resolved quotient of (5.1.2) $M_{l-1} = \widehat{W_{l-1}/G}$ and the period geometry of M_{l-1}^{l+1} is defined by the invariant periods of W_{l-1}/G depending on the G invariant l-dimensional deformation space. This construction is a special case of the construction of Batyrev and Borisov [35].

This suggests that the physical mass and momentum parameters should be identified in the high energy regime with the complexified Kähler parameters

$$\mathfrak{t}^k = \frac{1}{2\pi i} \int_{\mathbb{P}^1_k} (i\omega - b) \tag{5.1.3}$$

controlling the area[4] $A_k = \frac{1}{2\pi} \int_{\mathbb{P}^1_k} \omega$ of the kth $\mathbb{P}^1$ in (5.1.2) as

$$\mathfrak{t}^k \simeq \frac{1}{2\pi i} \log\left(\frac{M_k^2}{K^2}\right) = \frac{1}{2\pi i} \log(z_k) \qquad \text{for } k = 1,\dots,l+1 \ . \tag{5.1.4}$$

If this is true we expect that the large energy behaviour of the Feynman amplitude is exactly determined by the quantum cohomology of $W_{l-1} \subset F_l$ in the large volume limit of the geometry. In particular, if this beautiful picture holds we can infer the entire leading logarithmic structure of the Feynman graph from the central charge of the corresponding object in the derived category of coherent sheafs which can be described by the $\widehat{\Gamma}$-class conjecture in terms of the topological data of W_{l-1} as well as of F_l, which can be easily controlled for all l. Here z_k are the canonical complex structure variables of M_{l-1}, chosen so [17] that the point of maximal unipotent monodromy of the Picard-Fuchs– (or Gauss-Manin) system of M_{l-1} is at $z_k = 0$. We establish the equivalence of the two geometric descriptions, by first deriving the Picard-Fuchs equations of the Feynman graph geometry (4.1.20) and (5.1.1) as Calabi-Yau hypersurface in a toric variety by reduction of its GKZ system to the physical parameters and finding their solutions. These data can be compared to the GKZ system for the complete intersection (5.1.2) and its solutions given in [17] after a change of variables.

[2]This example is given in the link http://coates.ma.ic.ac.uk/fanosearch/?page_id=277#4-1.

[3]The lower index on the manifolds (apart from $\mathbb{P}^1_k$ of course) indicates their complex dimension in terms of the number of loops l of the Feyman diagram.

[4]Here ω is Kähler form and the complexification is by the expectation value of the Neveu-Schwarz $(1,1)$-form field b.

Note, however, that the GKZ systems given in [17] in generality do not yield immediately the complete Picard-Fuchs differential ideal for closed Calabi-Yau periods which entirely the maximal cut case. We solved this problem for the homogenous system for the Calabi-Yau periods and the extension to the inhomogenous system for the three-loop graph in [1] and for the four-loop graph in this work. In the general loop case we can check that the holomorphic solutions (5.1.9) and (5.2.37) that can be in both geometries derived from a simple residuum integral near the MUM point agree with a suitable identification of the variables.

5.1.1 Bessel function representation of l-loop banana integrals

Besides the parametric representation (4.1.20), we also recall a representation of the Feynman amplitude in terms of an integral over Bessel functions, which in its regime of validity,

$$t < \left(\sum_{i=1}^{l+1} \xi_i\right)^2 , \tag{5.1.5}$$

is well suited for numerical evaluation. Relegating a short derivation to appendix B, the Feynman integral (4.1.20) can be rewritten as

$$\mathcal{F}_{\sigma_l} = 2^l \int_0^\infty z\, I_0(\sqrt{t}z) \prod_{i=1}^{l+1} K_0(\xi_i z)\, \mathrm{d}z \ . \tag{5.1.6}$$

In particular, in the equal mass case the expression (5.1.6) contains the $(l+1)$th symmetric power of the Bessel function K_0.

As a side remark, in the on-shell case (defined via $t = \xi_i = 1$ for all i) the integral (5.1.6) becomes a special instance of a Bessel moment. Bessel moments differ in their powers of z, $I_0(z)$ and $K_0(z)$ in the integrand. The massive vacuum banana integrals also yield Bessel moments [74, 75]. Such Bessel moments have also caught the interest of number theorists, one reason being that they, in some cases, evaluate to critical values of L-series of certain modular forms. They satify many interesting relations [76–79] and are closely related to L-functions built from symmetric power moments of Kloosterman sums [80–82].

5.1.2 The maximal cut integral for large momentum

One goal our study is to analyze the l-loop banana graph in the regime $t > \left(\sum_{i=1}^{l+1} \xi_i\right)^2$ where the expression (5.1.6) becomes invalid. It turns out that there is an elegant expression for the so-called maximal cut integral associated with the banana graph, which still contains substantial information about the full Feynman integral $\mathcal{F}_{\sigma_l}$.

The maximal cut integral is obtained by replacing all[5] propagators by delta functions. As derived in [83] there is again a parametric representation of the maximal cut integral in

[5] One can also consider non-maximal cuts where only some propagators are replaced by delta functions. For our purpose these cut integrals are not relevant.

terms of the Symanzik polynomials. To get the maximal cut integral one simply changes the integration range from the simplex σ_l to the l-torus T^l. So for the banana integrals we obtain

$$\mathcal{F}_{T^l}(t,\xi_i) = \int_{T^l} \frac{\mu_l}{\left(t - \left(\sum_{i=1}^{l+1} \xi_i^2 x_i\right)\left(\sum_{i=1}^{l+1} x_i^{-1}\right)\right)\prod_{i=1}^{l+1} x_i} \ . \tag{5.1.7}$$

Now, for large momenta t, the maximal cut integral $\mathcal{F}_{T^l}$ can be obtained explicitly by a simple residue calculation. Introduce the variable $s = 1/t$, then for small s subsequent geometric series and multinomial expansion yields

$$\begin{aligned}
\mathcal{F}_{T^l}(t,\xi_i) &= \int_{T^l} \frac{s}{1 - s\left(\sum_{i=1}^{l+1} \xi_i^2 x_i\right)\left(\sum_{i=1}^{l+1} x_i^{-1}\right)} \ \frac{\mu_l}{\prod_{i=1}^{l+1} x_i} \\
&= \int_{T^l} \sum_{n=0}^{\infty} s^{n+1} \sum_{|k|=n} \binom{n}{k_1,\ldots,k_{l+1}} \prod_{i=1}^{l+1} (\xi_i^2 x_i)^{k_i} \\
&\qquad \cdot \sum_{|\tilde{k}|=n} \binom{n}{\tilde{k}_1,\ldots,\tilde{k}_{l+1}} \prod_{i=1}^{l+1} x_i^{-\tilde{k}_i} \ \frac{\mu_l}{\prod_{i=1}^{l+1} x_i} \\
&= (2\pi i)^l \sum_{n=0}^{\infty} s^{n+1} \sum_{|k|=n} \binom{n}{k_1,\ldots,k_{l+1}}^2 \prod_{i=1}^{l+1} \xi_i^{2k_i} \ .
\end{aligned} \tag{5.1.8}$$

Here we used the short hand notation $|k| = \sum_{i=1}^{l+1} k_i$ and evaluated a multidimensional residue in the last step. So up to normalization the maximal cut integral is for large momentum given by

$$\varpi_0(s,\xi_i) = \sum_{n=0}^{\infty} s^{n+1} \sum_{|k|=n} \binom{n}{k_1,\ldots,k_{l+1}}^2 \prod_{i=1}^{l+1} \xi_i^{2k_i} \ . \tag{5.1.9}$$

When expressed in terms of the variable $t = 1/s$, one recovers [83, eq. (123)].

5.2 The l-loop equal mass banana Feynman integral

In this section we focus on the equal mass case, i.e. $\xi_i = 1$ for $i = 1, \dots l+1$. We first derive an inhomogeneous differential equation for the equal mass Feynman integral. This equation is already known in the literature [84, 85], however, the derivation presented here is somewhat different. It is based on the observation that the maximal cut integral in the large momentum regime is given by the double Borel sum of a certain function for which one can easily construct an operator that annihilates it. This relation makes the computation of the desired differential equation conceptually clear and easy. For each l the differential equation thus obtained is related to the one in [85] by simply transforming it to the small momentum regime. We subquently explain the analytic properties of its solutions and compare to the actual Feynman integral. Coefficients relating local solutions in the large momentum regime to the Feynman integral are given. A conjectural relation for these coefficients to the so-called $\widehat{\Gamma}$-class is proposed. Moreover, these coefficients are linked to the Frobenius κ-constants as we explain before ending the section with some remarks about special points of the Feynman amplitude.

5.2.1 Inhomogeneous differential equation for the l-loop equal mass banana Feynman integral

In this subsection we give an elegant description for the l-loop banana Feynman integral which easily leads to its inhomogeneous differential equation.

First consider the maximal cut integral $\mathcal{F}_{T^l}$ for large momenta t, i.e. near $s = 0$, as given in equation (5.1.9). In the equal mass case, i.e. $\xi_i = 1$, the expression ϖ_0/s can be seen as the double Borel sum[6] of the $(l+1)$th symmetric power of the series

$$\sum_{k=0}^{\infty} \frac{1}{(k!)^2} x^k = I_0(2\sqrt{x}) \ . \tag{5.2.1}$$

Note that the double Borel sum resides, simply speaking, in the additional factor of $(n!)^2$ in the coefficients of (5.1.9), relative to those of the symmetric power of the Bessel function.

Hence, the differential equation annihilating the maximal cut integral (5.1.9) can be derived by three steps: First calculate the differential equation for the $(l+1)$th symmetric power of (5.2.1). Second, by a simple analysis of the (double) Borel sum we can infer the differential operator of the function ϖ_0/s from the operator of the symmetric power. Third, the additional factor of s is commuted into the differential operator to obtain the Picard-Fuchs equation for ϖ_0.

Step 1. The function $I_0(2\sqrt{x})$ is annihilated by the operator

$$\mathcal{D} = \theta^2 - x \tag{5.2.2}$$

with the logarithmic derivative $\theta = x\,\partial_x$. For the $(l+1)$th symmetric power of this function we use a result from [86, 87]:

[6] Or in other words, the $(l+1)$th symmetric power of I_0 is the Borel transform of the Borel transform of ϖ/s.

Lemma: Let $\mathcal{D} = \theta^2 + a(x)\theta + b(x)$ be a linear differential operator whose coefficients $a(x)$ and $b(x)$ are rational functions. Let $\mathcal{L}_0 = 1$, $\mathcal{L}_1 = \theta$ and for $k = 1, 2, \ldots, n$ define the operator $\mathcal{L}_{k+1}$ by

$$\mathcal{L}_{k+1} = (\theta + ka(x))\mathcal{L}_k + kb(x)(n-k+1)\mathcal{L}_{k-1} \ . \tag{5.2.3}$$

Then the symmetric power y^n of any solution to $\mathcal{D}y = 0$ is annihilated by $\mathcal{L}_{n+1}$.

In the case at hand we have $a(x) = 0$ and $b(x) = -x$ while $n = l + 1$.

Step 2. For the Borel summation we notice the following properties: Given a power series $\Psi(x) = \sum_n a_n x^n$, its Borel transform is defined by $\mathcal{B}\Psi(z) = \sum_n a_n \frac{z^n}{n!}$. The original series $\Psi(x)$ is obtained from the Borel transform $\mathcal{B}\Psi(z)$ by the back-transformation

$$\Psi(x) = \int_0^\infty \mathrm{e}^{-z}\, \mathcal{B}\Psi(zx)\ \mathrm{d}z \ , \tag{5.2.4}$$

which is similar to a Laplace transformation, the right hand side now being referred to as the Borel sum of $\Psi(x)$. Given a differential operator annihilating the Borel transform $\mathcal{B}\Psi(z)$ we can infer the corresponding operator annihilating the original function $\Psi(x)$, simply by analyzing the relation (5.2.4). The rules

$$\begin{aligned} &\theta_z^n \mathcal{B}\Psi(z) \longrightarrow \theta_x^n \Psi(x) \\ &z^n \mathcal{B}\Psi(z) \longrightarrow (x(1+\theta_x))^n \Psi(x) = \theta_x \left(x^n \prod_{k=1}^{n-1} (\theta_x + k) \right) \Psi(x) \end{aligned} \tag{5.2.5}$$

are useful in this respect, where $\theta_{x,z}$ are the logarithmic derivatives in x and z, respectively. After each back-transformation, i.e., application of the rules (5.2.5), we can factor out a logarithmic derivative θ_x since it turns out that the degree of the differential operator for the Borel transform of ϖ_0/s is increased by one compared to the original function ϖ_0/s.

Step 3. Finally, we remark that given a function $f(x)$ and an operator $\mathcal{D}$ with $\mathcal{D}f = 0$ the function $\phi(x) = xf(x)$ is annihilated by the operator $\tilde{\mathcal{D}}$, which is obtained from $\mathcal{D}$ by replacing $\theta \to \theta - 1$.

Putting all together we obtain the homogeneous degree l operator $\mathcal{L}_l$ annihilating the equal mass maximal cut integral $\mathcal{F}_{T^l}$. It turns out that this operator is of Fuchsian type for any l. Using a computer algebra program such as `mathematica` it is not hard to write a small program[7] to generate the differential operators. The first few are listed in Table 5.2.1.

For the full equal mass banana Feynman integral $\mathcal{F}_{\sigma_l}$ we have to extend these differential equations to inhomogeneous ones. By numerical evaluation of the integral $\mathcal{L}_l \mathcal{F}_{\sigma_l}$ one finds for the inhomogeneity

$$\mathcal{L}_l \mathcal{F}_{\sigma_l}(s, 1) = S_l := -(l+1)!\, s \ . \tag{5.2.6}$$

[7] On the webpage http://www.th.physik.uni-bonn.de/Groups/Klemm/data.php we upload a small `mathematica` file including a program to generate these operators. They are normalized that they start with one.

#Loops l	Differential operator $\mathcal{L}_l$
1	$1-2s+(-1+4s)\theta$
2	$1-3s+(-2+10s)\theta+(-1+s)(-1+9s)\theta^2$
3	$1-4s+(-3+18s)\theta+(3-30s)\theta^2-(-1+4s)(-1+16s)\theta^3$
4	$1-5s+(-4+28s)\theta+\left(6-63s+26s^2-225s^3\right)\theta^2+\left(-4+70s-450s^3\right)\theta^3$ $-(-1+s)(-1+9s)(-1+25s)\theta^4$
5	$1-6s+(-5+40s)\theta+\left(10-112s+1152s^3\right)\theta^2$ $+\left(-10+168s-236s^2+4608s^3\right)\theta^3+\left(5-140s+5760s^3\right)\theta^4$ $+(-1+4s)(-1+16s)(-1+36s)\theta^5$

Table 5.2.1: Homogeneous differential operators for maximal cut integrals

5.2.2 Analytic properties of the l-loop equal mass banana graph Feynman integral

In this subsection we study the analytic properties of the Frobenius basis corresponding to the (in-)homogeneous differential equaion (5.2.6) derived in the previous subsection. These properties partially descend to the actual Feynman integral, which is given by an appropriate linear combination. The coefficients of this linear combination will be computed in the next subsection.

We reserve the indices $k=0,\dots,l-1$ to the homogeneous solutions of $\mathcal{L}_l\varpi_k=0$, while the index $k=l$ refers to the special solution of the inhomogeneous equation $\mathcal{L}_l\varpi_l=S_l$. In this notation the Feynman amplitude $\mathcal{F}_{\sigma_l}$ is a linear combination of the ϖ_k with a non-zero contribution of the special solution ϖ_l. On the other hand, the maximal cut $\mathcal{F}_{T^l}$ of the Feynman amplitude only involves the homogeneous solutions ϖ_k with $k=0,\dots,l-1$.

First, we discuss the singular points of the differential equation. At $s=1/t=0$ we have a point of maximal unipotent monodromy, in short a MUM point. This means that the local exponents (i.e. the roots of the indicial equation) of $\mathcal{L}_l\varpi_k=0$ are all degenerate. In the case at hand they are all equal to one, which can be derived from the fact that $\mathcal{L}_l=(1-\theta)^l+\mathcal{O}(s)$. Moreover, in the s coordinate the singular loci are the roots of the discriminant $\Delta(\mathcal{L}_l)$, given by

$$\Delta(\mathcal{L}_l)=s\prod_{j=0}^{\lfloor\frac{l+1}{2}\rfloor}\left(1-s(l+1-2j)^2\right)\ . \tag{5.2.7}$$

So in general, we have a moduli space

$$\mathbb{P}^1\setminus\left(\bigcup_{j=0}^{\lceil\frac{l-1}{2}\rceil}\left\{\frac{1}{(l+1-2j)^2}\right\}\cup\{0,\infty\}\right)\ . \tag{5.2.8}$$

The actual Feynman integral $\mathcal{F}_{\sigma_l}$ is not singular at all of these points. From the Bessel function representation (5.1.6) of $\mathcal{F}_{\sigma_l}$, valid in a neighbourhood of the point $s=\infty$ (i.e. $t=0$) we know that it converges for $|s|>\frac{1}{(l+1)^2}$. In particular, this implies that the amplitude can

only be singular at $s = 0$ and $s = \frac{1}{(l+1)^2}$. This is also expected from the optical theorem since the latter point is a threshold for the $l+1$ particles in the loops (all of which have unit mass). At the other singular points of $\mathcal{L}_l$ the Feynman integral stays regular. In Figure 5.2.1 this behavior is shown.

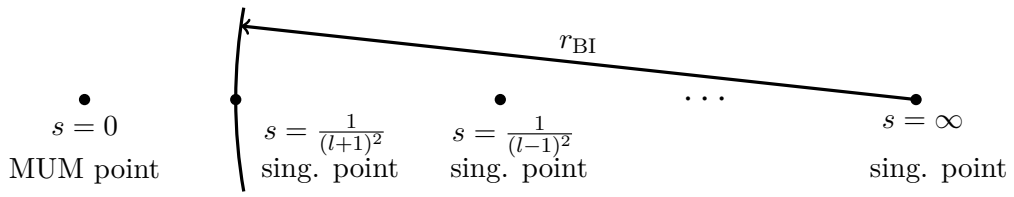

Figure 5.2.1: Singularities of the Fuchsian operator $\mathcal{L}_l$. The radius of convergence of the Bessel integral representation (5.1.6) of $\mathcal{F}_{\sigma_l}$ is denoted by $r_{\rm BI}$.

5.2.3 Frobenius basis at the MUM point

Around the MUM point the Frobenius basis takes a particularly nice form. The holomorphic solution ϖ_0 is given by (5.1.9) at $\xi_i = 1$ for $i = 1, \ldots, l+1$. The other solutions are given by[8]

$$\varpi_k = \sum_{j=0}^{k} \binom{k}{j} \log(s)^j \, \Sigma_{k-j} \qquad \text{for } k = 1, \ldots, l-1 \ , \tag{5.2.9}$$

where $\Sigma_0 = \varpi_0 = s + \mathcal{O}(s^2)$ and the power series Σ_k are determined by the operator $\mathcal{L}_l$ and the condition that they start as $\Sigma_k = \mathcal{O}(s^2)$ for $k \geq 1$. For example, the four-loop operator $\mathcal{L}_4$ has

$$\begin{aligned}
\varpi_0 &= s + 5s^2 + +45s^3 + 545s^4 + 7885s^5 + \cdots \\
\Sigma_1 &= 8s^2 + 100s^3 + \frac{4148}{3}s^4 + \frac{64198}{3}s^5 + \cdots \\
\Sigma_2 &= 2s^2 + \frac{197}{2}s^3 + \frac{33637}{18}s^4 + \frac{2402477}{72}s^5 + \cdots \\
\Sigma_3 &= -12s^2 - \frac{267}{2}s^3 - \frac{19295}{18}s^4 - \frac{933155}{144}s^5 + \cdots \ .
\end{aligned} \tag{5.2.10}$$

The special solution ϖ_l has one more logarithm and takes the form

$$\varpi_l = \sum_{j=0}^{l} \binom{l}{j} \log(s)^j \, \Sigma_{l-j} \ , \tag{5.2.11}$$

which, after multiplication with the constant $(-1)^{l+1}(l+1)$, satisfies (5.2.6). Again for the four-loop example we find

$$\Sigma_4 = 1830s^3 + \frac{112720}{3}s^4 + \frac{47200115}{72}s^5 + \cdots \tag{5.2.12}$$

[8]Note that the dependence on the loop order l is kept implicit in our notation for ϖ_k and Σ_k.

in the special solution ϖ_4.

The power series Σ_k can also be obtained from a generating function approach starting from the holomorphic solution ϖ_0. To this end rewrite (5.1.9) in the form

$$\varpi_0 = \sum_{k_1,\ldots,k_{l+1}\geq 0} \binom{|k|}{k_1,\ldots,k_{l+1}}^2 s^{|k|+1} \ , \tag{5.2.13}$$

where the summation is over all non-negative integers $k_1,\ldots,k_{l+1}$. Introduce formal parameters ϵ_i by replacing $k_i \to k_i+\epsilon_i$ in (5.2.13). Taking derivatives with respect to these parameters and subsequently putting the parameters to zero yields other Frobenius solutions[9]

$$\sum_{\{i_1,\ldots,i_k\}\in T_k^{(l+1)}} \frac{\partial^k}{\partial\epsilon_{i_1}\cdots\partial\epsilon_{i_k}}\varpi_0(\epsilon_i)\Big|_{\text{all } \epsilon_i=0} \quad \text{for } k=1,\ldots,l \ , \tag{5.2.14}$$

where $T_k^{(l+1)}$ denotes the set of all subsets of length k of the set $T^{(l+1)}=\{1,\ldots,l+1\}$.

5.2.4 Banana Feynman integral in terms of the MUM-Frobenius basis

Recall that in a local Frobenius basis (for us the region around the MUM point is most interesting) the l-loop banana Feynman amplitude is given by a linear combination

$$\mathcal{F}_{\sigma_l} = \sum_{k=0}^{l} \lambda_k^{(l)} \varpi_k \ . \tag{5.2.15}$$

In the following we explain how to obtain the coefficients $\lambda_k^{(l)}$.

The equal mass banana Feynman integrals $\mathcal{F}_{\sigma_l}$ can be evaluated numerically for fixed value of the variable s. For $l=2,3,4$ this can directly be done with the form given in (4.1.20), say using a numerical integration routine of `mathematica` or `pari`. Unfortunately, the multidimensional numerical integration gets too cumbersome for higher loop integrals due to the increase of the numerical error. On the other side, numerical integration is less problematic for the integral over Bessel functions (5.1.6), which can almost be computed for any loop order with any desired precision. However, around the MUM point $s=0$ the Bessel expression is not valid and analytic continuation is needed. As seen from Figure 5.2.1 we therefore have to analytically continue the solutions from $s=\frac{1}{(l+1)^2}$ to $s=0$. For this, the Bessel representation of $\mathcal{F}_{\sigma_l}$ is used to first fix the linear combination with respect to the local Frobenius basis[10] around $s=\frac{1}{(l+1)^2}$. Then, by subsequent numerical analytic continuation,

[9] The functions produced here may be linear combinations of the previously considered solutions to the homogeneous differential equation. In other words, by forming appropriate linear combinations of the expressions in (5.2.14) one in turn obtains the Σ_k as defined before.

[10] These are obtained by shifting the variable s to $\eta = s-\frac{1}{(l+1)^2}$ and solving the differential equation around $\eta=0$. It turns out that one obtains square root or logarithmic brunch cuts depending on whether l is odd or even, respectively.

the local Frobenius basis around $s = \frac{1}{(l+1)^2}$ is related to the local Frobenius basis at the MUM point $s = 0$. This numerically yields the desired coefficients $\lambda_k^{(l)}$ around $s = 0$.

In order to guess the exact analytic expression of the coefficient $\lambda_k^{(l)}$ we take as an ansatz[11] all possible products of zeta values and π that lead to a homogeneous transcendental weight of $l-k$ and linearly combine these products with rational coefficients to be determined. The latter are fitted by comparing the ansatz to the numerical values for $\lambda_k^{(l)}$ obtained in the previous paragraph.[12] We checked these fits with 300 digits precision up to the loop order $l = 17$ and with lower precision until $l = 20$. For example, in the four-loop case we thus find (see also Table 5.2.2)

$$\begin{aligned} &\lambda_0^{(4)} = -450\zeta(4) - i\pi \cdot 80\zeta(3) && \lambda_1^{(4)} = 80\zeta(3) - i\pi \cdot 120\zeta(2) && \\ &\lambda_2^{(4)} = 180\zeta(2) && \lambda_3^{(4)} = i\pi \cdot 20 && \lambda_4^{(4)} = -5 \ . \end{aligned} \tag{5.2.16}$$

In all examples considered we observe that the imaginary part factors into π and a sum of homogeneous transcendental weight $l-k-1$.

Moreover, all empirical results for $\lambda_k^{(l)}$ fit into the following combinatorial pattern: Let $\mathcal{P}(l)$ be the set of integer partitions of l. From $\mathcal{P}(l)$ we take only the set of partitions $P(l)$ with the property that any partition $p \in P(l)$ is given by a single even integer g, possibly zero, and s odd integers[13] o_i with $1 < o_1 < o_2 < \cdots < o_s$ such that

$$l = g + \sum_{i=1}^{s} m_i o_i \ , \tag{5.2.17}$$

so m_i is the multiplicity of o_i in the respective partition of l. In this case we may write $p = (g, o_1^{m_i}, \ldots, o_s^{m_s})$. With this notation the combinatorial pattern of the coefficients $\lambda_k^{(l)}$, where $k = 0, \ldots, l$, now reads[14]

$$\begin{aligned} \lambda_k^{(l)} = \quad & (-1)^{k+1} \frac{(l+1)!}{k!} \sum_{p \in P(l-k)} \frac{(-1)^{\frac{g}{2}} (\pi)^g}{g!} \prod_{i=1}^{s} \frac{2^{m_i}}{(o_i)^{m_i}\, m_i!} \zeta(o_i)^{m_i} \\ + i\pi \quad & (-1)^{k+1} \frac{(l+1)!}{k!} \sum_{p \in P(l-k-1)} \frac{(-1)^{\frac{g}{2}} (\pi)^g}{(g+1)!} \prod_{i=1}^{s} \frac{2^{m_i}}{(o_i)^{m_i}\, m_i!} \zeta(o_i)^{m_i} \ . \end{aligned} \tag{5.2.18}$$

Indeed, we can give a generating function for the values $\lambda_0^{(l)}$ by

$$\sum_{l=0}^{\infty} \lambda_0^{(l)} \frac{x^l}{(l+1)!} = -\mathrm{e}^{i\pi x + \sum_{k=1}^{\infty} \frac{2\zeta(2k+1)}{2k+1} x^{2k+1}} = -\frac{\Gamma(1-x)}{\Gamma(1+x)} \mathrm{e}^{-2\gamma x + i\pi x} \ , \tag{5.2.19}$$

[11] This ansatz is inspired by the $\widehat{\Gamma}$-conjecture, which will be addressed in the next subsection.

[12] If we write down the ansatz with even powers of π instead of even zeta values the coefficients in the ansatz turn out to be integers.

[13] Here s stands for any appropriate non-negative integer, that is of course not to be confused with the momentum parameter $s = 1/t$.

[14] With $\frac{(\pi i)^{2n}}{(2n)!} = -\frac{\zeta(2n)}{2^{2n-1} B_{2n}}$ we could also write the whole expression (5.2.18) in terms of zeta values and Bernoulli numbers.

where γ is the Euler-Mascheroni constant. The other coefficients are related to $\lambda_0^{(l)}$ by

$$\lambda_k^{(l)} = (-1)^k \binom{l+1}{k} \lambda_0^{(l-k)} \ . \tag{5.2.20}$$

Finally, we remark that $\sum_{k=0}^{l} \mathrm{Im}(\lambda_k^{(l)})\varpi_k$ is proportional to the vanishing period at $s = \frac{1}{(l+1)^2}$.

5.2.5 Euler numbers of Calabi-Yau hypersurfaces

In this section, we want to study Euler and Chern number of the ambient space and Calabi-Yau hypersurfaces.
First, we need to introduce a few definitions about polytopes. If the vertices of a polytope are primitive lattice points that polytope is a ***Fano polytope*** and if the only inner lattice point is the origin, it is called a ***canonical Fano polytope*** [88]. Some of the topological quantities of the toric varieties as the ambient space has been computed from the reflexive lattice polytope [89]. It is worth to note that, the number of the cones or in a star triangulation, the number of simplices gives the Euler number of the smooth (Fano) toric varieties.

For toric ambient space

Euler numbers: First we start with 16 reflexive 2 dimensional polytopes, including *del Pezzo surfaces*. The Euler number of the smooth toric variety is equal to the number of perimeter lattice points p, i.e. the number of all points on the edges or faces,

$$\chi(X(\Delta_2)) = p = (\Delta_2 \cap \mathbb{Z}^2) - 1, \tag{5.2.21}$$

which means for our case, for the sunset diagram, the Euler number of the ambient space is $\chi(dP3) = 6$.
For all 4319 three-dimensional reflexive polytopes, the Euler number is given by:

$$\chi(X(\Delta_3)) = 2\#(\Delta_3 \cap \mathbb{Z}^3) - 6 = 2p - 4. \tag{5.2.22}$$

For the three loop banana case, where in [89] the corresponding reflexive polytope is $\mathcal{X}_{1530}$, we have $\chi = 20$.

Chern numbers: For two dimensional reflexive polytopes one gets two Chern numbers by integration over the toric 2-fold,

$$(C(M_2), \chi(M_2)) = (p^*, p)$$

where $C(M_2) = \int_{M^2} c_1(M_2)^2$ and p and p^* are the number of lattice points for Δ and its dual $\hat{\Delta}$.

For the three dimensional case, the smooth Fano varieties, obtained from a fine regular star triangulation of a reflexive polytope Δ_3, have three natural integrals from the Chern classes $c_i(M_3) \in H^{2i}(M_3;\mathbb{Z})$,

$$\begin{aligned} C &:= \int_{M_3} c_1(M_3)^3 \\ C' &:= \int_{M_3} c_1(M_3)c_2(M_3) \\ \chi &= \int_{M_3} c_3(M_3), \end{aligned} \tag{5.2.23}$$

where all of them are integers. The second integral is equal to 24 for all 4319 reflexive three-dimensional polytopes and C and χ are related (check Fig.4. in [89]). C is given by,

$$C(X(\Delta_3)) = 2\#(\hat{\Delta_3} \cap \mathbb{Z}^3) - 6 = 2p^* - 4, \tag{5.2.24}$$

where for our case, i.e. three loop banana diagram, it is $C(X(\Delta_3)) = 24$.

These results have been cross checked by `Sage`. In $dim = 4$, the equivalence of the number of simplices in a star triangulation and Euler characteristic number, being $\chi = 70$ for both of our cases, has been tested by `Sage`, as well.

For Calabi-Yau hypersurfaces in the toric ambient space

Till now, we have computed the Euler number of the ambient space, but we need the topological numbers of the Calabi-Yau hypersurface in the toric varieties as the ambient space. In [90] the so-called *stringy Euler number* has been calculated and it is given by,

$$\chi(P_\Delta) = c_{d-1}(P_\Delta) = \sum_{k=1}^{d-2}(-1)^{k+1} \sum_{\substack{\theta \preceq \Delta \\ dim\theta = k}} v(\theta)\cdot v(\theta^*),$$

where θ is a face of the reflexive polytope Δ and θ^* is its dual, where they satisfy $dim\ \theta + dim\ \theta^* = d-1$. And also we have,

$$v(\theta) := k! \cdot vol_k(\Theta_\theta), \tag{5.2.25}$$

where $vol_k(\Theta_\theta)$ is the k-dimensional volume of the lattice polytope Θ_θ which is the convex hull of the origin and the primitive lattice generators of all 1-dimensional faces of θ [90].
For each of the polytopes one can define the so-called ***Ehrhart polynomial*** $\Lambda(t)$ which for any non-negative integer k we have $\Lambda(k) = l(k\Delta)$ where $l(k\Delta)$ is the number of integral points in the interior of $k\Delta$ [90]. For example the Ehrhart polynomial of the 5-dimensional polytope under the study looks like:

$$\Lambda_{\Delta_5}(t) = (21/10)\ t^5 + (21/4)\ t^4 + (28/3)\ t^3 + (35/4)\ t^2 + (137/30)\ t + 1. \tag{5.2.26}$$

Now, we can define Hilbert-Poincare series by,

$$P_\Delta(t) = \sum_{k\geq 0} \Lambda(k) t^k, \tag{5.2.27}$$

and

$$\Psi_\Delta(t) = \sum_{i\geq 0} \psi_i(\Delta) t^i := (1-t)^{d+1} P_\Delta(t). \tag{5.2.28}$$

This polynomial has some nice property and one of them is:

$$\Psi_\Delta(1) = \sum_{i\geq 0} \psi_i(\Delta) = v(\Delta), \tag{5.2.29}$$

where $v(\Delta)$ is equal to the Euler number of the ambient space up to a sign. And $\psi_1(\Delta) = l(\Delta) - d - 1$.
We have also Libgober-Wood identity for the Gorenstein toric Fano variety X corresponding to Δ,

$$\sum_{i\leq d} \psi_i(\Delta)(i - \frac{d}{2})^2 = \frac{d}{12} v(\Delta) + \frac{1}{6} \sum_{\substack{\theta \preceq \Delta \\ dim\theta = d-2}} v(\theta) \cdot v(\theta^*). \tag{5.2.30}$$

5.2.6 The $\widehat{\Gamma}$-class and zeta values at the point of maximal unipotent monodromy

In this subsection we will discuss those aspects, in particular the importance of the number of moduli, of the Calabi-Yau geometries[15] M_{l-1} shortly introduced in subsection 5.1, which are most relevant to discuss the $\widehat{\Gamma}$-class formalism. The latter fixes the coefficients of the expansion of the Feynman amplitude (4.1.20) in terms of a canonical Frobenius basis of solutions near the point of maximal unipotent monodromy. Eventually, this Frobenius basis can be related to period integrals over an integral basis of cycles in the middle dimensional cohomology of the Calabi-Yau geometry M_{l-1} and a single chain integral extension.

Recall that upon numerical analytic continuation from the region $1/s < (\sum_{i=1}^{l+1} \xi_i)^2$, where the amplitude can be calculated using the Bessel function realization (5.1.6), to the region $s < 1/(\sum_{i=1}^{l+1} \xi_i)^2$ we got in the equal mass case and for the first few loop orders $l \leq 6$ the coefficients $\lambda_k^{(l)}$ displayed in Table 5.2.2. Using further results up to $l = 15$ we could guess the pattern summarized in (5.2.18) or (5.2.19) combined with (5.2.20). This conjecturally determines all l-loop banana Feynman amplitudes in all regions of their physical parameter space, since the linear combinations for the non-equal mass case follow by a simple symmetric splitting (see Table 5.3.2 below).

Generally, the occurrence of powers of zeta values and of some special numbers in Table 5.2.2 that can be identified with Euler number integrals over combinations of top Chern classes, as well as equation (5.2.20), suggest that the coefficients come from a $\widehat{\Gamma}$-expansion integrated against the exponential $e^{\mathfrak{t}\omega}$ of a suitable Kähler form ω. Here we want to use the

[15] We drop from now on the superscript expressing the number of moduli.

l	ϖ_0	ϖ_1	ϖ_2	ϖ_3	ϖ_4	ϖ_5
1	$-2\pi i$					
2	$18\zeta(2)$	$6\pi i$				
3	$-16\zeta(3)+24i\pi\zeta(2)$	$-72\zeta(2)$	$-12\pi i$			
4	$-450\zeta(4)-80i\pi\zeta(3)$	$80\zeta(3)-120\pi i\zeta(2)$	$180\zeta(2)$	$20\pi i$		
5	$-288\zeta(5)+1440\zeta(2)\zeta(3)-$ $540i\pi\zeta(4)$	$2700\zeta(4)+$ $480i\pi\zeta(3)$	$-240\zeta(3)+$ $360\pi i\zeta(2)$	$-360\zeta(2)$	$-30\pi i$	
6	$6615\zeta(6)-1120\zeta(3)^2+$ $\pi i(3360\zeta(2)\zeta(3)-2016\zeta(5))$	$2016\zeta(5)-10080\zeta(2)\zeta(3)+$ $3780i\pi\zeta(4)$	$-9450\zeta(4)-$ $1680i\pi\zeta(3)$	$560\zeta(3)-$ $840\pi i\zeta(2)$	$630\zeta(2)$	$42\pi i$

Table 5.2.2: Numerically determined coefficients $\lambda_k^{(l)}$ for the equal mass Feynman integral w.r.t. the Frobenius basis ϖ_k at the MUM point for $l \leq 6$.

relevant Calabi-Yau varieties M_{l-1} and W_{l-1} together with a Fano geometry F_l to prove the equations (5.2.18) or (5.2.19) using the $\widehat{\Gamma}$-class formalism.

We start with the imaginary part of the numbers in (5.2.18) or Table 5.2.2. The analytic continuation as well as the monodromy worked out in section 5.2.7 reveals that this combination of periods corresponds to the one that vanishes at the nearest conifold $s = 1/(\sum_{i=1}^{l+1}\xi_i)^2$. Geometrically here a sphere S^{l-1} vanishes. The latter is in the integral middle cohomology of M_{l-1} and by Seidel-Thomas twist it corresponds to the D_{l-1} brane that wraps the full $(l-1)$-dimensional mirror Calabi-Yau space W_{l-1} in the derived category of coherent sheaves on W_{l-1}.

The $\widehat{\Gamma}$-class formalism[16] [92–95] allows to calculate the K-theory charge Z_{D_k} of any D-brane D_k via

$$Z_{D_k}(\mathfrak{t}) = \int_{W_{l-1}} e^{\omega\cdot\mathfrak{t}}\,\widehat{\Gamma}(TW_{l-1})\mathrm{Ch}(D_k) + \mathcal{O}(e^{\mathfrak{t}})\ . \tag{5.2.31}$$

Here ω is the Kähler form of W_{l-1} and $\omega\cdot\mathfrak{t} = \sum_{i=1}^{h^{1,1}}\omega_i\mathfrak{t}^i$ refers to an expansion of the latter in terms of Kähler parameters $\mathfrak{t}^i$ w.r.t. a basis ω_i of the Kähler cone of W_{l-1}. $\mathrm{Ch}(D_k)$ defines a cohomology class that specifies the D_k brane. In particular, for the top dimensional D_{l-1} brane $\mathrm{Ch}(D_{l-1}) = 1$. The mirror map at the point of maximal unipotent monodromy[17]

$$\mathfrak{t}^k = \frac{1}{2\pi i}\frac{\varpi_1^k}{\varpi_0} = \frac{1}{2\pi i}\log(z_k) + \tilde{\Sigma}_k(z) \tag{5.2.32}$$

allows to relate the latter to the corresponding period in the Frobenius basis. More precisely, the central charge $Z_{D_{l-1}}$ is identified with the period in question and the $\mathfrak{t}^k$-expansion can be identified with the logarithmic expansion in the Frobenius basis. In particular, to prove the occurence of the imaginary terms in the first column of Table 5.2.2, we only need to expand the $\widehat{\Gamma}$-class of the tangent sheaf TW_{l-1} of W_{l-1}. More generally, we consider the regularised

[16] First explanations of the $\zeta(3)\chi/(2(2\pi i))^3$ and the $\int_W c_2\wedge\omega_k/24$ values in the periods of three-folds as coming from derivates of the gamma function were made in [17]. See also [91].

[17] By ϖ_1^k, $k = 1,\ldots,h^{l-2,1}(M_{l-1})$ we denote all single logarithmic periods. If $h^{l-2,1}(M_{l-1}) = 1$ we omit the upper index.

$\widehat{\Gamma}$-class of a sheaf $\mathcal{F}$. For a sheaf of rank n the latter is defined as the symmetric expansion $\widehat{\Gamma}(\mathcal{F}) = \prod_{i=1}^{n} e^{\gamma\delta_i}\Gamma(1+\delta_i)$ in terms of the eigenvalues δ_i of $\mathcal{F}$ which in turn is re-expressed in terms of its Chern classes $c_k = s_k(\delta_1, \ldots, \delta_n)$. Here γ is the Euler-Mascheroni constant and the $e^{\gamma\delta_i}$ factors are introduced to cancel $e^{-\gamma c_1(\mathcal{F})}$ terms that would arise from the first derivative of just the $\Gamma(1+\delta_i)$ factors. For practical purposes it is faster to first write a closed formula in terms of the Chern characters $\mathrm{ch}_k(\mathcal{F})$ of $\mathcal{F}$. That yields the regularized $\widehat{\Gamma}(\mathcal{F})$-class as

$$\widehat{\Gamma}(\mathcal{F}) = \exp\left(\sum_{k\geq 2}(-1)^k(k-1)!\,\zeta(k)\,\mathrm{ch}_k(\mathcal{F})\right) \ . \tag{5.2.33}$$

The transition to the Chern classes c_k can be made by Newton's formula

$$\mathrm{ch}_k = (-1)^{(k+1)}k\left[\log\left(1+\sum_{i=1}^{\infty}c_i\,x^i\right)\right]_k \ , \tag{5.2.34}$$

where $[\cdot]_k$ means to take the kth coefficient (in x) of the expansion of the expression in the $[\cdot]$-bracket.

Let us now apply this to the geometry W_{l-1} in (5.1.2), the Fano variety F_l and its mirror M_{l-1} using the mirror symmetry formalism developed in [17]. Here a canonical subfamily with $l+1$ complex structure deformations of (5.1.2) is identified with the mirror manifold M_{l-1} to W_{l-1}. We first want to establish that the Picard-Fuchs equations and their solutions in the canonical Frobenius basis of M_{l-1} are the same as the one that we derived for the Feynman graph in the physical parametrization (5.1.7). According to [17] the period solutions of complete intersections in toric ambient spaces are specified by ℓ-vectors[18] $\ell^{(k)} = (\ell_{01}^{(k)}, \ldots, \ell_{0h}^{(k)}; \ell_1^{(k)}, \ldots, \ell_c^{(k)})$ for $k = 1, \ldots, h^{l-2,1}(M_{l-1})$. Here h is the number of complete intersection constraints, c is the number of homogenous coordinates of the ambient space and the $\ell_l^{(k)}$ for $l = 1, \ldots, c$, are the degrees of the constraints. In the case of M_{l-1} we have $h = 2$, $c = 2(l+1)$ and the $\ell^{(k)}$ read

$$\begin{aligned}
\ell^{(1)} &= (-1,-1;1,1,0,0,\cdots,0,0,0,0)\\
\ell^{(2)} &= (-1,-1;0,0,1,1,\cdots,0,0,0,0)\\
&\vdots\\
\ell^{(l)} &= (-1,-1;0,0,0,0,\cdots,1,1,0,0)\\
\ell^{(l+1)} &= (-1,-1;0,0,0,0,\cdots,0,0,1,1) \ .
\end{aligned} \tag{5.2.35}$$

From these ℓ-vectors one obtains a generalized Gelfand-Kapranov-Zelevinskĭ differential system with holomorphic solution

$$\omega_0(\underline{z};\underline{\epsilon}) = \sum_{n_1,\ldots,n_{l+1}\geq 0} c(\underline{n}+\underline{\epsilon})\,\underline{z}^{\underline{n}+\epsilon} \ . \tag{5.2.36}$$

[18] The terminology of ℓ-vectors employed here is of course not be confused with vectors that have l components or the like, which is why have chosen a different symbol ℓ.

Here the underlined quantities are $(l+1)$-tuples and the series coefficients $c(\underline{n})$ are determined by the $l+1$ ℓ-vectors via

$$c(\underline{n}) = \frac{\prod_{j=1}^{2}\left(-\sum_{k=1}^{l+1} l_{0j}^{(k)}\, n_k\right)!}{\prod_{i=1}^{2l+2}\left(\sum_{k=1}^{l+1} l_i^{(k)}\, n_k\right)!}\,. \tag{5.2.37}$$

The $c(\underline{n}+\underline{\epsilon})$ are as usual defined by promoting all factorials $*!$ in (5.2.37) to $\Gamma(*+1)$ and deforming each integer n_k to $n_k+\epsilon_k$. In particular, the unique holomorphic solution at the point of maximal unipotent monodromy is given by

$$\varpi_0(\underline{z}) = \omega_0(\underline{z};\underline{\epsilon})|_{\underline{\epsilon}=\underline{0}} = \sum_{n_1,\ldots,n_{l+1}\geq 0} \binom{|n|}{n_1,\ldots,n_{l+1}}^2 \prod_{k=1}^{l+1} z_k^{n_k}\,. \tag{5.2.38}$$

Comparing with (5.1.9) we see that the coordinates[19] z_k are related to the physical coordinates by

$$z_k = s\xi_k^2 \quad \text{for } k=1,\ldots,l+1\,. \tag{5.2.39}$$

The point here is that the period of M_{l-1} given in (5.2.38) is up to the simple parameter redefinition (5.2.39) equivalent to (5.1.9) after multiplying with the physical variable s. The other periods for both systems can be obtained by the Frobenius method as described in section 5.2.3 for the Feynman graph period and in [17] for the periods of M_{l-1}. The basic idea is to take certain combinations of derivatives w.r.t the deformations parameters $L_c^r = \sum_{j_1,\ldots,j_r} c_{j_1,\ldots,j_r}\partial_{\epsilon_{j_1}}\ldots\partial_{\epsilon_{j_r}}\omega_0(\underline{z};\underline{\epsilon})|_{\underline{\epsilon}=\underline{0}}$. In particular, the $\varpi_k = L^{(1)}_{\delta_{k,j}}/2\pi i$, $k=1,\ldots,h^{l-2,1}(M_{l-1}) = l+1$ are the single logarithmic solutions, which together with ϖ_0 determine the mirror map (5.2.32). The higher logarithmic solutions are fixed by the topological data of W_{l-1} and their numbers inferred by the differential ideal reported in Table 5.3.1 matches the primitive vertical Hodge numbers of W_{l-1} and primitive horizontal middle dimensional Hodge numbers of M_{l-1} discussed in [22, 23] for four-folds.

These identifications suggest that (5.1.2) is the right mirror W_{l-1} to the Calabi-Yau $(l-1)$-fold family M_{l-1} whose periods, together with the single chain integral extension, in the parametrization in (5.2.39) describe non-redundantly the Feyman graphs exactly in the physical parameters.

As we explained in the beginning of this subsection this implies that the evaluation of the $\widehat{\Gamma}$-class for W_{l-1} must reproduce the imaginary parts of (5.2.18). It follows by the adjunction formula that the Chern classes c_k of W_{l-1} are given by the degree k part of

$$c_k(W_{l-1}) = \left[\frac{\prod_{i=1}^{l+1}(1+H_i)^2}{(1+\sum_{i=1}^{l+1}H_i)^2}\right]_{\deg(H)=k}\,. \tag{5.2.40}$$

More precisely, since the hyperplane classes in each $\mathbb{P}^1$ fulfill $H_i^2=0$ we can express c_k in terms of elementary symmetric polynomials $s_k(\underline{H}) = \sum_{i_1<\ldots<i_k} H_{i_1}\cdots H_{i_k}$ as

$$c_k(W_{l-1}) = (-1)^k k!\sum_{j=0}^{k}\frac{(-2)^j(k+1-j)}{j!}s_k(\underline{H}) =: \mathcal{N}_k^{W_{l-1}} s_k(\underline{H})\,. \tag{5.2.41}$$

[19] These coordinates are also related to the redundant parameters multiplying the generic monomials of the Newton polytope associated to the complete intersection Calabi-Yau, see [17] for a definition.

Similarly, considering the power one of the normal bundle in the denominator of (5.2.40) (instead of two) we can write for the Chern classes of the ambient space

$$c_k(F_l) = (-1)^k k! \sum_{j=0}^{k} \frac{(-2)^j}{j!} s_k(\underline{H}) =: \mathcal{N}_k^{F_l} s_k(\underline{H}) \ . \tag{5.2.42}$$

Moreover, we notice that the integral of a top degree product of Chern classes c_{k_n} over $X = W_{l-1}$ or $X = F_l$ is given by

$$\int_X \prod_n c_{k_n} = (l+1)! \prod_n \frac{\mathcal{N}_{k_n}^X}{k_n!} \ . \tag{5.2.43}$$

Let us comment some more on primitive vertical homology of W_{l-1} and well as F_l and establish that W_{l-1} is the mirror of M_{l-1} for the three-fold case. Let us denote the homogenous coordinates of the kth $\mathbb{P}^1_k$ by $[x_k : y_k]$. Then in general the independent divisor classes of W_{l-1} and as well as of F_l are the restrictions of the hyperplane classes[20] $D_k = \{ax_k + by_k = 0\}$ in $(\mathbb{P}_1)^{l+1}$ with topology $(\mathbb{P}_1)^l$ for F_l or W_{l-1}, where they have topology F_{l-1} or W_{l-2}, respectively. We have $D_k^2 = 0$, $k = 1, \ldots, l+1$, and the top intersections are encoded in the coefficients of the rings

$$\mathcal{R}^{W_{l-1}} = 2 \sum_{i_1 < \ldots < i_{l-1}} D_{i_1} \ldots D_{i_{l-1}} \quad \text{and} \quad \mathcal{R}^{F_l} = \sum_{i_1 < \ldots < i_l} D_{i_1} \ldots D_{i_l} \ . \tag{5.2.44}$$

The D_k generate the primitive part of the vertical cohomology of $(\mathbb{P}^1)^{l+1}$, for which it is the full vertical cohomology with dimensions $h^{k,k}\left(\left(\mathbb{P}^1\right)^{l+1}\right) = \binom{l+1}{k}$, as well as for F_l and W_{l-1}, for which it is

$$h^{k,k}_{\text{prim}}(F_l) = \begin{cases} \binom{l+1}{k} & \text{if } k < \lceil \frac{l}{2} \rceil \\ \binom{l+1}{l-k} & \text{otherwise} \end{cases} \quad \text{and} \quad h^{k,k}_{\text{prim}}(W_{l-1}) = \begin{cases} \binom{l+1}{k} & \text{if } k < \lceil \frac{l}{2} \rceil - 1 \\ \binom{l+1}{l-1-k} & \text{otherwise} \end{cases} \ . \tag{5.2.45}$$

For high dimensions the primitive part is much smaller than the full vertical cohomology. The latter fact can be easily seen by calculating via the Hirzebruch-Riemann-Roch index theorem the elliptic genera $\chi_k = \sum (-1)^q h^{q,k}(X)$ by evaluating instead of the $\widehat{\Gamma}$-class the Todd class against $\mathrm{Ch}(\wedge^k TX)$.

According to [22, 23] this primitive part of the vertical cohomology should be mirror dual to the primitive horizontal middle cohomology which corresponds to solutions of those Picard-Fuchs equations as discussed in subsection 5.3.2. Luckily, it is only those solutions we need to describe the banana diagrams. The actual vertical– and horizontal cohomology groups are much bigger. For example for the differently polarized K3 surfaces called M_2 and W_2 we have $h^{1,1}_{\text{vert prim}}(W_2) = h^{1,1}_{\text{hor prim}}(M_2) = 4$ inside the twenty-dimensional group $H_{1,1}(\text{K3})$.

The D_k are dual to the rational curves $C_k = \mathbb{P}^1_k$ which span the Mori cone. The latter pair by integration $\int_{C_j} \omega_i = \delta_{ij}$ with the Kähler forms ω_k of the $\mathbb{P}^1_k$, which span the Kähler

[20] To ease the notation we denote the divisor classes on W_{l-1} and F_l again by D_k.

cone. To see e.g. that M_3 is really the mirror to W_3 we can check the mirror symmetry predictions at the level of the instantons. Using equations (5.2.35) and (5.2.44) we apply[21] the formalism of [17] for the prepotential of the case at hand and get up to order $\mathcal{O}(q^{11})$ and up to permutations

$$\begin{aligned}\mathcal{F}^{\text{prep}} &= 2\sum_{i<j<k}\mathfrak{t}^i\mathfrak{t}^j\mathfrak{t}^k+\sum_{i=k}^{5}\frac{24}{24}\mathfrak{t}^k-80\frac{\zeta(3)}{2(2\pi i)^3}+24\,\mathrm{Li}_3(q_1)+24\,\mathrm{Li}_3(q_1q_2)+112\,\mathrm{Li}_3(q_1q_2q_3)\\
&+1104\,\mathrm{Li}_3(q_1q_2q_3q_4)+19200\,\mathrm{Li}_3(q_1q_2q_3q_4q_5)+24\,\mathrm{Li}_3(q_1^2q_2q_3)+1104\,\mathrm{Li}_3(q_1^2q_2q_3q_4)\\
&+45408\,\mathrm{Li}_3(q_1^2q_3q_4q_5)+24\,\mathrm{Li}_3(q_1^2q_2^2q_3)+2800\,\mathrm{Li}_3(q_1^2q_2^2q_3q_4)+\\
&+212880\,\mathrm{Li}_3(q_1^2q_2^2q_3q_4q_5)+80\,\mathrm{Li}_3(q_1^2q_2^2q_3^2)+14496\,\mathrm{Li}_3(q_1^2q_2^2q_3^2q_4)\\
&+1691856\,\mathrm{Li}_3(q_1^2q_2^2q_3^2q_4q_5)+122352\,\mathrm{Li}_3(q_1^2q_2^2q_3^2q_4)\ .\end{aligned}$$

Here the $q_k=\exp(2\pi i\mathfrak{t}^k)$ keeps track of the (multi-) degree of a rational instanton contribution. $\mathrm{Li}_k(x)=\sum_{n=1}\frac{x^n}{n^k}$ denotes the polylogarithm and $\mathrm{Li}_3(x)$ subtracts the multi covering contributions to the $g=0$ curves. The integral coefficients of $\mathrm{Li}_3(\underline{q}^{\underline{d}})$ are denoted by $n_0^{\underline{d}}$. If the curves are smooth $n_0^{\underline{d}}=(-1)^{\dim(\mathcal{M}_{\underline{d}})}e(\mathcal{M}_{\underline{d}})$ is up to sign the Euler number of the moduli space $\mathcal{M}_{\underline{d}}$ of the rational curves of degree $\underline{d}$. We see that these instanton numbers are indeed as expected for W_3. For example each single degree one curve gives a contribution as $24\,\mathrm{Li}_3(q_1)$. Since the moduli space of such a curve is the K3 over which the $\mathbb{P}^1$ is fibered we get indeed $n_0^{(1,0,0,0,0)}=(-1)^2\chi(\mathrm{K3})=24$. The geometry W_{l-1} has an intriguing nested fibration structure. For example the K3 called W_2 is in four ways fibred by the elliptic curve W_1 over $\mathbb{P}^1_k$ for $k=1,\ldots,4$. While the Calabi-Yau three-fold W_3 for $l=4$ is in five ways fibered[22] with a K3 fiber of topology W_2, etc.

Now we can come to the main point and can use the mirror picture, the $\widehat{\Gamma}$-class conjecture and evaluation of the Chern classes to show that the leading logarithms (or $\mathfrak{t}$ powers) in the evaluation of the $\widehat{\Gamma}$-class

$$Z_{D_{l-1}}(\mathfrak{t})=\int_{W_{l-1}}e^{\omega\cdot\mathfrak{t}}\,\widehat{\Gamma}(TW_{l-1})+\mathcal{O}(e^{\mathfrak{t}}) \tag{5.2.46}$$

yield precisely the imaginary parts of Table 5.2.2 or more generally of (5.2.18).

Furthermore, we checked[23] that the leading logarithms (or $\mathfrak{t}$ powers) in the evaluation of

$$Z_{\mathcal{F}_{\sigma_l}}(\mathfrak{t})=\int_{F_l}e^{\omega\cdot\mathfrak{t}}\,\frac{1}{\widehat{\Gamma}^2(TF_l)}\widehat{A}(TF_l)+\mathcal{O}(e^{\mathfrak{t}})=\int_{F_l}e^{\omega\cdot\mathfrak{t}}\,\frac{\Gamma(1-c_1)}{\Gamma(1+c_1)}\cos(\pi c_1)+\mathcal{O}(e^{\mathfrak{t}}) \tag{5.2.47}$$

yield precisely the real part of Table 5.2.2 or more generally of (5.2.18). Here $\widehat{A}(TF_l)$ is the $\widehat{A}$-genus of the tangent sheaf TF_l which is generally defined for a rank n sheaf $\mathcal{F}$ as the

[21] This can be done with the program `Instanton` distributed with [17].

[22] The latter fact can be checked using the criterium of Oguiso [96] from the topological data that appears in the classical part of $\mathcal{F}^{\text{prep}}$.

[23] A few days after this preprint appeared in the arXiv, we received detailed e-mails from Hiroshi Iritani [97] indicating that the formula can be proven using the formalism [93, 95].

symmetric expansion $\widehat{A}(\mathcal{F}) = \prod_{i=1}^{n} \frac{2\pi i\delta_i}{\sinh(2\pi i\delta_i)}$ in terms of the eigenvalues δ_i of $\mathcal{F}$ and rewritten in terms of the Chern classes c_k.

Some remarks about (5.2.47) have to be said. First of all the two equalities in (5.2.47) were found by fitting an ansatz of a generalization of the $\widehat{\Gamma}$-class to the analytically computed values in (5.2.18). By this we observed that ansatze as in (5.2.47) reproduce the correct λ-coefficients. Notice that we are pretty sure that our ansatze are very special to the Fano variety F_l we are considering here. We do not believe that the relations in (5.2.47) are generally true. We leave it to future work to geometrically interpret and prove our modified $\widehat{\Gamma}$-class conjecture, see [98]. Secondly, we remark that the expected usual $\widehat{\Gamma}$-class ansatz as in (5.2.46) does not work even when ambiguities in the λ-coefficients are taken into account. These ambiguities arise due to analytic continuation of the Feynman amplitude around the MUM point. The monodromy of the Feynman amplitude is given by shifting each logarithm by $2\pi i$ such that λ-coefficients which contain even zeta values are shifted or in other words are ambiguous. Due to this ambiguity contributions containing only odd zeta values are ambiguity free and can naively be matched to the $\widehat{\Gamma}$-class. But also these terms are not correctly reproduced by a simple $\widehat{\Gamma}$-class[24]. Therefore, we take into account the more general form as given in (5.2.47) fitting to all even and odd zeta values in the λ-coefficients. Moreover, notice that the second equality in (5.2.47) is very useful since from it the real part of (5.2.20) follows trivially because the integral over F_l yields simply a contribution of $(l+1)!$ for c_1^l. But this term is again canceled in the generating series (5.2.20).

5.2.7 Monodromy

To each singular point s' of $\mathcal{L}_l$ (recall equation (5.2.7)) we can associate a monodromy matrix $M_{s'}^{(l)}$ acting on the Frobenius basis $\varpi_0, \ldots, \varpi_l$ around the MUM point $s = 0$ by

$$\begin{pmatrix} \varpi_0 \\ \vdots \\ \varpi_l \end{pmatrix} \longmapsto M_{s'}^{(l)} \begin{pmatrix} \varpi_0 \\ \vdots \\ \varpi_l \end{pmatrix} , \tag{5.2.48}$$

where we choose the analytic continuation along the upper half plane and encircle the singular point s' counterclockwise. For the MUM point $s' = 0$ one can directly read off $M_0^{(l)}$ from the structure of the Frobenius basis. At the singular points

$$\frac{1}{(l+1)^2} \ , \ \cdots \ , \ \frac{1}{(l+1-2\lfloor\frac{l+1}{2}\rfloor)^2} \tag{5.2.49}$$

the local Frobenius basis can in each case be chosen so that only one solution is singular, i.e. for these points the monodromy satisifies

$$\dim\Big(\text{image}(M_{s'}^{(l)} - \mathbb{1})\Big) = 1 \ . \tag{5.2.50}$$

This motivates the definition of the Frobenius constants $\kappa_k^{(l,s')}$ by

$$(M_{s'}^{(l)} - \mathbb{1})\varpi_k = \kappa_k^{(l,s')}(M_{s'}^{(l)} - \mathbb{1})\varpi_0 \ , \tag{5.2.51}$$

[24]For example for $l = 9$ the contribution of $\zeta(3)^3$ or for $l = 11$ the contribution of $\zeta(5)\zeta(3)^2$.

i.e. we choose the normalization such that $\kappa_0^{(l,s')} = 1$. Note that this only works when ϖ_0 is not invariant under $M_{s'}^{(l)}$.

The Feynman amplitude $\mathcal{F}_{\sigma_l}$ is only singular at $s' = 0$ and $s' = \frac{1}{(l+1)^2}$. For all other singular points s' satsifying (5.2.50) this implies[25] that the Frobenius constants are constrained by

$$\sum_{k=0}^{l} \lambda_k^{(l)} \kappa_k^{(l,s')} = 0 \ . \tag{5.2.52}$$

This can not hold for $s' = \frac{1}{(l+1)^2}$. However, numerically we find even stronger conditions for this point, i.e. we observe that the Frobenius constants do not depend on the loop order,

$$\kappa_k^{(l,1/(l+1)^2)} = \kappa_k^{(l',1/(l'+1)^2)} \quad \text{for } k \leq l, l' \ , \tag{5.2.53}$$

and that

$$\sum_{k=0}^{l} \kappa_k^{(l,1/(l+1)^2)} \lambda_k^{(l)} = -(2\pi i)^l \ . \tag{5.2.54}$$

Thus, restricting to the singular point $s' = \frac{1}{(l+1)^2}$, there is a series κ_k of Frobenius constants determined by

$$\sum_{k=0}^{\infty} \frac{\kappa_k}{k!} x^k = \frac{1}{\Gamma(1+x)^2} \ \mathrm{e}^{-2\gamma x} \ . \tag{5.2.55}$$

In terms of these Frobenius constants we can write the associated monodromy matrix as

$$M_{1/(l+1)^2}^{(l)} = \mathbb{1} + \begin{pmatrix} \kappa_0 \\ \vdots \\ \kappa_l \end{pmatrix} \left(\delta_0^{(l)}, ..., \delta_l^{(l)} \right) \tag{5.2.56}$$

for some constants $\delta_k^{(l)}$. These constants can now be determined using the fact[26]

$$M_0^{(l)} M_{1/(l+1)^2}^{(l)} \mathcal{F}_{\sigma_l} = \mathcal{F}_{\sigma_l} \ , \tag{5.2.57}$$

which gives

$$\sum_{l=1}^{\infty} \frac{\delta_0^{(l)}}{(l+1)!} x^l = -\frac{x}{\Gamma(1 - \frac{x}{2\pi i})^2} \ \mathrm{e}^{\gamma \frac{x}{i\pi}} \tag{5.2.58}$$

and the relation

$$\delta_k^{(l)} = \frac{1}{(2\pi i)^k} \binom{l+1}{k} \delta_0^{(l-k)} \ . \tag{5.2.59}$$

[25] Insert the definitions (5.2.15) and (5.2.51) in the trivial monodromy condition $(M_{s'}^{(l)} - \mathbb{1})\mathcal{F}_{\sigma_l} = 0$.

[26] The combined path of analytic continuation corresponding to the left hand side of (5.2.57) is contractible in $\mathbb{P}^1$, as $\mathcal{F}_{\sigma_l}$ picks up no non-trivial monodromies at the other singular points.

5.3 The l-loop non-equal mass banana Feynman integrals

Having discussed the equal mass banana Feynman graph, we want to focus in this section on the full non-equal mass case. We give a general description and method how to compute the l-loop non-equal mass banana Feynman graph, exemplified by the four-loop non-equal mass case. In [1] we have already discussed the two- and three-loop case.

5.3.1 Batyrev coordinates and the maximal cut integral

As in [1] we use Batyrev coordinates[27] z_k, defined by

$$z_k = \frac{\xi_k^2}{t - \sum_{i=1}^{l+1} \xi_i^2} \qquad \text{for } k = 1, \ldots, l+1 \ . \tag{5.3.1}$$

Furthermore, we include in the Feynman integral $\mathcal{F}_{\sigma_l}(t, \xi_i)$ the additional factor

$$a_0 = t - \sum_{i=1}^{l+1} \xi_i^2 = \frac{\xi_{l+1}^2}{z_{l+1}} \ , \tag{5.3.2}$$

which is related to the inner point of the polytope described by the polynomial constraint $P_l(t, \xi_i; x) = 0$. Then the expression we want to determine is

$$\hat{\mathcal{F}}_{\sigma_l} = \int_{\sigma_l} \frac{a_0 \mu_l}{P_l(t, \xi_i; x)} \ , \tag{5.3.3}$$

and will $\hat{\mathcal{F}}_{T^l}$ be defined by analogy. For large momenta we can use the expression (5.1.9) to find the non-equal mass maximal cut Feynman integral[28] including the inner point

$$\hat{\varpi}_0(z_i) = \sum_{k_1, \ldots, k_{l+1} \geq 0} \binom{|k|}{k_1, \ldots, k_{l+1}}^2 \left(\frac{1}{1 + \sum_{i=1}^{l+1} z_i} \right)^{1+|k|} \prod_{i=1}^{l+1} z_i^{k_i} \ . \tag{5.3.4}$$

Geometric series expansion gives a power series in the z_i with non-negative exponents, valid if all z_k are sufficiently small. The radius of convergence can be determined by the discriminant of the polynomial constraint $P_l(t, \xi; x)$ or later also from the differential operators annihilating (5.3.4). We claim that the discriminant[29] for the generic mass banana Feynman graph is given by

$$\Delta(\mathcal{D}^l)(t, \xi_i) = t \prod_{\{T_1, T_2\} \in \mathcal{T}} \left[t - \left(\sum_{i \in T_1} \xi_i - \sum_{i \in T_2} \xi_i \right)^2 \right] \ , \tag{5.3.5}$$

[27] Notice that these are not the same Batyrev coordinates as defined in (5.2.39) which correspond to the complete intersection model. Here now we consider the hypersurface model with other Batyrev coordinates.

[28] Again up to normalization.

[29] Or at least the discriminant factors up to multiplicities.

where the set

$$\mathcal{T} = \left\{ \{T_1, T_2\} \,\middle|\, T_1, T_2 \subseteq T^{(l+1)} \text{ disjoint and } T_1 \cup T_2 = T^{(l+1)} \right\} \tag{5.3.6}$$

gives all possibilities to distribute the $l+1$ indices among two subsets (identifying swaps of the two sets). We have explicitly checked $\Delta(\mathcal{D}^l)(t, \xi_i)$ for $l = 2, 3, 4$. The discriminant in the four-loop case is for instance given by

$$\begin{aligned}\Delta(\mathcal{D}^4)(t,\xi_i) = t \,&\big(t - (-\xi_1+\xi_2+\xi_3+\xi_4)^2\big)\,\big(t - (+\xi_1-\xi_2+\xi_3+\xi_4)^2\big)\\ &\big(t - (+\xi_1+\xi_2-\xi_3+\xi_4)^2\big)\,\big(t - (+\xi_1+\xi_2+\xi_3-\xi_4)^2\big)\\ &\big(t - (-\xi_1-\xi_2+\xi_3+\xi_4)^2\big)\,\big(t - (-\xi_1+\xi_2-\xi_3+\xi_4)^2\big)\\ &\big(t - (-\xi_1+\xi_2+\xi_3-\xi_4)^2\big)\,\big(t - (+\xi_1+\xi_2+\xi_3+\xi_4)^2\big)\ .\end{aligned} \tag{5.3.7}$$

In the equal mass case the discriminant $\Delta(\mathcal{D}^l)(t, \xi_i)$ reproduces the correct factors as stated in (5.2.7).

5.3.2 Differential equations for the non-equal mass case

Having found the holomorphic power series (5.3.4) describing the maximal cut Feynman integral for small values of z_k, as in [1] we now want to find a set of (in)homogeneous differential equations for it. With the help of (5.3.4) it can be checked that the second order operators[30]

$$\mathcal{D}_k = \theta_k^2 - z_k\left(\sum_{i=1}^{l+1}\theta_i - 2\theta_k\right)\left(1+\sum_{i=1}^{l+1}\theta_i\right) - z_k\left(\sum_{i=1}^{l+1} z_i - z_k\right)\left(1+\sum_{i=1}^{l+1}\theta_i\right)\left(1+\sum_{i=1}^{l+1}\theta_i\right) \tag{5.3.8}$$

for $k = 1, \ldots, l+1$ annihilate $\hat{\varpi}_0(z_i)$. Applying these operators to the full Feynman integral $\hat{\mathcal{F}}_{\sigma_l}$ and performing a numerical integration we find that the operators $\mathcal{D}_k$ are indeed homogeneous operators annihilating the full Feynman integral $\hat{\mathcal{F}}_{\sigma_l}$, see also section 2.3 in [1].

It turns out that these operators are enough to determine all solutions needed for the Feynman integral $\hat{\mathcal{F}}_{\sigma_l}$ — including those from integrals over closed cycles as well as the additional solution arising due to the chain integral — once the correct structure of solutions is imposed. Recall that the z_i are local coordinates around a MUM-point ($z_i = 0$ for all $i = 1, \ldots, l+1$), so there is a unique holomorphic solution up to normalization and the rest of the local Frobenius basis is spanned by solutions with increasing degree of the leading logarithms.[31] For periods coming from closed cycles the highest degree in logarithms of the $l+1$

[30] At this point we want to mention that it is also possible the obtain differential operators from the complete intersection model in 5.1. They follow directly from the ℓ-vector description, see [17], and are closely related to the ones in (5.3.8). The following discussion could have similarly been made also starting from these operators and analyzing the complete intersection model. Nevertheless, we focus in our discussion on the hypersurface model since this is how we originally invented our method.

[31] Here the notion of degree or better multidegree is such that for instance the periods $\hat{\varpi}_k^r$ in eqs. (5.3.11) have degree r, i.e. the arguments of the logs are irrelevant for this notion. Alternatively we call those r-fold logarithmic.

variables z_i is given by $l-1$, the (complex) dimension of the Calabi-Yau variety. Since in an algebraically realized Calabi-Yau variety, which fixes a polarization, only the primitive part of the horizontal subspace of the middle cohomology can be described by period integrals satisfying Picard-Fuchs equations [25], the number of r-fold logarithmic solutions corresponds to the dimension $h^{(l-1-r,r)}_{\text{hor prim}}$ of the respective piece in that subspace. Since the Feynman integral, i.e. the parametrization of the underlying Calabi-Yau variety, is completely symmetric in the z_i variables, solutions always come in complete orbits under permutations of the z_i.[32] On these grounds it is already possible to propose a generalization of the $l = 2, 3, 4$ results that we explicitly calculated. The number of periods over closed cycles is given by

$$
\begin{array}{ccccccccccccccccccccc}
 & & & & & & & & \#\text{hol} & & \#\log^1 & & & & & & & & & & \\
 & & & & & & & \#\text{hol} & & \#\log^1 & & \#\log^2 & & & & & & & & & \\
 & & & & & & \#\text{hol} & & \#\log^1 & & \#\log^2 & & \#\log^3 & & & & & & & & \\
 & & & & \#\text{hol} & & \#\log^1 & & \#\log^2 & & \#\log^3 & & \#\log^4 & & & & & & & & \\
 & & \#\text{hol} & & \#\log^1 & & \#\log^2 & & \#\log^3 & & \#\log^4 & & \#\log^5 & & & & & & & & \\
 & & & & & & & & & & & & & & & & & & & & \\
 & & & & & & & & & & & & & & & & & & & & \\
 & & & & & & & & & & & & & & & & & & & & \\
 & & & & & & & & & & & & & & & & & & & & \\
 & & & & & & & & & & & & & & & & & & & & \\
 & & & & & & & & & & & & & & & & & & & &
\end{array}
\quad \longrightarrow \quad
\begin{array}{ccccccccccccccccccccc}
 & & & & & & & & 1 & & 1 & & & & & & & & & & \\
 & & & & & & & 1 & & 4 & & 1 & & & & & & & & & \\
 & & & & & & 1 & & 5 & & 5 & & 1 & & & & & & & & \\
 & & & & & 1 & & 6 & & 15 & & 6 & & 1 & & & & & & & \\
 & & & & 1 & & 7 & & 21 & & 21 & & 7 & & 1 & & & & & & \\
 & & & & & & & & & & & & & & & & & & & & \\
 & & & & & & & & & & & & & & & & & & & & \\
 & & & & & & & & & & & & & & & & & & & & \\
 & & & & & & & & & & & & & & & & & & & & \\
 & & & & & & & & & & & & & & & & & & & & \\
 & & & & & & & & & & & & & & & & & & & &
\end{array}
$$

Table 5.3.1: The number of logarithmic solution for the non equal mass case for $l = 2, \ldots, 6$.

Here the entries in the nth row correspond to the number $d^{(l)}_r$ of basis elements at loop order $l = n+1$ that have the indicated degree r in logarithms, coinciding with the length of an orbit under permutations of the z_i. The left side is Pascal's triangle and the right side is fixed by the invariance of the primitive part of the horizontal Hodge numbers[33] of our variety under complex conjugation.

We shall further illucidate the combinatorial pattern that allows for a complete determation of a Frobenius basis and gives rise to the above numbers. After suitable normalization the holomorphic power series starts with unity

$$\hat{\varpi}_0(z_i) = 1 + \mathcal{O}(z_i^2) \ . \tag{5.3.9}$$

For $l > 2$ there are $l+1$ single logarithmic solutions of the form

$$\hat{\varpi}^k_1(z_i) = \log(z_k) + \mathcal{O}(z_i) \ . \tag{5.3.10}$$

Solutions of higher logarithmic degree $r \leq \lceil \frac{l}{2} \rceil - 1$ are of the form

$$\hat{\varpi}^k_r(z_i) = \prod_{i=1}^{r} \log(z_{j_i^{(k)}}) + \mathcal{O}(z_i) \qquad \text{for some} \quad \{j_1^{(k)}, \ldots, j_r^{(k)}\} \in T_r^{(l+1)} \ , \tag{5.3.11}$$

where $k = 1, \ldots, \binom{l+1}{r}$ now labels the elements of $T_r^{(l+1)}$, which we recall is the set of all subsets of $\{1, \ldots, l+1\}$ of length r.

[32] Similarly, the differential equations satisfied by the Feynman integrals always come in complete orbits.

[33] At that point we want to mention that Fernando Rodriguez Villegas told us that he actually found a motive from which one can directly calculate the horizontal Hodge numbers agreeing with our primitive horizontal Hodge numbers (5.2.45). We thank him for telling us this fact. Furthermore, we think that with some effort it is also possible to compute the full horizontal Hodge numbers from the complete intersection model described in section 5.1.

Further logarithmic solutions for $r > \lceil \frac{l}{2} \rceil - 1$ are obtained as follows. Label the $\binom{l+1}{l-r-1}$ subsets of $\{1, ..., l+1\}$ having exactly $l-r-1$ elements by k. For each k, i.e. a choice $N^{(k)} = \{n_1^{(k)}, \ldots, n_{l-r-1}^{(k)}\} \subseteq \{1, ..., l+1\}$, the solution $\hat{\varpi}_r^k$ only involves r-fold logarithms in the remaining $r+2$ variables and we have

$$\hat{\varpi}_r^k(z_i) = \sum_{\{j_1,\ldots,j_r\} \in \{1,\ldots,l+1\} \setminus N^{(k)}} \prod_{i=1}^{r} \log(z_{j_i}) + \mathcal{O}(z_i) \ . \tag{5.3.12}$$

As a consequence of these formulae, the total number of solutions (that correspond to integrals over closed cycles) is given by

$$\sum_{r=0}^{l-1} d_r^{(l)} = 2^{l+1} - \binom{l+2}{\lfloor \frac{l+2}{2} \rfloor} \ . \tag{5.3.13}$$

The additional (special) solution can be chosen to start as

$$\hat{\varpi}_l(z_i) = \prod_{i=1}^{l+1} \log(z_i) \sum_{i=1}^{l+1} \frac{1}{\log(z_i)} + \mathcal{O}(z_i) \ . \tag{5.3.14}$$

A generating function. As in the equal mass case we can define a generating function for a set of solutions by shifting $k_i \to k_i + \epsilon_i$ in the series (5.3.4). Derivatives with respect to the formal parameters ϵ_i then yield the higher logarithmic solutions. One has to take care that if the degree of the logarithms is larger than one, appropriate linear combinations of various derivatives have to be taken to get a correct solution. That is, these linear combinations should have the same combinatorial structure as the logarithmic solutions in (5.3.11), (5.3.12) and (5.3.14).

Loop reduction. An interesting feature of the solutions presented here is the following reduction property. Starting from those solutions for the l-loop banana integral which have no contribution from $\log(z_{l+1})$, those solutions of the $(l-1)$-loop integral which correspond to closed cycles are obtained from the former by setting z_{l+1} to zero. In this limit some l-loop solutions vanish and the number of non-zero logarithmic solutions of the $(l-1)$-loop geometry thus obtained nicely matches the number one expects according to the structure (5.3.9)-(5.3.12).

A four-loop example. To illustrate the structure of the solutions we consider the four-loop case, which is the lowest loop order that, to our knowledge, has not been treated analytically

in the non-equal mass case in the literature. Solutions start with

$$\begin{aligned}
\hat{\varpi}_0(z_i) &= 1 + 2\,(z_1z_2 + z_1z_3 + z_2z_3 + z_1z_4 + z_2z_4 + z_3z_4 + z_1z_5 + z_2z_5 \\
&\quad + z_3z_5 + z_4z_5) + \mathcal{O}(z_i)^3 \\
\hat{\varpi}^1_1(z_i) &= \log(z_1) - z_1 + z_2 + z_3 + z_4 + z_5 + \mathcal{O}(z_i)^2 \\
\hat{\varpi}^1_2(z_i) &= \log(z_2)\log(z_3) + \log(z_2)\log(z_4) + \log(z_3)\log(z_4) + \log(z_2)\log(z_5) \\
&\quad + \log(z_3)\log(z_5) + \log(z_4)\log(z_5) + \mathcal{O}(z_i) \\
\hat{\varpi}_3(z_i) &= \log(z_1)\log(z_2)\log(z_3) + \log(z_1)\log(z_2)\log(z_4) + \log(z_1)\log(z_3)\log(z_4) \\
&\quad + \log(z_2)\log(z_3)\log(z_4) + \log(z_1)\log(z_2)\log(z_5) + \log(z_1)\log(z_3)\log(z_5) \\
&\quad + \log(z_2)\log(z_3)\log(z_5) + \log(z_1)\log(z_4)\log(z_5) + \log(z_2)\log(z_4)\log(z_5) \\
&\quad + \log(z_3)\log(z_4)\log(z_5) + \mathcal{O}(z_i) \\
\hat{\varpi}_4(z_i) &= \log(z_1)\log(z_2)\log(z_3)\log(z_4) + \log(z_1)\log(z_2)\log(z_3)\log(z_5) + \mathcal{O}(z_i) \\
&\quad + \log(z_1)\log(z_2)\log(z_4)\log(z_5) + \log(z_1)\log(z_3)\log(z_4)\log(z_5) \\
&\quad + \log(z_2)\log(z_3)\log(z_4)\log(z_5) + \mathcal{O}(z_i)\ ,
\end{aligned} \tag{5.3.15}$$

where the other single- and double-logarithmic solutions are obtained by replacing $z_1 \leftrightarrow z_i$ by $i = 2, \ldots, 5$.

Analytic continuation by completing the differential ideal. To extend the solutions $\hat{\varpi}_n(z_i)$ for $n = 0, \ldots, l$ to other domains of the z_i-parameter space analytic continuation is needed. To this end it is necessary to have a complete set of differential equations. By these we mean a set of differential equations such that the number of corresponding solutions is equal to the number of solutions given in (5.3.13) plus the additional special solution. Notice that in general only the total number of solutions stays the same upon analytic continuation to other points. The precise logarithmic structure of the solutions changes, in particular for analytic continuation to non-singular points of the differential equations. With this (or these) additional differential equation(s) one can transform the local solutions of the MUM point to domains beyond the original domain of convergence by matching local Frobenius bases on overlapping regions.[34]

As we have explicitly seen in the two- and three-loop case[35] some differential equations get even extended with inhomogeneities if the whole Feynman integral $\hat{\mathcal{F}}_{\sigma_l}$ should satisfy them instead of just the maximal cut $\hat{\mathcal{F}}_{T^l}$. For the four-loop case we have found a second order operator with coefficients being polynomials of multidegree three in the five variables z_i, leading to an inhomogeneous differential equation given in appendix D. It is hard to give a general formula for the additional and perhaps inhomogeneous differential equation(s). In fact, it is not even clear whether one has to extend the operators $\mathcal{D}_k$ just by a single differential

[34] Of course, if one had again sufficient information about the analytic structure of a local Frobenius basis in the new region, one could construct a basis despite only knowing an incomplete set of differential equations, as was the case for the MUM point.

[35] For the two- and three-loop case these (inhomogeneous) differential equations are listed in [1] and for `mathematica`-file, see http://www.th.physik.uni-bonn.de/Groups/Klemm/data.php.

equation with or without an inhomogeneity. The general strategy to get a complete system of (inhomogeneous) differential equations is simply that one searches for new ones until only the expected number of solutions is determined by these operators. We suggest to search for second order operators by systematically increasing the multidegree of the coefficient polynomials multiplying the derivatives. At some point these are expected to yield a complete set of differential equations, as we checked for $l \leq 4$. If not, one has to go to higher degree equations in the ansatz.

5.3.3 Linear combination for the non-equal mass Feynman integral

Next we fix the linear combination of the previously constructed solutions that gives the full non-equal mass Feynman integral

$$\hat{\mathcal{F}}_{\sigma_l} = \sum_{r=0}^{l} \sum_{s=1}^{d_r^{(l)}} \lambda_{r,s}^{(l)} \, \hat{\varpi}_r^s \ . \tag{5.3.16}$$

As in the equal mass case we numerically compute $\hat{\mathcal{F}}_{\sigma_l}$ to fix the coefficients $\lambda_{r,s}^{(l)}$. These again turn out to be appropriate combinations of zeta values, closely related to the equal mass ones $\lambda_r^{(l)}$. For $l = 2, 3, 4$ and with respect to the basis of solutions given by (5.3.9), (5.3.10), (5.3.11),(5.3.12) and (5.3.14) we find the explicit values shown in Table 5.3.2. We see that

l	${\lambda_{0,s}}^{(l)}$	${\lambda_{1,s}}^{(l)}$	${\lambda_{2,s}}^{(l)}$	${\lambda_{3,s}}^{(l)}$	${\lambda_{4,s}}^{(l)}$
2	$18\zeta(2)$	$2\pi i$	1		
3	$-16\zeta(3)+24\pi\zeta(2)i$	$-18\zeta(2)$ $-18\zeta(2)$ $-18\zeta(2)$ $-18\zeta(2)$	$-2\pi i$	1	
4	$-450\zeta(4)$-$80\pi\zeta(3)i$	$16\zeta(3)$-$24\pi\zeta(2)i$ $16\zeta(3)$-$24\pi\zeta(2)i$ $16\zeta(3)$-$24\pi\zeta(2)i$ $16\zeta(3)$-$24\pi\zeta(2)i$ $16\zeta(3)$-$24\pi\zeta(2)i$	$6\zeta(2)$ $6\zeta(2)$ $6\zeta(2)$ $6\zeta(2)$ $6\zeta(2)$	$2\pi i$	1

Table 5.3.2: Coefficients giving the non-equal mass Feynman integral in the MUM point Frobenius basis of subsection 5.3.2.

with our choice of basis the equal mass values for $\lambda_r^{(l)}$ split symmetrically into the values $\lambda_{r,s}^{(l)}$. In general we claim that the non-equal mass values satisy

$$\lambda_{r,s}^{(l)} = \begin{cases} \lambda_r^{(l)} \cdot \binom{l+1}{r}^{-1} & \text{for } r \leq \lceil \frac{l}{2} \rceil - 1 \text{ and } s = 1, \ldots, \binom{l+1}{r} \\ \lambda_r^{(l)} \cdot \left(\binom{l+1}{l-r-1} \binom{r+2}{r} \right)^{-1} & \text{for } r > \lceil \frac{l}{2} \rceil - 1 \text{ and } s = 1, \ldots, \binom{l+1}{l-r-1} \\ 1 & \text{for } r = l \qquad \text{and } s = 1 \ . \end{cases} \tag{5.3.17}$$

We remark that the factor $\binom{r+2}{r}$ results from the $\binom{r+2}{r}$ terms in the sum of (5.3.12).

5.3.4 Remarks about master integrals for generalized banana Feynman integrals

Finally, we want to connect our results to certain master integrals for a (different kind of) family of banana type Feynman integrals. The latter family not only includes the Feynman integral $\mathcal{F}_{\sigma_l}$ with *fixed* loop order l, but also all integrals obtained by raising the propagators in the denominator to some non-negative powers ν_i and/or including polynomials in dot products of (external or loop) momenta in the numerator of the momentum space integrand. This constitutes a generalization of the kind of integrals considered so far in this work. By master integrals we then mean a finite subset of these integrals, i.e., a set of choices for the powers of propagators and powers of dot products, such that all other integrals in the family are obtained by linearly combining the master integrals, where the coefficients in general are rational functions[36] in the kinematic parameters (external momenta and masses).

For the two- and three-loop equal mass banana integrals sets of master integrals are known (see for instance [99] and [58]). In the non-equal mass case less is known. To the best of our knowledge only in the two-loop case all master integrals and their relations to the other integrals where found [100]. At least results for the number of higher loop master integrals are available in [101, 102].

Given our solution for $\mathcal{F}_{\sigma_l}$ we can at least construct a (sub-)set of master integrals which is possibly neither complete nor linearly independent[37], namely those integrals with trivial dot products in the numerator (of the standard momentum space represenation) but positive powers of the propagators in the denominator. For this note that raising the kth propagator to the power ν_k means taking the $(\nu_k - 1)$th derivative of the original Feynman integral $\mathcal{F}_{\sigma_l}$ (where all $\nu_i = 1$) with respect to the mass parameter ξ_k^2, i.e.

$$\mathcal{F}_{\sigma_l}(t, \xi_i; \nu_1, \ldots, \nu_{l+1}) = \prod_{k=1}^{l+1} \partial_{\xi_k^2}^{\nu_k - 1} \mathcal{F}_{\sigma_l}(t, \xi_i; 1, \ldots, 1) = \prod_{k=1}^{l+1} \partial_{\xi_k^2}^{\nu_k - 1} \mathcal{F}_{\sigma_l}(t, \xi_i) \ . \tag{5.3.18}$$

Since we have fixed the linear combination of the MUM-point Frobenius basis yielding the original Feynman integral $\mathcal{F}_{\sigma_l}$, we also have the correct linear combination for the mentioned (master) integrals $\mathcal{F}_{\sigma_l}(t, \xi_i; \nu_1, \ldots, \nu_{l+1})$ by the relation (5.3.18). As a consequence, expansions in the masses ξ_i^2 and the momentum t are readily available.

For the master integrals in the equal mass case we expect less independent functions. Of course, one can first construct the non-equal mass banana master integrals and at the end restrict to the equal mass case by setting all masses to unity. However, it is actually much simpler to consider only the derivatives

$$\frac{1}{r!} \left[\prod_{k=1}^{r} (\theta_t + k) \right] \mathcal{F}_{\sigma_l}(t, 1) \ , \tag{5.3.19}$$

[36] The precise definition of master integrals is immaterial at this points, as the only claims made will concern a set of integrals that, as we believe, should be amongst the master integrals in any reasonable defintion.

[37] Here again linear dependence refers to coefficients being rational functions in the kinematic parameters.

for at least $r \leq l-1$. These derivatives correspond to the integrals

$$\int_{\sigma_l} \frac{\mathcal{U}^r}{\mathcal{F}^{r+1}} \left(\sum_{k=1}^{l+1} x_i \right)^r \mu_l \ , \tag{5.3.20}$$

where

$$\mathcal{U} = \prod_{k=1}^{l+1} x_k \sum_{k=1}^{l+1} \tfrac{1}{x_k} \qquad \text{and} \qquad \mathcal{F} = \mathcal{U} \sum_{k=1}^{l+1} x_k \xi_k^2 - t \prod_{k=1}^{l+1} x_k \tag{5.3.21}$$

are the two Symanzik polynomials for the banana graphs. We expect that these integrals form part[38] of the basis for the equal mass l-loop family of banana integrals.

[38] At least one has to extend this set of master integrals by the constant function corresponding to the tadpole integral, which arises as a subtopology of the banana graph.

Chapter 6

Inhomogeneous Picard-Fuchs equation

By studying the variation of relative cohomology of a smooth projective hypersurface, one can construct an inhomogeneous Picard-Fuchs equation [12].
Let $\mathcal{D}_x$ be a Picard-Fuchs operator and Ω_x a family of nonzero holomorphic n-form on an n-dimensional projective variety parameterized by variable x. Then there exists a $(n-1)$-form β_x such that:

$$\mathcal{D}_x\Omega_x = -d\beta_x, \tag{6.0.1}$$

when it is integrated over a closed cycle, the exact term $d\beta_x$ does not contribute. It is related to closed string periods which satisfy homogeneous Picard-Fuchs equations. But in the open string period integrals, we integrate over a chain which has non-trivial boundary. This leads to have inhomogeneous Picard-Fuchs equations,

$$\int_\Gamma \mathcal{D}_x\Omega_x = -\int_{\partial\Gamma} \beta_x, \tag{6.0.2}$$

where Γ is the chain and $\partial\Gamma$ is its boundary. Let's give an example; consider X_x is a family of Calabi-Yau three-fold parameterized by variable x and Ω_x is a family of nonzero holomorphic 3-forms on X^x. By introducing a family of divisors $Y^{x,u}$ with an extra parameter u which deform in X_x, we can define a relative homology class $\Gamma \in \mathrm{H}_3(X_x, Y_{x,u})$. Now We obtain the relative period by,

$$\int_\Gamma \Omega_x, \tag{6.0.3}$$

and it is called a relative period for *B-brane*. There are two approaches to compute relative periods. One of them is similar to Griffiths-Dwork reduction [103], but the other approach is similar to GKZ approach and they propose an enlarged polytope to encode both the geometry of the toric variety, e.g. the Calabi-Yau X_x and the B-brane geometry [104]. The GKZ for relative periods yields a special solution at a critical point in u which give us a solution to the original inhomogeneous Picard-Fuchs equation.

We define the family of relative cohomology class $H^n(X_t, Y_t)$, where Y is a family of smooth subvariety of X and t a closed point, by the cohomology of the complex of pairs

$\Gamma(\Omega^n(X_t)) \oplus \Gamma(\Omega^{n-1}(Y_t))$. Where $\Omega^n(X_t)$ and $\Omega^{n-1}(Y_t)$ are sheaves of De Rahm differential n-forms on X_t and $(n-1)$-forms on Y_t and Γ is the smooth global section.
Let P_Δ to denote the toric variety corresponding to the polytope Δ and define a Calabi-Yau hypersurface in the toric variety by following equation,

$$f_{\hat{\Delta}}(X) = \sum_{\hat{v}_i \in \hat{\Delta}} a_i X^{\hat{v}_i}, \tag{6.0.4}$$

where X_i are toric coordinates. Each toric coordinate represent a corresponding monomial in the polynomial that defines the hypersurface, therefore one can easily find the relation between the homogeneous coordinates and toric coordinates. Now we can have a relevant rational form with pole of order one along the hypersurface by:

$$\Omega(a) = \frac{1}{f_{\hat{\Delta}}(X)} \prod_{j=1}^{n} \frac{dX_j}{X_j}, \tag{6.0.5}$$

we also define a 1-parameter family of automorphisms as:

$$\phi : X_i \to \frac{a_0}{a_i} X_i, \tag{6.0.6}$$

which transform the form that is parameterized by the Batyrev coordinate. Using this automorphism to reform our rational form and get $\tilde{\Pi}(z) = a_0 \phi^* \Pi(a)$, we redefine GKZ system as,

$$\tilde{\mathcal{D}} = \prod_{j=1}^{l_0>0} (a_0 \partial_{a_0} - j) \prod_{i \neq 0, l_i > 0} \prod_{j=0}^{l_i - 1} (a_i \partial_{a_i} - j) - a^l \prod_{j=1}^{-l_0>0} (a_0 \partial_{a_0} - j) \prod_{i \neq 0, -l_i > 0} \prod_{j=0}^{-l_i - 1} (a_i \partial_{a_i} - j). \tag{6.0.7}$$

Now if we replace following operators in $\tilde{\mathcal{D}}$, the new differential equation annihilates $\tilde{\Pi}(z)$,

$$\begin{aligned} a_0 \partial_{a_0} &\mapsto a_0 \partial_{a_0} - \mathcal{L}_{\sum_{j=1}^n X_j \partial_{X_j}} \\ a_j \partial_{a_j} &\mapsto a_j \partial_{a_j} + \mathcal{L}_{X_j \partial_{X_j}}, \quad \text{for } 1 \leq j \leq n \\ a_j \partial_{a_j} &\mapsto a_j \partial_{a_j}, \quad \text{for } j > n. \end{aligned} \tag{6.0.8}$$

then it leads to,

$$\begin{aligned} &(\prod_{j=1}^{l_0>0} (a_0 \partial_{a_0} - j) \prod_{i \neq 0, l_i > 0} \prod_{j=0}^{l_i - 1} (a_i \partial_{a_i} - j + \delta_{1 \leq i \leq n+1} \mathcal{L}_{X_j \partial_{X_j}}) \\ &- a^l \prod_{j=1}^{-l_0>0} (a_0 \partial_{a_0} - j) \prod_{i \neq 0, -l_i > 0} \prod_{j=0}^{-l_i - 1} (a_i \partial_{a_i} - j + \delta_{1 \leq i \leq n+1} \mathcal{L}_{X_j \partial_{X_j}})) \tilde{\Pi}(z) = 0, \end{aligned} \tag{6.0.9}$$

$\mathcal{L}_{X_j \partial_{X_j}}$ is the Lie derivative and commutes with all the logarithmic derivatives in the equation. For a vector V by the Cartan-Lie formula we have $\mathcal{L}_V = d\iota_V + \iota_V d$. Here ι_V is a interior product which is the contraction of a differential form with a vector field on the manifold M,

$$\iota_V : \Omega^p(M) \to \Omega^{p-1}(M), \tag{6.0.10}$$

it maps a p-form $\omega \in \Omega^p(M)$ to the $(p-1)$-form $\iota_V \omega \in \Omega^{p-1}(M)$. then the inhomogeneous GKZ system looks like,

$$\tilde{\mathcal{D}}\tilde{\Pi}(z) = -d\beta_l. \tag{6.0.11}$$

We can use this method to derive the inhomogeneous GKZ system for banana Feynman integrals. For this aim, we need to define the boundary of the integration domain by a corresponding divisor in the related Calabi-Yau manifold. After obtaining the divisor we can construct the enhanced polytope and from the enhanced polytope we obtain the inhomogeneous GKZ system.

Chapter 7

Conclusion

The geometric interpretation of Feynman integrals enables us to relate Feynman integrals to Calabi-Yau chain integrals and provides new and powerful methods to compute them. The new method is the resonant GKZ differential system that was used previously in the context of mirror symmetry to obtain the period integrals of Calabi-Yau hypersurfaces in toric varieties [16, 11, 10]. By applying this method, it becomes straightforward to compute the maximal cut integral at the point of maximal unipotent monodromy. The GKZ differential system benefits the symmetries of the Newton polytopes associated to the banana graphs very efficiently. But, as expected, it results in redundant solutions and variables which are more than the actual Calabi-Yau periods and Feynman integrals. The extra solutions are eliminated using methods from the mirror symmetry application of the GKZ system [16, 11, 10]. The intersection numbers allow us to derive the complete homogeneous Picard-Fuchs differential ideal in the physical parameters and its solutions characterize the analytic form of the maximal cut integral everywhere in the physical parameter space. It turns out that taking the advantage of the symmetries in this approach is more efficient than the multi parameter Griffiths-Dwork reduction method. One can find the relations which lead to master integrals and are derived by using Griffiths-Dwork reduction method for different classes of Feynman graphs in the physics literature like in [105–107].

We determined the inhomogeneity at the point of maximal unipotent monodromy by integrating the geometrical chain integral directly after applying the generators of the homogeneous Picard-Fuchs differential ideal on its integrand. It results in very simple form of functions as the corresponding inhomogeneities and that helps us to find an inhomogeneous solution. This leads to expressing the full mass dependence of the three-loop banana graph analytically, for the first time. By deriving the inhomogeneous Picard-Fuchs system of differential equations, we can relate the result of the Feynman integral to the relative periods that appear in the calculation of open topological string amplitudes [12].

After relating GKZ integrals to Calabi-Yau geometries by using the scaling invariance in Feynman integrals, we benefited a straightforward desingularizations of the hypersurfaces in toric varieties. But, this can be much more complicated for different geometries, like complete intersections in toric varieties or more interesting cases like Paffian Calabi-Yau spaces in Grassmanians or flag manifolds. Nevertheless, we expect that many aspects of the general approach outlined in our work can be applied further, as it has been done for example in

application of the GKZ to the complete intersection three-fold case [17–19], and to higher dimensional Calabi-Yau manifolds in [20–23].

After using GKZ method for banana integrals by relating them to the Calabi-Yau hypersurfaces, we got familiar with techniques developed in the interface of algebraic geometry and algebraic number theory with mathematical physics mostly in the context of string theory. We employed those techniques to describe the complete analytic structure of the l-loop banana integrals. In [48] for low energy region $t < (\sum_{i=1}^{l+1} \xi_i)^2$, the Bessel function integrals have been used to compute the banana integrals. As an extension of this work to the region $t \geq (\sum_{i=1}^{l+1} \xi_i)^2$ and into the high energy regime, we noted the realization of the Feynman amplitudes as periods of very symmetric complete intersection Calabi-Yau $(l-1)$-folds and their extension.

A geometrical interpretation was also observed for the coefficients of solutions of GKZ system in the large energy limit. These coefficients which are products of zeta values, have been explained by the $\widehat{\Gamma}$-class evaluation. Our application of the $\widehat{\Gamma}$-class to the Fano variety has been proved numerically, but it is still conjectural and poses an interesting challenge to prove it in mathematical rigor. Further studies might show that at special points, interesting (conjecturally transcendental) numbers, such as multiple zeta values (MZV) or critical values of modular L-functions appear as the evaluation of Feynman integrals.

To sum up, by understanding the geometrical structure of some special Feynman integral, we achieved to use GKZ methods to calculate those integrals very fast with a very high numerical precision. We are interested in applying our method to the other types of integrals. The GKZ method can be extended, as mentioned in [8], to more general rational integrals to find the same or a similar analytic structure like at the point of maximally unipotent monodromy. We have noticed that the evaluated $\widehat{\Gamma}$-class is proportional to the number of different dimensional faces of the corresponding Newton polytopes. Since the $\widehat{\Gamma}$-class evaluation is not always straightforward to compute, with further studies, one might be able to obtain them from the Newton polytope of the ambient space.

Moreover, it is worth to study the solution of the inhomogeneous Picard-Fuchs equation by the help of an enlarged polytope and use this method to solve the Feynman integrals totally by encoding the geometry of the integrand and the boundaries of the integral [12]. We applied the general theory of periods to the closed string mirror symmetry, but, it is also possible to use it in the open string case. By defining the so-called B-brane as the divisor, one can obtain the boundary terms and derive the solutions of the inhomogeneous Picard-Fuchs equation. Since computational efforts for triangulating polytopes in higher dimensions grows exponentially and it is crucial to get the Mori cone generators from a triangulation, one needs to investigate a general method for triangulating reflexive polytopes more precisely.

Appendices

Appendix A

Griffiths-Dwork reduction for a quintic hypersurface

Here we want to show step by step the Griffiths-Dwork reduction for a smooth quintic hypersurface in a projective space $\mathbb{P}$.
As we already mentioned in chapter 2, a quintic hypersurface in $\mathbb{P}$ is a Calabi-Yau 3-fold and it is defined by,

$$P = \sum_{i=1}^{5} \frac{1}{5} x_i^5 - a \prod_{i=1}^{5} x_i \tag{A.0.1}$$

where x_i are homogeneous coordinates and a is the moduli parameter. From the degree of the polynomial constraint we know that for the first step we have to take the derivative four times w.r.t. the moduli parameters from $\frac{\Pi(a)}{a} = \tilde{\Pi}(a) = \int_\gamma \frac{\mu}{P}$ and that leads to as shown already:

$$\frac{\partial^4}{\partial a^4}\tilde{\Pi}(a) = \int_\gamma \frac{4! \prod_{i=1}^{5} x_i^4 \ \mu}{P^5} = \frac{4!(a^4 x_1^4 (x_2x_3x_4x_5)^3 \partial_{x_1} P + a^3 x_1^7 x_2^3 (x_3x_4x_5)^2 \partial_{x_2} P + a^2 (x_1x_2)^6 x_3^2 x_4x_5 \partial_{x_3} P + a(x_1x_2x_3)^5 x_4 \partial_{x_4} P + (x_1x_2x_3x_4)^4 \partial_{x_5} P)}{(1-a^5)P^5} \tag{A.0.2}$$

now we have to obtain the third, second and first order derivative of the period in the ideal of $[\partial_{x_i} P]$. For this aim we use the integration by part relations to express the denominator with monomials without the partial derivatives. We can use following relation [27],

$$\frac{arQ(x,a)\partial_k P}{P^{r+1}} = \frac{a\partial_k Q(x,a)}{P^r}, \tag{A.0.3}$$

after applying it on equation A.0.2 and denoting $\partial_{x_i} P = \partial_i P$, it looks like,

$$\begin{aligned}
\frac{\partial^4}{\partial a^4}\tilde{\Pi}(a) &= \frac{3!(4a^4\prod_{i=1}^5 x_i^3 + 3a^3x_1^7(x_2x_3x_4x_5)^2 + 2a^2(x_1x_2)^6x_3x_4x_5 + a(x_1x_2x_3)^5)}{(1-a^5)P^4} \\
&= \frac{3!(4a^4\prod_{i=1}^5 x_i^3 + 3a^3x_1^7(x_2x_3x_4x_5)^2 + 3a^2(x_1x_2)^6x_3x_4x_5 + a(x_1x_2)^5x_3\partial_3 P)}{(1-a^5)P^4} \\
&= \frac{3!(4a^4\prod_{i=1}^5 x_i^3 + 6a^3x_1^7(x_2x_3x_4x_5)^2 + 3a^2x_1^6x_2^2x_3x_4x_5\partial_2 P + a(x_1x_2)^5x_3\partial_3 P)}{(1-a^5)P^4} \\
&= \frac{3!(10a^4\prod_{i=1}^5 x_i^3 + 6a^3x_1^3(x_2x_3x_4x_5)^2\partial_1 P + 3a^2x_1^6x_2^2x_3x_4x_5\partial_2 P + a(x_1x_2)^5x_3\partial_3 P)}{(1-a^5)P^4} \\
&= \frac{10a^4}{(1-a^5)}\frac{\partial^3}{\partial a^3}\tilde{\Pi}(a) + \frac{3!(6a^3x_1^3(x_2x_3x_4x_5)^2\partial_1 P + 3a^2x_1^6x_2^2x_3x_4x_5\partial_2 P + a(x_1x_2)^5x_3\partial_3 P)}{(1-a^5)P^4} \\
&= \frac{10a^4}{(1-a^5)}\frac{\partial^3}{\partial a^3}\tilde{\Pi}(a) + \frac{3!(6a^3\prod_{i=1}^5 x_i^2 + 2a^2x_1^6x_2x_3x_4x_5) + 2a(x_1x_2)^5}{(1-a^5)P^3} \\
&= \frac{10a^4}{(1-a^5)}\frac{\partial^3}{\partial a^3}\tilde{\Pi}(a) + \frac{36a^3\prod_{i=1}^5 x_i^2 + 14a^2x_1^6x_2x_3x_4x_5 + 2ax_1^5x_2\partial_2 P}{(1-a^5)P^3} \\
&= \frac{10a^4}{(1-a^5)}\frac{\partial^3}{\partial a^3}\tilde{\Pi}(a) + \frac{50a^3\prod_{i=1}^5 x_i^2 + 14a^2x_1^2x_2x_3x_4x_5\partial_1 P + 2ax_1^5x_2\partial_2 P}{(1-a^5)P^3} \\
&= \frac{10a^4}{(1-a^5)}\frac{\partial^3}{\partial a^3}\tilde{\Pi}(a) + \frac{25a^3}{(1-a^5)}\frac{\partial^2}{\partial a^2}\tilde{\Pi}(a) + \frac{14a^2x_1x_2x_3x_4x_5 + ax_1^5}{(1-a^5)P^2} \\
&= \frac{10a^4}{(1-a^5)}\frac{\partial^3}{\partial a^3}\tilde{\Pi}(a) + \frac{25a^3}{(1-a^5)}\frac{\partial^2}{\partial a^2}\tilde{\Pi}(a) + \frac{15a^2}{(1-a^5)}\frac{\partial}{\partial a}\tilde{\Pi}(a) + \frac{a}{(1-a^5)}\tilde{\Pi}(a)
\end{aligned} \tag{A.0.4}$$

and we have,

$$(a^5-1)\frac{\partial^4}{\partial a^4}\tilde{\Pi}(a) + 10a^4\frac{\partial^3}{\partial a^3}\tilde{\Pi}(a) + 25a^3\frac{\partial^2}{\partial a^2}\tilde{\Pi}(a) + 15a^2\frac{\partial}{\partial a}\tilde{\Pi}(a) + a\tilde{\Pi}(a) = 0 \tag{A.0.5}$$

and after replacing $t = a^{-5}$ and the logarithmic derivative $t\partial_t = \theta$, we have it in a generalized hypergeometric form,

$$\big[\theta^4 - t(\theta+\frac{1}{5})(\theta+\frac{2}{5})(\theta+\frac{3}{5})(\theta+\frac{4}{5})\big]a\tilde{\Pi}(a) = 0. \tag{A.0.6}$$

Appendix B

Derivation of the Bessel function representation

In this appendix we rewrite the Feynman integral (4.1.20) in terms of an integral over Bessel functions, closely follow the discussion in [85].

Starting from (4.1.20) one expands a factor in the denominator in terms of a geometric series,

$$\mathcal{F}_{\sigma_l} = -\sum_{k=0}^{\infty} t^k \int_{\sigma_l} \left(\frac{1}{\left(\sum_i \xi_i^2 x_i\right)\left(\sum_i x_i^{-1}\right)} \right)^{k+1} \frac{\mu_l}{\prod_i x_i} \ , \tag{B.0.1}$$

converging if $t < \left(\sum_i \xi_i^2 x_i\right)\left(\sum_i \frac{1}{x_i}\right)$. Since $x_i \geq 0$ we require

$$t < \left(\sum_{i=1}^{l+1} \xi_i \right)^2 \tag{B.0.2}$$

for equation (B.0.1) to hold. Furthermore, we can use the identity

$$\left(\frac{1}{a}\right)^{k+1} = \frac{1}{k!} \int_0^{\infty} \mathrm{e}^{-ax} x^k \ \mathrm{d}x \ , \tag{B.0.3}$$

which is valid for $\mathrm{Re}(a) > 0$ and $k > -1$, to rewrite the denominator in (B.0.1) introducing two new integrations

$$\mathcal{F}_{\sigma_l} = -\sum_{k=0}^{\infty} \frac{t^k}{(k!)^2} \int_{\sigma_l} \int_0^{\infty} \int_0^{\infty} \mathrm{e}^{-u\sum_i \xi_i^2 x_i - v\sum_i \frac{1}{x_i}} \ \frac{\mathrm{d}u\mathrm{d}v}{u^{-k}v^{-k}} \frac{\mu_l}{\prod_i x_i} \ . \tag{B.0.4}$$

The projective integral over σ_l can be performed using the identity

$$\int_0^{\infty} \mathrm{e}^{-um^2 x - \frac{v}{x}} \ \frac{\mathrm{d}x}{x} = 2K_0(2m\sqrt{uv}) \tag{B.0.5}$$

involving the Bessel function of the second kind K_0. We obtain

$$\mathcal{F}_{\sigma_l} = -2^l \sum_{k=0}^{\infty} \frac{t^k}{(k!)^2} \int_0^{\infty} \int_0^{\infty} \prod_{i=1}^{l} K_0\left(2\xi_i\sqrt{uv}\right) \mathrm{e}^{-u\ \xi_{l+1}^2 - v}\ \frac{\mathrm{d}u\mathrm{d}v}{u^{-k}v^{-k}}\ . \tag{B.0.6}$$

Introducing new variables $y = v$ and $z = 2\sqrt{uv}$ with $\mathrm{d}u\mathrm{d}v = \frac{z}{2y}\ \mathrm{d}y\mathrm{d}z$ and integrating subsequently over y we find

$$\mathcal{F}_{\sigma_l} = -2^{l+1} \sum_{k=0}^{\infty} \frac{t^k}{(k!)^2} \int_0^{\infty} \prod_{i=1}^{l+1} K_0(2\xi_i) \left(\frac{z}{2}\right)^{2k+1}\ \mathrm{d}z\ . \tag{B.0.7}$$

The Bessel function of the first kind I_0 has a series representation given by

$$I_0(x) = \sum_{k=0}^{\infty} \left(\frac{x}{2}\right)^{2k} \frac{1}{(k!)^2}\ , \tag{B.0.8}$$

which simplifies $\mathcal{F}_{\sigma_l}$ to the final expression

$$\mathcal{F}_{\sigma_l} = 2^l \int_0^{\infty} z\, I_0(\sqrt{t}z) \prod_{i=1}^{l+1} K_0(\xi_i z)\ \mathrm{d}z\ . \tag{B.0.9}$$

Appendix C

Differential operator ideal of the banana graph

Here we list a generating set of differential operators which describes the three-loop banana graph in all four physically important Batyrev coordinates.

$$\begin{aligned}\mathcal{D}_1 = &(\theta_1-\theta_2)\,(\theta_3-\theta_4)\\ &+z_1(\theta_3-\theta_4)(\theta_1-\theta_2-\theta_3-\theta_4)+z_2(\theta_3-\theta_4)(\theta_1-\theta_2+\theta_3+\theta_4)\\ &-2(z_1-z_2)\,(z_3(\theta_3+1)-z_4(\theta_4+1))\,(\theta_1+\theta_2+\theta_3+\theta_4+1)\end{aligned} \tag{C.0.1}$$

$$\begin{aligned}\mathcal{D}_2 = &5(\theta_1-\theta_2)\theta_4-6\theta_2^2\\ &+z_1\left(2\theta_1^2-8\theta_1\theta_2+6\theta_2^2-6\theta_3^2-11\theta_4^2+4\,(\theta_1+\theta_2)\,\theta_3+(9\theta_1-\theta_2-13\theta_3)\,\theta_4\right)\\ &+z_2\left(17\theta_4^2+(13\theta_1-9\theta_2+25\theta_3+6)\,\theta_4-2\,(\theta_2-\theta_3)\,(4\theta_2+6\theta_3+3)+\theta_1\,(8\theta_2+8\theta_3+6)\right)\\ &+2\left[5z_3z_4(\theta_2-\theta_1)+z_1^2(\theta_1-\theta_2-\theta_3-\theta_4)+z_2^2(\theta_1-\theta_2+\theta_3+\theta_4)\right.\\ &+z_1z_4(3\theta_1+3\theta_2-2\theta_3-8\theta_4-5)+z_1z_3(3\,(\theta_1+\theta_2-\theta_3)-2\theta_4)\\ &+3z_1z_2(-\theta_1+3\theta_2+\theta_3+\theta_4+2)+z_2z_3(6\theta_3+5\theta_4+6)\\ &\left.+z_2z_4(5\theta_3+11\theta_4+11)\right]\,(\theta_1+\theta_2+\theta_3+\theta_4+1)\end{aligned} \tag{C.0.2}$$

$$\begin{aligned}\mathcal{D}_3 = &-3\theta_2^2-2\theta_2\theta_4+\theta_1\,(3\theta_2-2\theta_4)+\theta_4\,(\theta_3+\theta_4)\\ &-3z_1\theta_2\,(-\theta_1+\theta_2+\theta_3)-z_1\theta_4(2\theta_1+\theta_2-2\theta_3)-z_3\theta_4(\theta_1+\theta_2-\theta_3)+(2z_1-z_3)\theta_4^2\\ &-z_4\,(\theta_1+\theta_2+\theta_3-\theta_4)\,(\theta_4+1)+z_2\,(\theta_1-\theta_2+\theta_3+\theta_4)\,(3\theta_2+8\theta_4+3)\\ &+2\left[-2z_3z_4(\theta_4+1)+z_1z_4-3z_1z_3\theta_2+z_1(z_3+z_4)\theta_4+z_2z_3(3\theta_2+4\theta_4+3)\right.\\ &\left.+4z_2z_4+4z_2(z_1+z_4)\theta_4\right]\,(\theta_1+\theta_2+\theta_3+\theta_4+1)\end{aligned} \tag{C.0.3}$$

$$
\begin{aligned}
\mathcal{D}_4 = &-\theta_2\left(\theta_2+5\theta_3-5\theta_4\right)\\
&+z_1(2\theta_1^2-\left(3\theta_2+\theta_3-4\theta_4\right)\theta_1+\theta_2^2-\theta_3^2-6\theta_4^2+4\theta_2\theta_3-\left(\theta_2+3\theta_3\right)\theta_4)\\
&+5z_4\left(\theta_1-\theta_2-\theta_3\right)\left(\theta_1+\theta_2+\theta_3-\theta_4\right)+5z_3\theta_4\left(\theta_1+\theta_2-\theta_3+\theta_4\right)\\
&+z_2\left[-3\theta_2^2+\left(-14\theta_3+11\theta_4-1\right)\theta_2+17\theta_3^2-8\theta_4^2+\theta_3+\theta_1\left(3\theta_2+13\theta_3-12\theta_4+1\right)\right.\\
&\left.+5\theta_3\theta_4+\theta_4\right]\\
&+\left[2z_1^2(\theta_1-\theta_2-\theta_3-\theta_4)+z_1z_4(11\theta_1-9\theta_2+\theta_3-11\theta_4)\right.\\
&+z_1z_2(-\theta_1+3\theta_2+11\theta_3-9\theta_4+2)+z_1z_3(\theta_1+11\theta_2-\theta_3+\theta_4)\\
&+2z_2z_3(-5\theta_2+11\theta_3-5\theta_4+6)+2z_2z_4(5\theta_3-4\theta_4-4)+10z_3z_4(\theta_4-\theta_3)\\
&\left.+2z_2^2(\theta_1-\theta_2+\theta_3+\theta_4)\right]\left(\theta_1+\theta_2+\theta_3+\theta_4+1\right)
\end{aligned}
\tag{C.0.4}
$$

Appendix D

Inhomogeneous differential equation for the four-loop case

In this appendix we give an inhomogeneous differential equation

$$\mathcal{D}\hat{\mathcal{F}}_{\sigma_4} = S, \tag{D.0.1}$$

satisfied by the four-loop banana Feynman integral $\hat{\mathcal{F}}_{\sigma_4}$ (which includes the extra factor (5.3.2) in the numerator) in the case of generic masses. Operators $\mathcal{D}_k$ leading to homogeneous differential equations for $\hat{\mathcal{F}}_{\sigma_4}$ have already been given in (5.3.8). Indeed, here we only present the leading contribution in z_i to $\mathcal{D}$, which reads

$$\begin{aligned}\mathcal{D} = &-63\,\theta_2^2 - 416\,\theta_1\theta_3 - 13\,\theta_2\theta_3 + 206\,\theta_3^2 - 180\,\theta_1\theta_4 + 102\,\theta_2\theta_4 + 507\,\theta_3\theta_4 + 180\,\theta_4^2 \\ &+ 596\,\theta_1\theta_5 - 89\,\theta_2\theta_5 - 78\,\theta_3\theta_5 - 429\,\theta_4\theta_5 - 323\,\theta_5^2 + \mathcal{O}(z_i)\ .\end{aligned} \tag{D.0.2}$$

The complete expression of this second-order operator $\mathcal{D}$ can be found in a supplementary `mathematica`-file on our web page[1]. Furthermore, the inhomogeneity to $\mathcal{D}$ is given by

$$\begin{aligned}S = \ &(-42z_1 + 168z_2 - 101z_3 + 282z_4 - 139z_5)\log(z_1)\log(z_2) \\ &+ (-416 - 556z_1 + 283z_2 + 105z_3 - 15z_4 - 128z_5)\log(z_1)\log(z_3) \\ &+ (-180 - 180z_1 - 345z_2 - 195z_3 + 540z_5)\log(z_1)\log(z_4) \\ &+ (596 + 778z_1 - 106z_2 + 191z_3 - 267z_4 - 273z_5)\log(z_1)\log(z_5) \\ &+ (-13 + 533z_1 + 203z_2 - 21z_3 - 15z_4 - 128z_5)\log(z_2)\log(z_3) \\ &+ (102 + 123z_1 + 168z_2 - 195z_3 - 6z_5)\log(z_2)\log(z_4) \\ &+ (-89 - 614z_1 - 539z_2 + 317z_3 - 267z_4 + 273z_5)\log(z_2)\log(z_5) \\ &+ (507 + 122z_1 - 477z_2 + 407z_3 - 252z_4 - 139z_5)\log(z_3)\log(z_4) \\ &+ (-78 - 99z_1 - 9z_2 - 491z_3 + 282z_4 + 395z_5)\log(z_3)\log(z_5) \\ &+ (-429 - 65z_1 + 654z_2 - 17z_3 + 252z_4 - 395z_5)\log(z_4)\log(z_5)\ .\end{aligned} \tag{D.0.3}$$

[1] http://www.th.physik.uni-bonn.de/Groups/Klemm/data.php

Bibliography

[1] A. Klemm, C. Nega, and R. Safari, "The l-loop Banana Amplitude from GKZ Systems and relative Calabi-Yau Periods," *JHEP* **04** (2020) 088, arXiv:1912.06201 [hep-th].

[2] K. Boenisch, F. Fischbach, A. Klemm, C. Nega, and R. Safari, "Analytic structure of all loop banana integrals," *JHEP* **05** (2021) 066, arXiv:2008.10574 [hep-th].

[3] S. Bloch, M. Kerr, and P. Vanhove, "Local mirror symmetry and the sunset Feynman integral," *Adv. Theor. Math. Phys.* **21** no. 6, (2017) 1373–1454.

[4] C. Bogner and S. Weinzierl, "Feynman graph polynomials," *Int. J. Mod. Phys. A* **25** (2010) 2585–2618, arXiv:1002.3458 [hep-ph].

[5] "Integration by parts: The algorithm to calculate -functions in 4 loops," *Nuclear Physics B* **192** no. 1, (1981) 159–204.

[6] V. A. Smirnov, *Analytic tools for Feynman integrals*, vol. 250. 2012.

[7] Müller-Stach, Stefan and Weinzierl, Stefan and Zayadeh, Raphael, "Picard-Fuchs equations for Feynman integrals," *Commun. Math. Phys.* **326** (2014) 237–249, arXiv:1212.4389 [hep-ph].

[8] I. M. Gel′ fand, A. V. Zelevinskiĭ, and M. M. Kapranov, "Hypergeometric functions and toric varieties," *Funktsional. Anal. i Prilozhen.* **23** no. 2, (1989) 12–26. https://doi.org/10.1007/BF01078777.

[9] C. Bogner and S. Weinzierl, "Periods and Feynman integrals," *J. Math. Phys.* **50** (2009) 042302, arXiv:0711.4863 [hep-th].

[10] S. Hosono, B. H. Lian, and S.-T. Yau, "Gkz generalized hypergeometric systems in mirror symmetry of calabi-yau hypersurfaces," *Commun. Math. Phys.* **182** (1996) 535–578, arXiv:alg-geom/9511001 [alg-geom].

[11] S. Hosono, A. Klemm, S. Theisen, and S.-T. Yau, "Mirror symmetry, mirror map and applications to calabi-yau hypersurfaces," *Commun. Math. Phys.* **167** (1995) 301–350, arXiv:hep-th/9308122 [hep-th].

[12] S. Li, B. H. Lian, and S.-T. Yau, "Picard-fuchs equations for relative periods and abel-jacobi map for calabi-yau hypersurfaces," arXiv:0910.4215 [math.AG].

[13] S. Groote, J. G. Korner, and A. A. Pivovarov, "On the evaluation of sunset - type Feynman diagrams," *Nucl. Phys. B* **542** (1999) 515–547, arXiv:hep-ph/9806402.

[14] S. Bauberger, M. Böhm, G. Weiglein, F. A. Berends, and M. Buza, "Calculation of two-loop self-energies in the electroweak Standard Model," *Nucl. Phys. B Proc. Suppl.* **37** no. 2, (1994) 95–114, arXiv:hep-ph/9406404.

[15] R. Bonciani, V. Del Duca, H. Frellesvig, J. M. Henn, M. Hidding, L. Maestri, F. Moriello, G. Salvatori, and V. A. Smirnov, "Evaluating a family of two-loop non-planar master integrals for Higgs + jet production with full heavy-quark mass dependence," *JHEP* **01** (2020) 132, arXiv:1907.13156 [hep-ph].

[16] V. V. Batyrev, "Dual polyhedra and mirror symmetry for Calabi-Yau hypersurfaces in toric varieties," *J. Algebraic Geom.* **3** no. 3, (1994) 493–535.

[17] S. Hosono, A. Klemm, S. Theisen, and S.-T. Yau, "Mirror symmetry, mirror map and applications to complete intersection Calabi-Yau spaces," *Nucl. Phys.* **B433** (1995) 501–554, arXiv:hep-th/9406055 [hep-th]. [AMS/IP Stud. Adv. Math.1,545(1996)].

[18] V. V. Batyrev and D. van Straten, "Generalized hypergeometric functions and rational curves on Calabi-Yau complete intersections in toric varieties," *Comm. Math. Phys.* **168** no. 3, (1995) 493–533. http://projecteuclid.org/euclid.cmp/1104272487.

[19] V. V. Batyrev and L. A. Borisov, "On Calabi-Yau complete intersections in toric varieties," in *Higher-dimensional complex varieties (Trento, 1994)*, pp. 39–65. de Gruyter, Berlin, 1996.

[20] B. R. Greene, D. R. Morrison, and M. R. Plesser, "Mirror manifolds in higher dimension," *Commun. Math. Phys.* **173** (1995) 559–598, arXiv:hep-th/9402119 [hep-th]. [AMS/IP Stud. Adv. Math.1,745(1996)].

[21] P. Mayr, "Mirror symmetry, N=1 superpotentials and tensionless strings on Calabi-Yau four folds," *Nucl. Phys.* **B494** (1997) 489–545, arXiv:hep-th/9610162 [hep-th].

[22] A. Klemm, B. Lian, S. S. Roan, and S.-T. Yau, "Calabi-Yau fourfolds for M theory and F theory compactifications," *Nucl. Phys.* **B518** (1998) 515–574, arXiv:hep-th/9701023 [hep-th].

[23] N. Cabo Bizet, A. Klemm, and D. Vieira Lopes, "Landscaping with fluxes and the E8 Yukawa Point in F-theory," arXiv:1404.7645 [hep-th].

[24] A. Gerhardus and H. Jockers, "Quantum periods of Calabi–Yau fourfolds," *Nucl. Phys.* **B913** (2016) 425–474, arXiv:1604.05325 [hep-th].

[25] A. Klemm, "The B-model approach to topological string theory on Calabi-Yau n-folds," in *B-model Gromov-Witten theory*, Trends Math., pp. 79–397. Birkhäuser/Springer, Cham, 2018.

[26] M. Kontsevich and D. Zagier, "Periods," in *Mathematics unlimited—2001 and beyond*, pp. 771–808. Springer, Berlin, 2001.

[27] A. Klemm, *The B-Model Approach to Topological String Theory on Calabi-Yau n-Folds*. 2018.

[28] K. Kikkawa and M. Yamasaki, "Casimir Effects in Superstring Theories," *Phys. Lett. B* **149** (1984) 357–360.

[29] N. Sakai and I. Senda, "Vacuum Energies of String Compactified on Torus," *Prog. Theor. Phys.* **75** (1986) 692. [Erratum: Prog.Theor.Phys. 77, 773 (1987)].

[30] P. Candelas, G. T. Horowitz, A. Strominger, and E. Witten, "Vacuum Configurations for Superstrings," *Nucl. Phys. B* **258** (1985) 46–74.

[31] W. Lerche, C. Vafa, and N. P. Warner, "Chiral Rings in N=2 Superconformal Theories," *Nucl. Phys. B* **324** (1989) 427–474.

[32] K. Hori, S. Katz, A. Klemm, R. Pandharipande, R. Thomas, C. Vafa, R. Vakil, and E. Zaslow, *Mirror symmetry*, vol. 1 of *Clay mathematics monographs*. AMS, Providence, USA, 2003.

[33] D. A. Cox and S. Katz, *Mirror symmetry and algebraic geometry*. 2000.

[34] V. V. Batyrev, "Dual Polyhedra and Mirror Symmetry for Calabi-Yau Hypersurfaces in Toric Varieties," *arXiv e-prints* (Oct., 1993) alg–geom/9310003, `arXiv:alg-geom/9310003 [math.AG]`.

[35] V. V. Batyrev and L. A. Borisov, "On Calabi-Yau complete intersections in toric varieties," `arXiv:alg-geom/9412017`.

[36] R. N. Lee, "Presenting LiteRed: a tool for the Loop InTEgrals REDuction," `arXiv:1212.2685 [hep-ph]`.

[37] "Fire6: Feynman integral reduction with modular arithmetic," *Computer Physics Communications* **247** (2020) 106877.

[38] P. Maierhöfer, J. Usovitsch, and P. Uwer, "Kira—A Feynman integral reduction program," *Comput. Phys. Commun.* **230** (2018) 99–112, `arXiv:1705.05610 [hep-ph]`.

[39] A. V. Smirnov and V. A. Smirnov, "How to choose master integrals," *Nucl. Phys. B* **960** (2020) 115213, `arXiv:2002.08042 [hep-ph]`.

[40] J. M. Henn, "Lectures on differential equations for feynman integrals," *Journal of Physics A: Mathematical and Theoretical* **48** no. 15, (mar, 2015) 153001.

[41] T. Gehrmann and E. Remiddi, "Differential equations for two loop four point functions," *Nucl. Phys. B* **580** (2000) 485–518, `arXiv:hep-ph/9912329`.

[42] M. A. Bezuglov, "Integral representation for three-loop banana graph," arXiv:2104.14681 [hep-ph].

[43] C. Itzykson and J. B. Zuber, *Quantum Field Theory*. International Series In Pure and Applied Physics. McGraw-Hill, New York, 1980. http://dx.doi.org/10.1063/1.2916419.

[44] S. Weinzierl, "The Art of computing loop integrals," *Fields Inst. Commun.* **50** (2007) 345–395, arXiv:hep-ph/0604068.

[45] R. Bott and L. W. Tu, *Differential forms in algebraic topology*, vol. 82 of *Graduate Texts in Mathematics*. Springer-Verlag, New York-Berlin, 1982.

[46] D. A. Cox, J. B. Little, and H. K. Schenck, *Toric varieties*, vol. 124 of *Graduate Studies in Mathematics*. American Mathematical Society, Providence, RI, 2011. https://doi.org/10.1090/gsm/124.

[47] http://doc.sagemath.org/html/en/reference/schemes/sage/schemes/toric/variety.html.

[48] S. Bloch, M. Kerr, and P. Vanhove, "Local mirror symmetry and the sunset feynman integral," *Adv. Theor. Math. Phys.* **21** (2017) 1373–1453, arXiv:1601.08181 [hep-th].

[49] I. M. Gel′ fand, A. V. Zelevinskiĭ, and M. M. Kapranov, "Newton polyhedra of principal A-determinants," *Dokl. Akad. Nauk SSSR* **308** no. 1, (1989) 20–23.

[50] V. V. Batyrev and D. van Straten, "Generalized hypergeometric functions and rational curves on calabi-yau complete intersections in toric varieties," *Commun. Math. Phys.* **168** (1995) 493–534, arXiv:alg-geom/9307010 [alg-geom].

[51] P. A. Griffiths, "On the periods of certain rational integrals. I, II," *Ann. of Math. (2) 90 (1969), 460-495; ibid. (2)* **90** (1969) 496–541. https://doi.org/10.2307/1970746.

[52] J. M. Henn, "Lectures on differential equations for Feynman integrals," *J. Phys.* **A48** (2015) 153001, arXiv:1412.2296 [hep-ph].

[53] I. M. Gel′ fand, M. M. Kapranov, and A. V. Zelevinsky, "Generalized Euler integrals and A-hypergeometric functions," *Adv. Math.* **84** no. 2, (1990) 255–271. https://doi.org/10.1016/0001-8708(90)90048-R.

[54] R. L. Bryant and P. A. Griffiths, "Some observations on the infinitesimal period relations for regular threefolds with trivial canonical bundle," in *Arithmetic and geometry, Vol. II*, vol. 36 of *Progr. Math.*, pp. 77–102. Birkhäuser Boston, Boston, MA, 1983.

[55] P. Vanhove, "The physics and the mixed Hodge structure of Feynman integrals," *Proc. Symp. Pure Math.* **88** (2014) 161–194, arXiv:1401.6438 [hep-th].

[56] M.-X. Huang, A. Klemm, and M. Poretschkin, "Refined stable pair invariants for E-, M- and $[p, q]$-strings," *JHEP* **11** (2013) 112, arXiv:1308.0619 [hep-th].

[57] J. Broedel, C. Duhr, F. Dulat, R. Marzucca, B. Penante, and L. Tancredi, "An analytic solution for the equal-mass banana graph," *JHEP* **09** (2019) 112, arXiv:1907.03787 [hep-th].

[58] A. Primo and L. Tancredi, "Maximal cuts and differential equations for Feynman integrals. An application to the three-loop massive banana graph," *Nucl. Phys.* **B921** (2017) 316–356, arXiv:1704.05465 [hep-ph].

[59] D. Maulik, R. Pandharipande, and R. P. Thomas, "Curves on $K3$ surfaces and modular forms," *J. Topol.* **3** no. 4, (2010) 937–996. https://doi.org/10.1112/jtopol/jtq030. With an appendix by A. Pixton.

[60] G. Oberdieck and R. Pandharipande, "Curve counting on $K3 \times E$, the Igusa cusp form χ_{10}, and descendent integration," in *K3 surfaces and their moduli*, vol. 315 of *Progr. Math.*, pp. 245–278. Birkhäuser/Springer, [Cham], 2016. https://doi.org/10.1007/978-3-319-29959-410.

[61] H. A. Verrill, "Root lattices and pencils of varieties," *J. Math. Kyoto Univ.* **36** no. 2, (1996) 423–446. https://doi.org/10.1215/kjm/1250518557.

[62] B. H. Lian and S.-T. Yau, "Mirror maps, modular relations and hypergeometric series 1," arXiv:hep-th/9507151 [hep-th].

[63] J. H. Conway and S. P. Norton, "Monstrous moonshine," *Bull. London Math. Soc.* **11** no. 3, (1979) 308–339. https://doi.org/10.1112/blms/11.3.308.

[64] A. R. Forsyth, *Theory of differential equations. 1. Exact equations and Pfaff's problem; 2, 3. Ordinary equations, not linear; 4. Ordinary linear equations; 5, 6. Partial differential equations.* Six volumes bound as three. Dover Publications, Inc., New York, 1959.

[65] W. Lerche, D. J. Smit, and N. P. Warner, "Differential equations for periods and flat coordinates in two-dimensional topological matter theories," *Nucl. Phys.* **B372** (1992) 87–112, arXiv:hep-th/9108013 [hep-th].

[66] R. E. Borcherds, "Automorphic forms with singularities on Grassmannians," *Invent. Math.* **132** no. 3, (1998) 491–562. https://doi.org/10.1007/s002220050232.

[67] A. Klemm and M. Marino, "Counting BPS states on the enriques Calabi-Yau," *Commun. Math. Phys.* **280** (2008) 27–76, arXiv:hep-th/0512227 [hep-th].

[68] T. W. Grimm, A. Klemm, M. Marino, and M. Weiss, "Direct Integration of the Topological String," *JHEP* **08** (2007) 058, arXiv:hep-th/0702187 [HEP-TH].

[69] G. Almkvist, C. van Enckevort, D. van Straten, and W. Zudilin, "Tables of calabi-yau equations." arXiv:math/0507430v2 [math.AG].

[70] D. van Straten, "Calabi-Yau operators," in *Uniformization, Riemann-Hilbert correspondence, Calabi-Yau manifolds & Picard-Fuchs equations*, vol. 42 of *Adv. Lect. Math. (ALM)*, pp. 401–451. Int. Press, Somerville, MA, 2018.

[71] P. Candelas, X. de la Ossa, M. Elmi, and D. van Straten, "A one parameter family of calabi-yau manifolds with attractor points of rank two." to appear.

[72] K. Boenisch, A. Klemm, E. Scheidegger, and D. Zagier, "Periods and quasiperiods of modular forms and d-brane masses for the mirror quintic." to appear.

[73] T. Coates, A. Corti, S. Galkin, V. Golyshev, and A. Kasprzyk, "Fano varieties and extremal laurent polynomials: A collaborative research blog." HTTP://COATES.MA.IC.AC.UK/FANOSEARCH/, since December 2012.

[74] D. H. Bailey, J. M. Borwein, D. Broadhurst, and M. Glasser, "Elliptic integral evaluations of bessel moments and applications," *Journal of Physics A: Mathematical and Theoretical* **41** no. 20, (2008) 205203.

[75] D. Broadhurst, *Multiple Zeta Values and Modular Forms in Quantum Field Theory*, pp. 33–73. Springer Vienna, 2013.

[76] D. Broadhurst and D. P. Roberts, "Quadratic relations between Feynman integrals," *PoS* **LL2018** (2018) 053.

[77] Y. Zhou, "Wrońskian factorizations and Broadhurst–Mellit determinant formulae," *Commun. Num. Theor. Phys.* **12** (2018) 355–407, arXiv:1711.01829 [math.CA].

[78] Y. Zhou, "Some algebraic and arithmetic properties of Feynman diagrams," in *KMPB Conference: Elliptic Integrals, Elliptic Functions and Modular Forms in Quantum Field Theory*, pp. 485–509. 2019. arXiv:1801.05555 [math.NT].

[79] Y. Zhou, "$\mathbb{Q}$-linear dependence of certain Bessel moments," arXiv:1911.04141 [math.NT].

[80] D. Broadhurst, "Feynman integrals, L-series and Kloosterman moments," *Commun. Num. Theor. Phys.* **10** (2016) 527–569, arXiv:1604.03057 [physics.gen-ph].

[81] J. Fresán, C. Sabbah, and J.-D. Yu, "Hodge theory of Kloosterman connections," arXiv:1810.06454 [math.AG].

[82] J. Fresán, C. Sabbah, and J.-D. Yu, "Quadratic relations between Bessel moments," arXiv:2006.02702 [math.AG].

[83] P. Vanhove, "Feynman integrals, toric geometry and mirror symmetry," in *KMPB Conference: Elliptic Integrals, Elliptic Functions and Modular Forms in Quantum Field Theory*, pp. 415–458. 2019. arXiv:1807.11466 [hep-th].

[84] H. A. Verrill, "Sums of squares of binomial coefficients, with applications to Picard-Fuchs equations," arXiv:math/0407327 [math.CO].

[85] P. Vanhove, "The physics and the mixed Hodge structure of Feynman integrals," *Proc. Symp. Pure Math.* **88** (2014) 161–194, `arXiv:1401.6438 [hep-th]`.

[86] J. M. Borwein and B. Salvy, "A proof of a recurrence for bessel moments," *Experimental Mathematics* **17** no. 2, (Jan, 2008) 223–230. http://dx.doi.org/10.1080/10586458.2008.10129032.

[87] M. Bronstein, T. Mulders, and J.-A. Weil, "On symmetric powers of differential operators," in *Proceedings of the 1997 International Symposium on Symbolic and Algebraic Computation (Kihei, HI)*, pp. 156–163. ACM, New York, 1997.

[88] B. Nill, "Gorenstein toric Fano varieties," *arXiv Mathematics e-prints* (May, 2004) math/0405448, `arXiv:math/0405448 [math.AG]`.

[89] Y.-H. He, R.-K. Seong, and S.-T. Yau, "Calabi-Yau Volumes and Reflexive Polytopes," *Commun. Math. Phys.* **361** no. 1, (2018) 155–204, `arXiv:1704.03462 [hep-th]`.

[90] V. Batyrev and K. Schaller, "Stringy Chern classes of singular toric varieties and their applications," *Commun. Num. Theor. Phys.* **11** (2017) 1–40, `arXiv:1607.04135 [math.AG]`.

[91] A. Libgober, "Chern classes and the periods of mirrors," *Math. Res. Lett.* **6** no. 2, (1999) 141–149. https://doi.org/10.4310/MRL.1999.v6.n2.a2.

[92] S. Hosono, "Local mirror symmetry and type IIA monodromy of Calabi-Yau manifolds," *Adv. Theor. Math. Phys.* **4** no. 2, (2000) 335–376. https://doi.org/10.4310/ATMP.2000.v4.n2.a5.

[93] H. Iritani, "Ruan's conjecture and integral structures in quantum cohomology," in *New developments in algebraic geometry, integrable systems and mirror symmetry (RIMS, Kyoto, 2008)*, vol. 59 of *Adv. Stud. Pure Math.*, pp. 111–166. Math. Soc. Japan, Tokyo, 2010. https://doi.org/10.2969/aspm/05910111.

[94] L. Katzarkov, M. Kontsevich, and T. Pantev, "Hodge theoretic aspects of mirror symmetry," in *From Hodge theory to integrability and TQFT tt*-geometry*, vol. 78 of *Proc. Sympos. Pure Math.*, pp. 87–174. Amer. Math. Soc., Providence, RI, 2008. https://doi.org/10.1090/pspum/078/2483750.

[95] S. Galkin, V. Golyshev, and H. Iritani, "Gamma classes and quantum cohomology of Fano manifolds: gamma conjectures," *Duke Math. J.* **165** no. 11, (2016) 2005–2077. https://doi.org/10.1215/00127094-3476593.

[96] K. Oguiso, "On algebraic fiber space structures on a Calabi-Yau 3-fold," *Internat. J. Math.* **4** no. 3, (1993) 439–465. https://doi.org/10.1142/S0129167X93000248. With an appendix by Noboru Nakayama.

[97] H. Iritani, "Private communication,".

[98] M. Kerr, "Work in progress,".

[99] S. Laporta and E. Remiddi, "Analytic treatment of the two loop equal mass sunrise graph," *Nucl. Phys. B* **704** (2005) 349–386, arXiv:hep-ph/0406160.

[100] M. Caffo, H. Czyz, S. Laporta, and E. Remiddi, "The Master differential equations for the two loop sunrise selfmass amplitudes," *Nuovo Cim. A* **111** (1998) 365–389, arXiv:hep-th/9805118.

[101] M. Y. Kalmykov and B. A. Kniehl, "Counting the number of master integrals for sunrise diagrams via the Mellin-Barnes representation," *JHEP* **07** (2017) 031, arXiv:1612.06637 [hep-th].

[102] T. Bitoun, C. Bogner, R. P. Klausen, and E. Panzer, "Feynman integral relations from parametric annihilators," *Lett. Math. Phys.* **109** no. 3, (2019) 497–564, arXiv:1712.09215 [hep-th].

[103] H. Jockers and M. Soroush, "Effective superpotentials for compact D5-brane Calabi-Yau geometries," *Commun. Math. Phys.* **290** (2009) 249–290, arXiv:0808.0761 [hep-th].

[104] M. Alim, M. Hecht, P. Mayr, and A. Mertens, "Mirror Symmetry for Toric Branes on Compact Hypersurfaces," *JHEP* **09** (2009) 126, arXiv:0901.2937 [hep-th].

[105] H. Frellesvig and C. G. Papadopoulos, "Cuts of Feynman Integrals in Baikov representation," *JHEP* **04** (2017) 083, arXiv:1701.07356 [hep-ph].

[106] J. Bosma, M. Sogaard, and Y. Zhang, "Maximal Cuts in Arbitrary Dimension," *JHEP* **08** (2017) 051, arXiv:1704.04255 [hep-th].

[107] M. Harley, F. Moriello, and R. M. Schabinger, "Baikov-Lee Representations Of Cut Feynman Integrals," *JHEP* **06** (2017) 049, arXiv:1705.03478 [hep-ph].